SOFT MICROGEL PARTICLES AT FLUID INTERFACES

Omkar Suresh Deshmukh

SOFT MICROGEL PARTICLES AT FLUID INTERFACES

Omkar Suresh Deshmukh

Physics of Complex Fluids Group,
University of Twente

Committee

Prof. Hans Hilgenkamp (Chairperson)	University of Twente
Prof. Frieder Mugele (Promoter)	University of Twente
Prof. Martien Cohen Stuart (Assistant promoter)	University of Twente
Dr. Dirk van den Ende (Assistant promoter)	University of Twente
Prof. Walter Richtering	RWTH Aachen
Prof. Matthias Wessling	RWTH Aachen
Prof. Jurrian Huskens	University of Twente
Dr. Wouter den Otter	University of Twente

The work described in this thesis has been carried out in the group of Physics of Complex Fluids at University of Twente. The work described in the thesis was carried out under the FOM program on "Jamming and Rheophysics" and is supported by Foundation for Fundamental Research on Matter (FOM) which is funded by the Netherlands Organization for Scientific Research (NWO).

Physics of Complex Fluids group is a part of the research program of the MESA+ Institute and the J.M. Burgerscentrum.

ISBN: 978-90-365-3830-5

Printing: Gildeprint, Enschede

SOFT MICROGEL PARTICLES AT FLUID INTERFACES

PROEFSCHRIFT

ter verkrijging van

de graad van doctor aan de Universiteit Twente,

op gezag van de rector magnificus,

prof. dr. H. Brinksma

volgens het besluit van het College voor Promoties

in het openbaar te verdedigen

op vrijdag 16 Januari 2015 om 16.45 uur

door

OMKAR SURESH DESHMUKH

geboren op 20 maart 1985

te SOLAPUR, INDIA

This dissertation has been approved by:

Prof. Frieder Mugele	Promoter
Prof. Martien Cohen Stuart	Assistant promoter
Dr. Dirk van den Ende	Assistant promoter

Contents

1 Introduction

1.1 General Background

In his Nobel lecture in 1991[1], Pierre-Gilles de Gennes introduced the world to the term Soft Matter. The term soft matter encompasses a very wide range of materials which as the name suggests, can be easily deformed. They include liquids, colloids, polymers, foams, emulsions, gels, liquid crystals, granular materials and biological materials. From the toothpaste that we squeeze out of a tube in the morning to the caramel pudding that we have for desserts after dinner, we encounter countless examples of soft materials in our daily life.

In his Nobel lecture and in subsequent publications[2], de Gennes referred to colloidal systems as *ultra divided matter* and highlighted their ubiquitous nature. The term *colloid* was coined by Scottish chemist Thomas Graham in 1861[3]. In general colloidal material consists of an ensemble of microscopic particles dispersed in a continuous phase. Depending on what the dispersed and continuous phases are, they are further classified as liquid aerosol (liquid dispersed in gas), solid aerosol (solid dispersed in gas), foam (gas dispersed in liquid), emulsion (liquid dispersed in liquid), sol (solid dispersed in liquid), solid foam (gas dispersed in solid), gel (liquid dispersed in solid) and solid sol (solid dispersed in solid). Figure 1.1 shows various examples of colloids mentioned above. In this thesis however, we focus only on solid particles suspended in water specifically at particles at air-water or oil-water interfaces. The size of the dispersed phase is usually between 10nm and 10μm. Such small sizes mean that the thermal energy is relevant at the level of these individual dispersed particles and other forces like gravity can be ignored. The thermal energy of the system is enough to move the particles constantly in a random fash-

ion. This random motion of particles is called as Brownian motion after Robert Brown who first observed such random motion of pollen grains in a water droplet.

Figure 1.1: Examples of colloids that we encounter.(a)Aerosol spray(liquid aerosol), (b)Ash plume in a volcanic eruption(solid aerosol), (c)Whipped cream(foam), (d)Mayonnaise(emulsion), (e)Pigmented ink(sol), (f)Aluminium foam(solid foam), (g)Strawberry jelly(gel), (h)Cranberry glass(solid sol). (All images taken from Wikipedia, Creative Commons license)

Emulsions are colloidal systems where one liquid phase is dispersed in another immiscible liquid phase. They are thermodynamically metastable systems. Instability of emulsions arises due to the high energy associated with a liquid-liquid interface. Coalescence, creaming and Ostwald ripening are the main types of instabilities that occur in emulsions. Traditionally, emulsions have been stabilised by the use of emulsifying agents. These are nothing but species that assemble at the liquid-liquid interface and prevent individual droplets from coming in contact. In addition, they also significantly improve the rheological properties of the interface thereby preventing rupture of the interface. Conventional emulsion stabilisers include surfactant and biopolymers like proteins.

Colloidal particles can also attach to liquid-liquid interfaces resulting in efficient stabilisation of droplets in an emulsion. Such particle stabilised emulsions are called Pickering (Ramsden) emulsions[4, 5]. The reason why solid particles are efficient in stabilizing emulsions lies in their ability to irreversibly adsorb onto fluid interfaces. The energy of desorption of such particles depends on their contact angle at the interface and scales as the square of their radius. Even for particles as small as a few tens of nanometers, the energy required to desorb the particle is as high as $10^3 - 10^4 k_B T$. Furthermore, the particles provide steric and sometimes electrostatic repulsion between the droplets which helps in the emulsion stability.

1.2 PNIPAM microgel particles

Microgel particles consist of a highly cross-linked network of high molecular weight polymers. These polymer networks can be swollen in presence of a solvent under appropriate conditions. The degree of swelling depends on the quality of the solvent and the cross-link density [6, 7]. The solvent-polymer interactions can be tuned via external stimuli such as temperature[8], pH, ionic strength[9] and electric field[10].

Amongst all the polymer microgel systems studied, the ones based on Poly-N-Isopropylacrylamide (PNIPAM) have garnered much attention. PNIPAM is a water soluble polymer which undergoes a coil to glob-

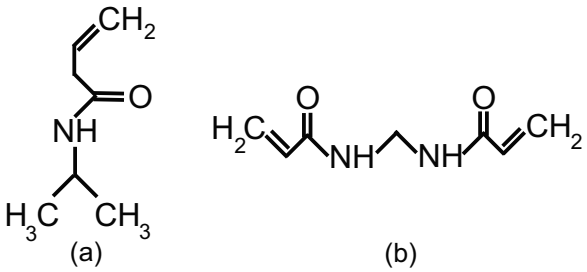

Figure 1.2: Structure of (a) N isopropylacrylamide (NIPA) monomer and (b) N,N'-Methylene -bisacrylamide(BIS) crosslinker.

ule transition at lower critical solution temperature (LCST) of around 32°C. The thermoresponsive nature of these microgels lies in the chemical structure of the polymers. The monomer NIPA as shown in figure 1.2(a) contains a hydrophilic amide group and a hydrophobic isopropyl group. Below the LCST, water forms hydrogen bonds with the acrylamide groups. This keeps the hydrophobic groups apart. However as the temperature increases above the LCST, these hydrogen bonds break. The hydrophobic interactions thus drive the polymer from a coil state to a globule state. This coil to globule transition also reflects in the behaviour of PNIPAM microgel particles. They undergo a volume phase transition around the same temperature (VPTT) as the LCST. This happens to be around the same as the human body temperature. Hence PNIPAM microgels are considered as promising systems for controlled drug delivery applications[11, 12]. However, the VPTT may or may not be same as the LCST and depends upon various factors like addition of a hydrophilic or hydrophobic co-monomer during synthesis, salt concentration, pressure and added surfactant[13].

Microgels in their swollen state have a core-shell type of structure (figure 1.3 (a)). They have a highly cross-linked core and loosely cross-linked brush-like region at the periphery. In the swollen state, the peripheral brush-like structure provides steric stabilization. The van der Waals attraction between such swollen particles is also very weak. In addition to these, the particles also posses a slight negative charge due to the initia-

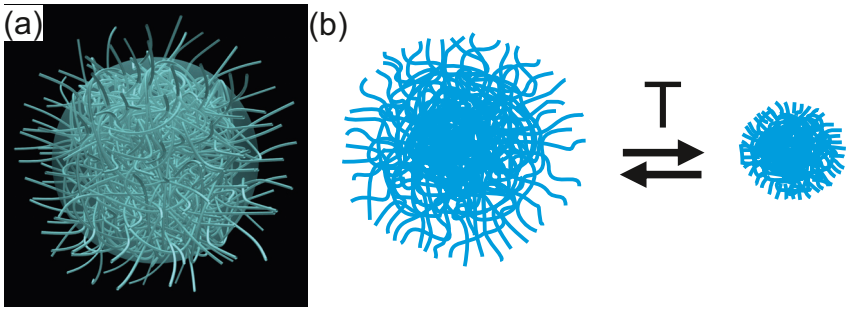

Figure 1.3: (a)Artist's sketch of a swollen PNIPAM microgel particle (image reproduced with permission from Prof. Frank Scheffold[14] and Dr. Jean-François Dechézelles[15] (b)Schematic picture of the change in structure of a microgel particle upon changes in temperature.

tor used in the synthesis. This prevents the particles from aggregating. Above the VPTT, the brush collapses and the particles are morphologically similar to stiff colloidal particles as shown in figure 1.3 (b).

The adsorption and self assembly of microgel particles at fluid interfaces has been a topic of study for many researchers for the past few years. Soft microgel particles at fluid interfaces provide many interesting challenges. Firstly, their nature is somewhere in between that of stiff colloidal particles and soft polymer molecules[16]. This proves to be extremely useful since they posses the advantages of both the systems. For example, just like polymers or surfactant molecules, they adsorb readily on to an interface. But polymeric molecules are small and can also desorb easily from an interface. In this respect, microgel particles behave like colloidal particles that are irreversibly adsorbed on to an interface. Secondly, being at an interface, the broken symmetry gives rise to complex interactions and morphological conformations which have lately come under intense scrutiny. These aspects in addition to their stimuli responsive nature, make microgel particles potential candidates as Pickering stabilizers for emulsions with tunable stability. These microgel stabilized tunable/smart emulsions are also referred to as *Mickering emulsions*[17] to highlight the fact that they are different from the conventional Pickering emulsions.

1.3 Outline of the thesis

In this thesis, I investigate the interactions between PNIPAM microgel particles on an interface. In particular, I study the effect of temperature on these interactions and consequently on the rheology of the interfacial monolayer. This thesis comprises of a total of 7 chapters including this introductory chapter.

Chapter 2: In this chapter, I try to provide a comprehensive review of the existing literature regarding adsorption, interactions, self assembly and rheology of particulate layers at fluid interfaces. I have tried to make a comparative study of hard particle systems and soft microgel systems within the framework mentioned above.

Chapter 3: This chapter delineates the various experimental methods and protocols that I have followed. I begin with describing the synthesis and characterisation of the microgel particles that I have used for my experiments. This is followed by explanation of the working principles of the equipment used in my experiments such as the Langmuir balance and Drop tensiometer.

Chapter 4: This chapter deals with the adsorption kinetics of the microgel particles at an air-water interface. I establish an experimental equation of state (EOS) for these microgels using compression isotherms on a Langmuir film balance. I use this EOS to convert the dynamic surface pressure data into surface concentration. We can thus study how the surface concentration of the microgel particles evolve over time starting with a bare interface. We can see that the adsorption process clearly consists of two regimes. Initially the adsorption is controlled by the diffusion of particles from bulk to the interface. However as the interface gets filled with particles, a kinetic barrier is created for adsorption of newer particles on to the interface. At long time, this barrier become the limiting mechanism.

Chapter 5: I extend the adsorption kinetics study carried out in the previous chapter. Given the thermoresponsive nature of the particles, I study the effect of temperature on the adsorption kinetics. I investigate the EOS for various temperatures and surprisingly, the interactions at

higher temperatures seem to be softer. I also try to build a model which considers the short time diffusion limited regime as well as the long time barrier controlled mechanism to predict the behaviour of the adsorption curves. We fit the model to our experimental data and extract parameters like the diffusion coefficient and the rate constant.

Chapter 6: I consider the adsorption and interactions of microgels on oil-water interfaces in this chapter. I try to explain the counter intuitive observations of increase in surface pressure with temperatures using an argument that the inter-particle interactions cross over from being predominantly steric at lower temperatures to long range dipolar repulsion at higher temperatures. The electrophoretic mobility measurements modelled using the Ohshima theory support this argument.

Chapter 7: In the conclusions and outlook chapter, I summarise my findings and try to make recommendations for a possible future line of study.

Bibliography

[1] Pierre-Gilles de Gennes. Soft matter. Nobel lecture(`http://www.nobelprize.org/nobel_prizes/physics/laureates/1991/gennes-lecture.pdf`), 1991.

[2] Pierre-Gilles de Gennes. Ultradivided matter. *Nature*, 412(6845):385–385, 2001.

[3] T. Graham. Liquid diffusion applied to analysis. *Phil.Roy.Soc.*, 151:183–224, 1861.

[4] Spencer Umfreville Pickering. Cxcvi.-emulsions. *Journal of the Chemical Society, Transactions*, 91(0):2001–2021, 1907.

[5] W. Ramsden. Separation of solids in the surface-layers of solutions and 'suspensions' (observations on surface-membranes, bubbles, emulsions, and mechanical coagulation). – preliminary account. *Proceedings of the Royal Society of London*, 72(477-486):156–164, 1903.

[6] Brian R. Saunders and Brian Vincent. Microgel particles as model colloids: theory, properties and applications. *Advances in Colloid and Interface Science*, 80(1):1 – 25, 1999.

[7] H. Senff and W. Richtering. Influence of cross-link density on rheological properties of temperature-sensitive microgel suspensions. *Colloid and Polymer Science*, 278(9):830–840, 2000.

[8] R.H. Pelton and P. Chibante. Preparation of aqueous latices with n-isopropylacrylamide. *Colloids and Surfaces*, 20(3):247 – 256, 1986.

[9] Mitsuhiro Shibayama, Fumiyoshi Ikkai, Satoshi Inamoto, Shunji Nomura, and Charles C. Han. ph and salt concentration dependence of the microstructure of poly(nisopropylacrylamidecoacrylic acid) gels. *The Journal of Chemical Physics*, 105(10):4358–4366, 1996.

[10] R. H. Pelton, H. M. Pelton, A. Morphesis, and R. L. Rowell. Particle sizes and electrophoretic mobilities of poly(n-isopropylacrylamide) latex. *Langmuir*, 5(3):816–818, 1989.

[11] Ying Guan and Yongjun Zhang. Pnipam microgels for biomedical applications: from dispersed particles to 3d assemblies. *Soft Matter*, 7:6375–6384, 2011.

[12] Christine T. Schwall and Ipsita A. Banerjee. Micro- and nanoscale hydrogel systems for drug delivery and tissue engineering. *Materials*, 2(2):577–612, 2009.

[13] Samruddhi Kamble. *Probing Structure and Dynamics of Soft Colloidal Glasses using Rheology and Light Scattering*. PhD thesis, Indian Institute of Technology Bombay, Mumbai, India, September 2013.

[14] Frank Scheffold. `http://frimat.unifr.ch/frimat/en/page/445/`.

[15] Jean-François Dechézelles. `http://www.am-institute.ch/about/people/staff/jean-francois-dechezelles`.

[16] L. Andrew Lyon and Alberto Fernandez-Nieves. The polymer/colloid duality of microgel suspensions. *Annual Review of Physical Chemistry*, 63(1):25–43, 2012.

[17] Sabrina Schmidt, Tingting Liu, Stephan Rutten, Kim-Ho Phan, Martin Moller, and Walter Richtering. Influence of microgel architecture and oil polarity on stabilization of emulsions by stimuli-sensitive core–shell poly(n-isopropylacrylamide-co-methacrylic acid) microgels: Mickering versus pickering behavior? *Langmuir*, 27(16):9801–9806, 2011.

2 Literature review

Abstract Soft microgel particles inherently possess qualities of both polymers as well as particles. In this chapter I review the similarities and differences between soft microgel particles and stiff colloids at fluid-fluid interfaces. Based on the existing literature, I compare two fundamental aspects of particle-laden interfaces namely the adsorption kinetics and the interactions between adsorbed particles. Although it is well established that the transport of both hard particles and microgels to the interface is driven by diffusion, the analysis of the adsorption kinetics needs reconsideration and a proper equation of state relating the surface pressure to the adsorbed mass should be used. I provide an overview of the theoretical and experimental investigations into the interactions of particles at the interface. The rheology of the interfacial layers is intimately related to the interactions, and the differences between hard particles and microgels become pronounced. The assembly of particles into the layer is another distinguishing factor that separates hard particles from soft microgel particles. Microgels deform substantially upon adsorption and the stability of a microgel-stabilized emulsion depends on the conformational changes triggered by external stimuli.

This chapter has been published as Deshmukh OS, *et al.*, Hard and soft colloids at fluid interfaces: Adsorption, interactions, assembly & rheology, Adv Colloid Interface Sci (2014), http://dx.doi.org/10.1016/j.cis.2014.09.003

2.1 Introduction

While coarse emulsions have widespread applications ranging from food products, pharmaceuticals and cosmetics to oil recovery[1, 2], they also share the property of thermodynamic metastability. In most cases the tendency of the droplets to assemble into a large volume of fluid, is detrimental to the application (e.g. in many food products), while in other cases this proclivity is exploited to break the emulsion (e.g. in oil recovery). Clearly in both scenarios the thermodynamic properties of the emulsion are of utmost importance, and a thorough understanding of how the system is (thermodynamically or kinetically) stabilized is needed. Even though emulsions are known for a very long time, their stability is still an active area of research, in which new formulations and new theoretical descriptions are being explored[3–7].

Emulsion instability arises from the high energy associated to a liquid/liquid interface. Coalescence (film rupture) and Ostwald Ripening (due to differences in Laplace pressure of the drops) are the most important processes involved in destabilization. A classical way to eliminate (or at least counteract) these processes is to add amphiphilic molecules, i.e. surfactants. Alternatively, also colloidal particles can be used. Such particle-stabilized emulsions are known as (Ramsden)-Pickering emulsions[8–10]. Conventional Pickering stabilizers include rigid micro- or nano-sized particles of highly cross-linked polymers like PolyMethylMethacrylate(PMMA), Poly-styrene(PS) or amorphous solids like silica[11, 12]. Since recently, also softer (i.e. deformable) particles like polymers or proteins have been used effectively for stabilizing emulsions and foams[13–15].

The efficiency of colloidal particles in stabilizing emulsions originates from the thermodynamics of their adsorption. The energy required to desorb a spherical particle from a fluid interface is given by:

$$E = \pi R^2 \gamma (1 \pm \cos\theta)^2 \tag{2.1}$$

Where R is the radius of the particle, γ is the interfacial tension and θ is the contact angle at the interface. The sign inside the brackets is

positive or negative depending on whether the particle is being desorbed into air/oil phase or water phase. Already for particles with a size of a few tens of nanometers, this energy takes values of the order of $10^3 k_B T$ for contact angles that are not close to 0° or 180°[16]. For bigger colloids this energy becomes even larger and hence the adsorption can be considered as irreversible. This situation is in strong contrast to that of amphiphilic molecules which, due to their small desorption energies of the order of $10^0 - 10^1$ $k_B T$, can desorb on a relatively short timescale, and hence cannot always completely preclude instability events.

While adsorption at a fluid interface is thus always thermodynamically favoured for particles, the process can be significantly slowed down in practice, which points at the possible presence of an adsorption barrier [17]. Sometimes this energy barrier is so high that Pickering emulsions can only be made by vigorous mechanical shaking, or a spreading solvent has to be used to deposit particles at an interface[18–20].

To understand the stability of a Pickering emulsion, one clearly has to consider much more than the adsorption alone. Eventually the reason why particle-coated droplets can maintain their integrity is that the particle layers on the encountering droplets repel each other strongly enough[10]. This first of all requires the particles to be present at sufficiently high (local) surface density, and secondly it requires a mechanism for the inter-particle repulsion.

This aspect of particle interactions is where the complexity of Pickering emulsions becomes manifest. The interaction of an adsorbed particle with another particle in the same layer is fundamentally different from that between two particles that are adsorbed on different droplets (and thus interact through the continuous phase), while both contribute to the stability of the emulsion droplets. In the simplest case, the particles would be rigid spheres interacting only via their excluded volume; stability would then require a sufficiently high packing density (to be achieved before the droplets encounter each other). In practice, electrostatic forces due to surface charges often play a role as well, and in a complex way, since the counterion distributions are different in the two phases[21–23] and also the volume distribution of the adsorbed particle over the two

phases must be considered as a degree of freedom Curvature of the droplet adds another dimension to the problem[24, 25]. It is therefore not surprising that a variety of particle layer structures has been observed, and that different particle interactions were proposed to explain the different cases[21, 26, 27].

In the last decade, also a new class of particles, namely microgels, has generated interest as potential Pickering emulsion stabilizers. Microgel particles are made from a chemically cross-linked polymer that can be swollen by a solvent. The degree of swelling depends on the solvent quality and cross-link density[28, 29]. Microgel particles made from thermosensitive polymers such as poly N-isopropyl acrylamide (PNIPAM) undergo reversible swelling/shrinking transitions at temperatures around the body temperature, and therefore are considered as promising particles for thermo-stimulated control of drug delivery[30, 31]. The particle chemistry can also be varied, e.g., by incorporating charged co-monomers like acrylic or methacrylic acid to make them pH-responsive[32]. Also their hybrid physical character makes them interesting: the fact that they are particles makes them adsorb very strongly to the interface. On the other hand, their polymeric character strongly facilitates their attachment from solutions onto fluid interfaces. This combination of properties makes microgel particles ideal candidates for preparing emulsions with tunable stability[33]. Schmidt*et al.*[34] have coined the term *"Mickering emulsions"* for emulsions stabilized by microgel particles to highlight the fact that although these are conceptually similar to conventional Pickering emulsions stabilized by hard particles, the underlying mechanisms responsible for stabilization of these emulsions are drastically different.

Owing to these attractive properties, in particular PNIPAM (based) particles at fluid interfaces were intensively studied in the past few years. Several insightful studies were performed[35–39] and the suitability of PNIPAM as an emulsifier was demonstrated[34, 37]. However, and remarkably, the kinetics of adsorption and thermodynamics of the interactions between microgels particles adsorbed in the same layer, were addressed only in a few studies up till now[35].

Since excellent books and review papers have been written on Pick-

ering emulsions (e.g. [16] and references therein) and on (PNIPAM) microgels[28–34], we will refer to these sources for further details. The specific focus of this review will be the state-of-the-art in understanding the behaviour of PNIPAM microgels at fluid interfaces, with a special emphasis on the kinetics of adsorption and the thermodynamic interactions between particles in the same layer. Comparisons with the behaviour of hard (spherical) particles at interfaces will serve as a reference case to highlight the similarities and differences with soft microgels.

One method that is particularly well suited to study both the interfacial adsorption kinetics and the subsequent interaction between colloidal particles, is interfacial rheology. Also for this topic an excellent review book is available[40]. Therefore in this article we will shortly explain the concepts, and then more elaborately discuss the most recent developments in this field.

2.2 Adsorption dynamics

Although several experimental studies into particles adsorbing at fluid-fluid interfaces have been performed, most of them with stiff colloids[41–45] and a few with soft microgel particles[35, 46], the processes controlling the kinetics of adsorption are generally complex and at present not clearly understood.

For the adsorption of colloidal particles, electrostatic interactions between the interface and the particle must play a role. This is most strongly evidenced by experiments in which no mechanical energy is supplied in order to assist the adsorption. It is experimentally established that air-water or oil-water interface is negatively charged, even though the origin of this negative charge is still a matter of debate[47–49]. Thus, depending on the ionic strength, negative particles repelled by the interface adsorb either very slowly or not at all, whereas positively charged particles adsorb readily[50]. Also combinations of electrostatics and wettability can play a role. For example silica particles, which are both negatively charged and inherently hydrophilic, are found to adsorb onto the interface only after making their surface more hydrophobic, by letting cationic surfactants

like CTAB adsorb on their surface[51–53]. Also other wetting phenomena' can contribute to an adsorption barrier. For example in case of PS particles adsorbing onto air/water interface it is found that completion of the adsorption process (for a single particle) could take a long time (weeks or even months), which is attributed to relaxation of the three phase contact line[26, 54] (similar to contact angle hysteresis on macroscopic surfaces).

In physical modelling of the adsorption kinetics, a distinction is usually made between diffusion controlled transport to a thin sublayer, and the adsorption from the sublayer. This approach is similar to that of adsorbing surfactants, as presented for example by Ward and Tordai[55]. Briefly, in the absence of external flow fields, the transport of particles is governed by Fickian diffusion. This produces a mass transport rate:

$$\frac{\partial c}{\partial t} = D\frac{\partial^2 c}{\partial x^2} \tag{2.2}$$

Where c is the bulk concentration, D the diffusion coefficient of the particles and x the distance from the interface. Assuming as initial conditions a bare interface, i.e. $\Gamma(0) = 0$ with $\Gamma(t)$ the time dependent surface concentration, and a uniform concentration $c(x, 0) = c_\infty$ in the bulk liquid, the boundary condition is given by:

$$\frac{d\Gamma}{dt} = D\left[\frac{\partial c(x,t)}{\partial x}\right]_{x=0} \tag{2.3}$$

Then, assuming absence of an adsorption barrier and an interfacial area that is so small that even the maximum adsorption would not significantly deplete particles from the liquid, i.e. $c(\infty, t) = c_\infty$, equations 2 and 3 result in the well known expression of Ward and Tordai[55]. In case of irreversible adsorption and complete depletion of the sublayer, it can be expressed as:

$$\Gamma(t) = 2c_\infty\sqrt{\frac{Dt}{\pi}} \tag{2.4}$$

In case the particles have to cross an adsorption barrier, the description has to be extended. Fig 1. shows a schematic representation of the

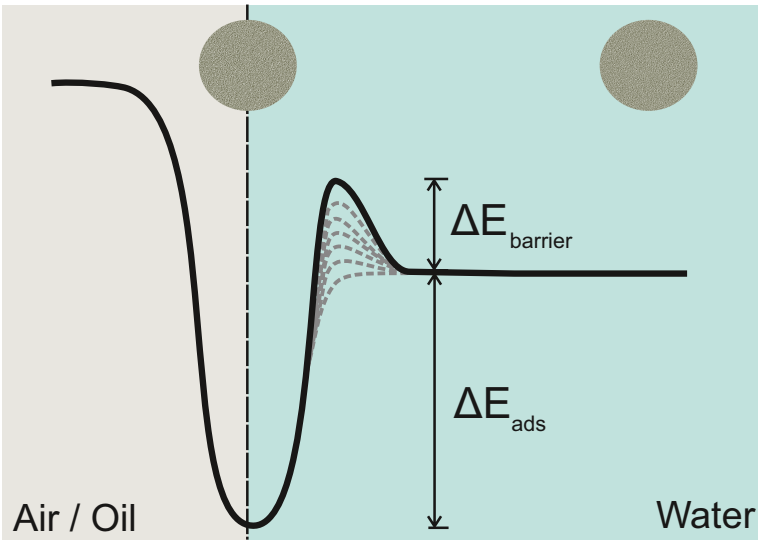

Figure 2.1: Schematic representation of the energy landscape at the air-water or oil-water interface. The energy barrier $\Delta E_{barrier}$ increases as the surface gets covered with particles.

energy landscape associated with the adsorption process. Electrostatic interactions are generally incorporated in an exponential term[56], while the effect of area (fraction) that is occupied by already adsorbed particles is taken into account by a linear term. This approach is similar to that of Adamcyzk and co-workers[57, 58] who study the role of electrostatic interactions in adsorption of particles on solid-liquid interfaces. Several of the mentioned studies into interfacial particle adsorption are performed by measuring the Dynamic Surface Tension using axisymmetric drop shape analysis[41–45, 59]. An obstacle with this approach is, that one does not directly obtain $\Gamma(t)$: an equation of state i.e. $\Pi(\Gamma)$, with Π the surface pressure, is needed. Here $\Pi(t) = \gamma - \gamma_0$ is the surface pressure, γ is the instantaneous interfacial tension and γ_0 is the value of interfacial tension of the bare interface. Note that use of an equation of state (EOS) assumes a thermodynamic equilibrium within the adsorbed layer. Most studies use

the EOS for an ideal 'surface gas':

$$\Pi(t) = RT\Gamma(t) \tag{2.5}$$

This assumption leads to qualitatively correct predictions: in many experiments, an initial decay in γ that is proportional to $t^{1/2}$ is followed by an exponential relaxation of γ; which according to Eqn. 5 then gives an adsorption that rises quickly initially, and then gradually saturates. However, in the quantitative sense, something is clearly missing. When analysing the implications of this approach (with Eqns. 2-5), it turns out that the corresponding diffusion coefficients would have to be as much as $10^{13} - 10^{15}$ times larger than the values predicted from the Stokes-Einstein relation[45, 59].

In case of charged particles at an interface, the surface pressure is strongly dominated by the electrostatic interactions. Aveyard *et al.*[60] derive an analytical expression for Π as a function of reduced trough area assuming pair-wise additive dipole-dipole repulsion between the adsorbed particles. Recently, this expression was improved further by taking into account the collective effects (beyond the pair-wise additivity) by Petkov *et al.* [61]. These expressions can be treated as a surface equation of state for charged colloidal particles adsorbed on an oil-water interface.

Recently Deshmukh *et al.* [46] use a Langmuir trough to compress spread monolayers of soft PNIPAM microgel particles on an air-water interface. Since adsorbed particles do not leave the interface, their Pressure-Area isotherm can be interpreted as a Pressure-Mass relationship; in other words, an equation of state, allowing $\Pi(t)$ data to be converted into $\Gamma(t)$ data. They find that an 'Ideal gas' equation of state is indeed very inadequate for relating the pressure to the adsorbed mass. They report that the adsorption process can be clearly separated into two regimes. At short times, the adsorption process is controlled by the diffusion of the particles from bulk to the interface. At long times, the interface gets filled with particles thereby creating a barrier for newer particles to adsorb onto the interface. This leads to an exponential relaxation of Γ.

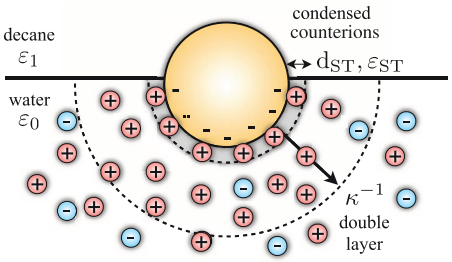

Figure 2.2: Schematic drawing of the charge distribution around a colloidal particle at an oil-water interface. Taken from Masschaele *et al.*[22] with permission from APS.

2.3 Interfacial interactions

2.3.1 Electrostatic interactions

Colloidal particles very often carry electrical charge on their surface. This clearly has to be the case for the far majority of water-dispersible colloids, which are also the systems most often studied at liquid-liquid interfaces. This charge may arise from a dissociation or deprotonation of the native surface groups (e.g. silica), from dissociation of initiator molecules (e.g. PS latex) or from adsorbed or grafted surfactants or polymers with an ionic character[62]. The interactions between charged particles in (aqueous) bulk are generally well described by the Derjaguin-Landau-Verwey-Overbeek (DLVO) theory[63]. Also in non-polar solvents, particles can carry charge[64] but the origin of the charge is not always clear and its contribution to colloidal stability is usually considered less important.

When colloidal particles transfer from the bulk polar liquid (e.g. water) to an interface with a non-polar phase (e.g. oil), the interactions can change profoundly. The part of the particle immersed in the polar phase will remain charged but for the part in the non-polar phase, it is energetically favourable to re-neutralize the surface groups. This then results

in an asymmetric double layer[65] as shown in Figure 2. The resulting overall interaction between the adsorbed particles (in the same interfacial layer) can become (strongly) dependent on several parameters, like the relative volume distribution over the two phases, the dielectric constant of (and presence of counter charges in) the non-polar phase, and the degree of charge screening in the aqueous phase[66–68].

The theoretical modelling of the interactions between hard particles at a fluid-fluid interface has made considerable progress, especially in the last decade. An early contribution was made by Stillinger[69] who derived an expression for the pair interaction potential between point charges separated by a distance r at an electrolyte-air interface, using the Debye-Hückel theory[65]:

$$U(r) = \frac{2Z^2e^2}{4\pi\varepsilon\varepsilon_0 r}\int_0^\infty \frac{xJ_0(x)}{[x^2 + (\kappa r)^2]^{1/2} + x/\varepsilon}dx \tag{2.6}$$

Where Z,e,ε,ε_0 are the valency of the ions, the unit electrical charge, the dielectric constant of the liquid, and the permittivity of vacuum, respectively. $J_0(x)$ is the zero order Bessel function and κ is the inverse of the Debye screening length. Hurd[70] simplified this expression to show that the potential crosses over from a screened Coulombic interaction at small distances to a dipole-dipole interaction at larger separations.

As common in physics, the improvement of the theoretical description has gone hand in hand with the possibility to do more sophisticated experiments. The first experimental observations of electrostatic interactions between particles at a fluid-fluid interface were made in 1980 by Pieranski[71] who looked at ordered and disordered patterns formed by charged polystyrene latex particles adsorbed at an air-water interface. More than two decades later, a major step forward was made when optical tweezers were used to measure the interaction force between two individual colloids at an oil-water interface[72]. Herewith it was confirmed that the dominant contributions to the pair potential U(r) are a screened Coulombic repulsion at short distances, plus a long range dipolar

repulsion at large distances:

$$U(r) = \frac{a_1 k_B T}{3r} e^{-\kappa r} + \frac{a_2 k_B T}{r^3} \tag{2.7}$$

Where a_1 and a_2 are numerical constants. The calculation of a_2 involved a charge re-normalization. The validity of this expression was further corroborated by additional laser tweezers experiments, measurements of the pair correlation function and measurements of the macroscopic shear modulus of a 2D colloidal crystal at the interface[73]. Differences in the magnitude of interaction potential measured with the different techniques were attributed to the heterogeneity in the electrostatic repulsion[20]. To date, this expression appears to give the best description of pair interactions between hard spherical particles at liquid-liquid interfaces.

Very recently numerical studies were carried out[74] using the standard Poisson-Nernst-Planck equations for interactions between two spherical particles. The calculations showed that the particle size was important especially when the particles are close to each other. These findings were in good agreement with the experimental data from Masschaele *et.al.*[22].

2.3.2 Van der Waals interactions

In principle, Van der Waals interactions can play a role as well. These short range attractive interactions between particles of the same type, resulting from dipole-dipole interactions between the individual molecules constituting the particles, are more difficult to calculate for particles at an interface. In a simplistic scenario for the potential between spherical colloidal particles dispersed in a single phase, one finds[75]

$$U_{vw}(r) = -\frac{A_H}{6}\left(\frac{2a^2}{(r^2-4a^2)} + \frac{2a^2}{r^2} + ln\frac{(r^2-4a^2)}{r^2}\right) \tag{2.8}$$

Where r is the distance between the particle centers, a is their radius and A_H is the Hamaker constant. Clearly, for interfacial particles the (effective) Hamaker constant should depend on the fractional volume of particles immersed in each phase. More importantly, the van der Waals

interaction is usually negligible small. It can play a role if the particles approach each other very closely, but this rarely happens since in many practical cases, the strong repulsions prevent this from happening.

2.3.3 Capillary interactions

Adsorption of colloidal particles results in local deformation of the liquid interface. For large particles, the balance of the gravity and buoyancy forces in combination with the wetting properties of the particles, deforms the interface and causes the particles at interface to attract or repel depending on the local curvature of the interface. This phenomenon is often referred to as the *"Cheerios effect"*[76] after the common observation that breakfast cereals floating in a bowl of milk often clump together in the centre or migrate to the edge of the bowl. The aggregation of non-colloidal particles due to capillary attraction has been well formulated[77, 78].

For micron sized or sub-micron sized particles however, the weight of the particles is not enough to deform the interface. But yet, various studies have shown systems comprising of small colloidal particles or protein macromolecules to form clusters or larger ordered domains([79] and references therein). In this case the interfacial deformations are created because the contact line at the surface of the particle is undulated or irregularly shaped. This may happen if the solid surface is rough or heterogeneous[80–82]. Undulated contact lines may form if the surface of the particles is smooth but the particles are anisotropic[83, 84].

The deformation of the interface along the contact line can be assumed to be small enough so that the Young-Laplace equation can be linearised. The interfacial deformation can then be written as a Fourier multi-polar expansion [85].

$$\zeta = \sum_{m=0}^{\infty} h_m \frac{K_m(q\rho)}{K_m(qr)} cos\left[m\left(\phi - \phi_m\right)\right] \tag{2.9}$$

Where, (ρ, ϕ) are polar co-ordinates associated with the particle, K_m is the modified Bessel function of the second kind and order m, h_m and ϕ_m are the amplitude and phase shift for the m-th mode of the undulation of

the particle contact line, r is the radius of its vertical projection on the xy-plane and $q = \sqrt{(\Delta\rho g \backslash \gamma)}$ is the inverse of the capillary length.

For the case of large particles, the deformation of the meniscus is predominantly due to the weight of the particle and can be expressed as a capillary monopole ($m = 0$). The interaction potential between two monopoles each of strength f separated by distance d is given by[86]:

$$U_{cap} = -\frac{f^2}{2\pi\gamma} K_0(qd) \tag{2.10}$$

In case of colloidal particles, the effect of gravity on the deformation of the interface is negligible hence the monopoles can be neglected. Similarly, there is no external torque that can rotate the particles relative to the interface. Hence the dipolar term ($m = 1$) can also be neglected. Thus, for colloidal particles, the leading term that defines the interfacial deformation is quadrupole ($m = 2$)[85]. The interaction energy for two identical particles (A and B) of radius r_c, separated by a distance d is then given by[80]:

$$\Delta E = -12\pi\gamma h_2^2 \cos\left[2(\phi_A - \phi_B)\right] \frac{r_c^4}{d^4} \tag{2.11}$$

It must be noted that these approximations are valid for large separations between the particles. When the particles come closer (typically of the order of the particle radius) the scenario is much more complicated since higher multi-pole orders come into play. These higher orders are non monotonic and the potential may even become repulsive at very small distances[80, 85]. The effective interaction potential is always a result of a superposition of capillary and electrostatic interactions.

2.3.4 Interactions between microgel particles

We now turn to microgel particles at a fluid-fluid interface. Since these particles exhibit a behaviour that is intermediate to that of hard particles and polymers, their thermodynamic interactions at an interface can be expected to be different from those of hard particles. Because the particles

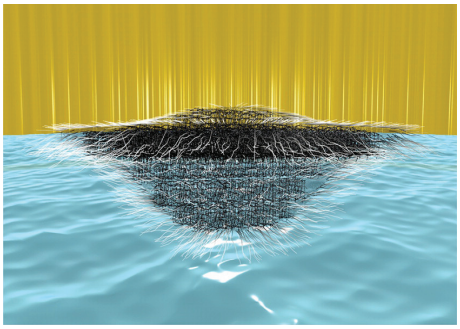

Figure 2.3: Artist impression of the deformation of a soft microgel particle at an oil-water interface. Taken from [95] with permission from ACS.

are strongly swollen, the Van der Waals attractions will be very weak, which also means that microgels do not need to carry much electrical charge in order to be stable. In other words, the interactions that are dominant for hard particles could be very weak for microgel particles. Furthermore, the ability of microgels to deform in bulk[29, 87–91] and at an interface[34, 92–95] adds important new degrees of freedom to the system.

The interaction potential between PNIPAM microgel particles in bulk liquid has been studied. For low to intermediate concentrations (effective volume fraction of the swollen particle below 0.3) it is very similar to that of hard sphere systems. But as the concentration is increased to the point where the particles have to deform, the softness suddenly becomes apparent. This has been described with an effective potential [96].

When these particles adsorb onto an interface, they will deform in a completely different manner. According to the generally accepted view, the particles are stretched out when the surface coverage is low. The reason for this is that free energy gain (i.e. reduction) of covering a bigger interfacial area is high as compared to the energy cost that is related to the elastic deformation of the particle. Besides that, a major part of the particle remains in the aqueous phase, while only a small portion protrudes into the oil phase[95] as sketched in the cartoon in

Fig. 3[95]. What happens to the shape and embedding of the particle when more particles adsorb and thus increase the surface density, can only be reasoned in a qualitative manner: from the moment that the adsorbed microgels are touching each other, it should be energetically more favourable for them to stretch less. This will reduce the elastic energy, while the liquid-liquid interface will still be covered.

These degrees of freedom (embedding and deformation) make it difficult to estimate the interaction potential between microgel particles at an interface. First experiments in this regard have been conducted only very recently by Geisel *et al.* [97] who reported the remarkable finding that even charge introduced via acidic / dissociating co monomers on microgel particles does not directly influence their compression behaviour.

In case of soft particles, it is known that the capillary attraction is stronger as compared to hard particles since the wetting radius is larger and extremely rough and heterogeneous due to the deformable nature of particles[98, 99]. Cohin *et al.*[39] observe clusters of PNIPAM microgel particles at an air water interface. They note that the cluster formation was irreversible and occurred at very low concentrations. Also the particles seem to form clusters at the interface but do not form aggregates in bulk. This leads them to conclude that the clustering primarily occurs due to the long range capillary interactions. Once the particles are close to each other, the overlapping dangling polymer segments can also interact through short range forces.

From these recent findings it becomes clear that while important differences have been identified in the mechanisms via which hard particles and microgels interact at an interface, there is also a dire need of further experimental and theoretical studies on interactions between soft microgel particles at interfaces. Knowledge about the interactions as the particles change their morphology as a response to external stimuli is essential if PNIPAM microgels have to claim a place in the league of Pickering stabilizers and to highlight their ability to create emulsions with tunable stability.

2.4 Interfacial Rheology

Rheology is the study of flow or deformation in materials when they are subjected to a stress or load. For bulk fluids, it provides a unique and indispensable tool for understanding mechanical interactions between supramolecular entities (droplets, particles, polymers) in flow. The strength of the method is that the different contributions to the stress (tensor) in the fluid e.g. hydrodynamic and electrostatic interactions between particles, deformability of particles, are measured in a direct way. Understanding the rheology of complex fluids can be difficult for the same reason. Often one has to simplify the real system in order to analyse it, or resort to (numerical) simulations that are capable of integrating the thermodynamic and hydrodynamic interactions[100].

For the rheology of interfacial layers containing colloidal particles the situation is similar. The rheological properties of the layer reflect the thermodynamic and hydrodynamic interactions between particles inside the layer and with the surrounding fluids. In principle this can present a very complex problem, but if the mechanical properties of the layer are dominant, simplifications can be made. Like for bulk fluids, the rheological behaviour by itself (even if it is not quantitatively understood) can be an important tool in understanding stability. This certainly applies to emulsions and foams[101, 102].

In case of interfaces, deformations are possible via their area or via their shape. Dilatational rheology is the study of response of the interface to a change in area while conserving the shape, whereas shear rheology studies the response to a change in shape while the area remains the same[40]. Below, we briefly outline the different rheological concepts before discussing experimental studies.

2.4.1 Macroscopic Methods

Dilatational rheology

Dilatation (and compression) of the interface can be achieved with a Langmuir trough or a pendant drop (/captive bubble). Consider an interfacial

area that is perturbed by a very small amount $\delta A(t)$. The response of the system is characterized by a change in the surface pressure $\delta\Pi(t)$. If no material can be exchanged between interfacial and sublayer (dilatational elasticity), the change in $\Pi(t)$ will immediately follow the change in $A(t)$, which can be described by an equation of state. Often however, there are relaxation processes within the layer that involve dissipation and cause a delay in the response. This is characterized by a dilatational viscosity. The general response of the surface pressure is given by[40, 103]

$$-\Delta\Pi(t) = \int_{-\infty}^{t} \tilde{E}(t-s)\dot{u}(s)ds = \left[E + \zeta\frac{\partial}{\partial t}\right]u(t) \tag{2.12}$$

Where $u(t) = \delta A(t)/A_0$ is the relative change in area and $\tilde{E}$ a viscoelastic memory function. For most purposes the integral can be simplified to the right hand side of Eq. 12, where:

$$E = -\left(\frac{\partial\Pi}{\partial A/A}\right)_T \tag{2.13}$$

is the dilatational elastic modulus, and ζ the dilatational viscosity. If the perturbation of the interfacial area is sinusoidal, it can be expressed as $u(t) = u_0 e^{(i\omega t)}$. The surface stress response $\sigma(t) = \Pi(t) - \Pi_0$, then follows the imposed deformation with a phase lag ϕ. In this case, the viscoelastic modulus E* is a complex quantity in which the elastic component (the dilatational storage modulus $E'(\omega)$) constitutes the real part and the viscous dissipation (the dilatational loss modulus $E''(\omega)$) constitutes the imaginary part. This analysis is valid only if the deformations are small enough so that the response is linear. Non-linear response can be studied by considering the Fourier expansion of the stress response[104]

Experimentally, dilatational rheology is mostly carried out with pendant drops or captive bubbles, oscillated at low frequencies (< 1Hz). At higher frequencies, interpretation can become obscured by the shear flows that are involved in the volume changes of the drop[105].

Shear Rheology

Various experimental techniques have been employed to carry out shear rheology at interfaces. The most popular ones are oscillatory shear rheometers, which are designed to characterize interfaces. Depending on the type of probe used they are called knife-edge, blunt-knife, plate, bi-cone or double wall ring type surface viscometer[106]. Recently magnetic probes have been used to make very sensitive measurements[107]. The shear rheology of 2D interfacial layers uses similar rheological concepts as have been developed for 3D systems. Thus the stress response of the monolayer(σ_{xy}) is directly proportional to the applied strain (u_{xy}), the proportionality constant being the interfacial shear modulus:

$$\sigma_{xy} = \int_{-\infty}^{t} \tilde{G}(t-s)\dot{u}_{xy}(s)ds = \left[G + \eta_s \frac{d}{dt}\right] u_{xy} \tag{2.14}$$

Again the right hand side is a simplification of the memory integral. The interfacial stress response to small amplitude shear deformations at a frequency ω can be defined by a complex interfacial shear modulus $G^*(\omega)$ which has the elastic component (storage modulus $G'(\omega)$) as the real part and the viscous component (loss modulus $G''(\omega)$) as the imaginary part[108].

2.4.2 Microscopic methods

Most available rheometers that measure interfacial shear properties have a detection limit of around 10^{-6}Ns/m[40, 109]. For layers with lower shear viscosities, micro-rheological techniques have been looked upon as a promising technique that could enable measurement of surface shear viscosities as low as 10^{-10}Ns/m [106]. In fact interfacial micro-rheology comprises different methods, which have in common that small probes are used to measure or impose very small forces or displacements [110, 111]. Most methods appear to be inspired by micro-rheological methods for bulk samples, which have been developed in the past two decades, and for which excellent reviews exist[112–115].

Micro-rheological techniques can be classified into active and passive ones. Here 'active' means that forces or deformations are imposed via external controls like electromagnetic fields, whereas 'passive' implies that displacements are driven by thermal motion. Active techniques have so far mainly been used to characterize bulk systems. One technique that has been adapted for use at interfaces is Optical Tweezers[116]. An advantage of this technique is that the measured interfacial shear viscosity can also be used to measure the particle interactions and the drag coefficient of the particle; provided that the trap is calibrated [21]. Another recent technique uses magnetic nano-wires [117] or microscopic magnetic disks[118]. This method is based on Fuller's Interfacial Stress Rheometer (ISR)[107] but uses a microscopic probe combined with video microscopy which leads to higher sensitivities.

Passive techniques that have been adapted for interfacial rheology include Dynamic Light Scattering at interfaces using evanescent waves[119, 120] and Fluorescence Correlation Spectroscopy(FCS)[121, 122]. Recently also Particle Tracking micro-rheology has emerged as a technique for interfacial rheology. The relative ease (in terms of labour and cost) of doing the experiments makes this method potentially attractive; therefore it is discussed in more detail.

Particle Tracking

This technique uses (high speed) microscopy to record the motions of colloidal probe particles that have been deposited onto an air-liquid or liquid-liquid interface. After the recordings, the particles are localized, and trajectories are constructed, mostly using the same software that is also used in particle tracking in bulk[123]. By averaging over different particles and/or times, one then obtains the Mean Squared Displacement (MSD) as a function of lag time τ, which is often expressed as[106]:

$$\left\langle \Delta r^2(\tau) \right\rangle = 2dD\tau^{\alpha} \tag{2.15}$$

Where d is the dimensionality of the system and D a constant. For a purely viscous (e.g. bare) interface, the exponent α equals unity, and D

is the interfacial diffusion coefficient. For interfaces like lipid monolayers, dense polymer monolayers or biological systems where particle motion is hindered by obstacles or restricted to specific regions, a sub-diffusive behaviour with $\alpha < 1$ is found[106]. The diffusion coefficient D is related to the hydrodynamic drag coefficient (f) on the particle:

$$D = \frac{k_B T}{f} \tag{2.16}$$

In bulk, i.e. 3D systems, and for non-deformable particles f is equal to the Stokes drag $6\pi\eta R$, with η the solvent viscosity and R the radius of the particle. For particles at an interface, this expression is no longer valid, since motion of the particle along the interface causes flow patterns in each of the two fluid phases. This makes the drag coefficient dependent on the relative embedding in each fluid phase, and the corresponding viscosities. Even in the simplest (i.e. 'symmetric') case of equal embedding and equal viscosities (like for PS spheres at water/decane interface)[124] the drag coefficient will still be slightly higher as compared to bulk liquid.

While $\langle \Delta r^2(\tau) \rangle$ could be interpreted in terms of rheological properties (see e.g.[106]) this is not always done as the relation between the MSD and the mechanical properties is not always straightforward. These complications were highlighted by recent studies of interfacial layers of polymers. The interfacial shear viscosities measured with micro-rheology were 3-4 orders of magnitude smaller than the ones measured with macroscopic methods[106, 125, 126]. Samaniuk and Vermant[126] point out various reasons for this discrepancy such as tracking errors, large scale heterogeneities in the interfacial layers and dilatation effects in macroscopic measurements.

Quantitative interpretation of MSDs measured at an interface can be obscured by several issues: besides the already mentioned mechanical contributions of the bulk liquid phases [127], there can also be uncertainties about how the probe is mechanically coupled to its environment, and how the probe volume is distributed over the two phases[128]. Also the lack of a single model to extract mechanical properties of the layer from the particle trajectories has been pointed out[106]. Different equations exist for

specific cases. This underlines that truly quantitative information about material properties of the layer cannot be expected by default. New variants of the method are still being explored, e.g. by Shlomovitz *et al.*[128], who choose to not immerse the probe particles inside the layer but close to it. Also two point interfacial micro-rheology has been applied in one study[129].

Attractive sides of interfacial particle tracking are the relative ease of doing the experiment and the sensitivity that can be obtained by using small probe particles: the more contact between the probe and the matrix, the less 'background signal' is picked up by the measurement (as expressed by the Boussinesq number[106]). For interfacial layers containing particles, colloidal probes might thus provide the best possible tuning between probe size and layer thickness.

The Particle Tracking method could also be attractive for specific types of interfacial layers. In particular, interfacial layers of soft microgels should be easier to study than layers of hard particles: Due to the polymer-like character, the mesh size (i.e. minimum length scale) of the interfacial layer will be much smaller than that of the microgel particles themselves[46], allowing for a broad range of probe particle sizes. In contrast, interfacial layers of hard particles will require much larger probe particles (in view of the 'mesh size') which in turn can cause new problems like very small displacements or additional contributions due to capillary effects (for micron-sized particles). The first success of interfacial particle tracking rheology was demonstrated by Cohin *et al.*[39] who simply calculated an interfacial diffusion coefficient for PNIPAM at an air-water interface. In this way, they were able to quantify the weight fraction at which dynamic arrest occurred at the interface.

2.4.3 Rheology of particle laden interfaces

Dilatational rheology

Most of the experimental studies on particle-laden interfaces have focused on silica (with or without surfactants) or latex particles. Experimental work in this area has been carried out mainly in the past decade; earlier

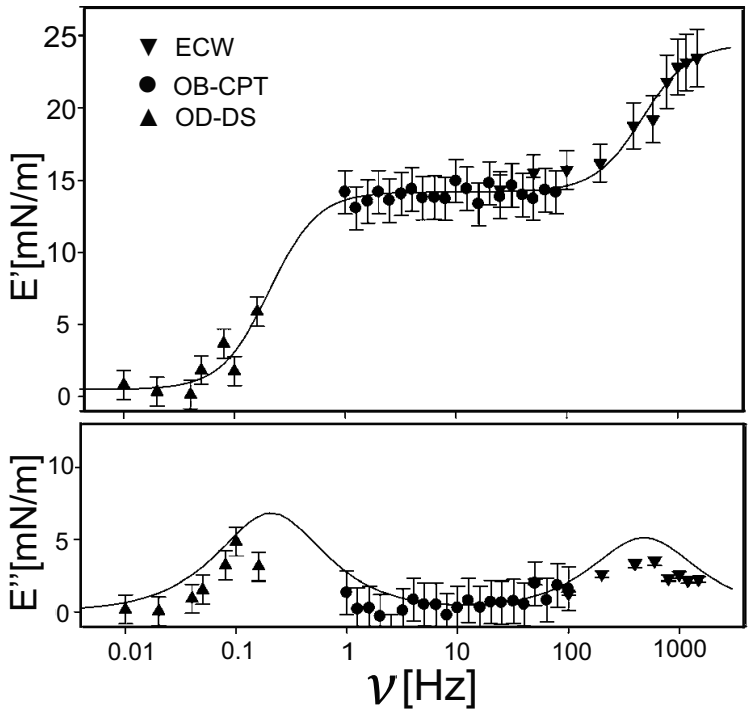

Figure 2.4: Elastic(top) and viscous(bottom) contributions to the dilatational viscoelastic moduli for 1%w/w silica particles with 0.1mM CTAB at an air-water interface. Different symbols indicate different experimental techniques. Solid lines are theoretical predictions by Ravera *et al.*[131]. Reproduced from Liggieri *et al.*[132] with permission from RSC.

contributions include those by Tambe and Sharma[101]. The theoretical framework for dilatational rheology of a system of particle with or without surfactants was given by Miller *et al.*[130].

Safouane *et al.*[133] studied the dilatational rheology of fumed silica particle monolayers at an air-water interface using the capillary wave technique. They reported that the storage modulus was always greater than

the loss modulus, irrespective of the particle hydrophobicity or the surface coverage of the interface by particles. The elastic moduli increased as the surface of the silica particles was grafted with an increasing number of (hydrophobic) methyl groups. Dilatational rheology of surfactant-decorated silica monolayers has been examined in several studies, due to the ability of these systems to form extremely stable foams and emulsions. Ravera *et al.*[53] investigated the adsorption properties and dilatational rheology of silica particles with CTAB at both air-water and oil-water interface in the low frequency range (0.005-0.2 Hz) using the oscillating drop method. They found that the surfactant formed complexes with the silica particles, thus fostering their adsorption to the interface. The elastic moduli for surfactant+particle layers were always higher than those of pure surfactant layers adsorbed on the interface. Furthermore, particle + surfactant layers formed at an oil-water interface were more elastic than similar layers formed at an air-water interface. This work was extended to higher frequencies by using other techniques like Capillary Pressure Tensiometry (CPT)[131]. Liggieri *et al.*[132] studied the same system using 3 different techniques: Oscillating Barrier, CPT and Elastocapillary Waves. This enabled them to probe the response of silica+surfactant interfacial layers over an unprecedented range of frequencies (10^{-2} – 10^{3}Hz). The experimental data obtained by these 3 techniques agreed very well, and when analysed in the theoretical framework developed previously [131] they revealed different relaxation mechanisms associated with different characteristic frequencies. The relaxation at low frequencies was governed by the diffusion of particles towards the interface and at high frequencies by surface kinetic processes like molecular reorientation, aggregation or chemical reactions. For charged Poly(Styrene) latex particles, it was reported that they formed elastic monolayers even at low surface coverage[134]. The linear regime was very small and experiments had to be performed at low frequencies. Dilatational rheology of PS latex particles at an air-water interface was carried out by Kobayashi and Kawaguchi[135], using the Oscillating Barrier technique at very low frequencies. They reported a crossover from a viscous to an elastic regime at frequencies of around 12 mHz. In their recent work on dilatational rheology of spread monolayers

of PS particles, Bykov *et al.*[136] report that the entire range of surface pressure-area isotherms can be divided into three zones. First one is characterised by a relatively low surface elasticity (< 50mN/m) that is a result of electrostatic interactions. In the second region, the surface elasticity is extremely high (~500 mN/m) due to strong hydrophobic attraction. Finally in the third region, the collapse and folding of the monolayer results in an almost zero surface elasticity.

Shear Rheology

Safouane *et al.*[133] in their work on fumed silica particles of varying hydrophobicity at an air-water interface, reported that the shear moduli of silica monolayers were small and dependent on the particle wettability. At low hydrophobicity the layers had negligible shear moduli whereas for very hydrophobic particles, $G' > G''$. The authors defined a gel point at intermediate hydrophobicity where $G' = G''$. This work was extended by Zang *et al.*[137, 138], who showed that the behaviour of a 2D layer is similar to that of a 3D soft solid, characterized by a decrease in the structural relaxation time with increasing strain amplitude. They also applied the Strain-Rate-Frequency-Superposition (SRFS) principle developed for 3D systems by Wyss *et al.*[139], to interfacial measurements. The relaxation time scaled inversely with shear-rate. Silica particles in combination with various lipids were studied by Maas *et al.*[73]. They concluded that particles + lipid layers at the oil-water interface were elastic in nature with a very small critical strain (i.e. a brittle network).

Silver nanoparticles at a toluene-water interface exhibited a frequency independent elastic response at low frequencies[140]. Amplitude sweep measurements showed shear thinning at large strain amplitudes. Steady shear measurements revealed a finite yield stress. All of these are characteristics of a 2D soft glassy material. In contrast to these findings, gold nanoparticles at air-water interface showed a gel-like behaviour[141]. The viscoelastic moduli increased with the particle coverage, following a power law behaviour that was correlated to percolation phenomena. The storage modulus was independent of frequency whereas the loss modulus

increased at higher frequencies.

Charged polystyrene latex particles surprisingly showed a completely different behaviour. Cicuta *et al.*[142] found the interfacial layers of these particles to exhibit a viscous behaviour ($G'' > G'$), with increasing moduli as the surface coverage increased. In the same study these authors also compared the interfacial rheology of latex particles (hard disk-like) and β-lactoglobulin (soft, deformable disk-like) systems and concluded that the viscoelastic response of systems with very different interaction potentials was similar. In their recent study, Barman and Christopher [143] performed shear rheology using a double wall ring geometry and simultaneously observed the interfacial micro-structure. They find that at high surface coverages the interface undergoes a transition from shear thinning to a yielding behaviour. Surprisingly this transition occurs much before the maximum coverage is reached indicating that the yielding does not necessarily require a fully jammed interface. These findings highlight the fact that interfacial rheological measurements must always be carefully evaluated.

As a general remark about interfacial rheology of stiff particles at interface, we can say that the dilatational rheological studies of particle monolayers at interface show a very small linear viscoelastic range, whereas the deformations that occur in most real life scenarios are much higher. This points towards a need of non-linear rheological study of interfacial particulate layers. Shear rheology suggest that the surface elasticity is strongly dependent on the surface concentration of particles. Jamming of particles at the interface is an aspect that could be a possible area of interest in the near future.

2.4.4 Rheology of microgel laden interfaces

Microgels have recently garnered a lot of attention from the scientific community as possible emulsion stabilizers. Yet the interfacial rheology of microgel layers at fluid-fluid interfaces and its effect on emulsion stability has not received much attention. The first systematic study was carried out by Brugger *et al.*[92], who used the oscillating drop technique

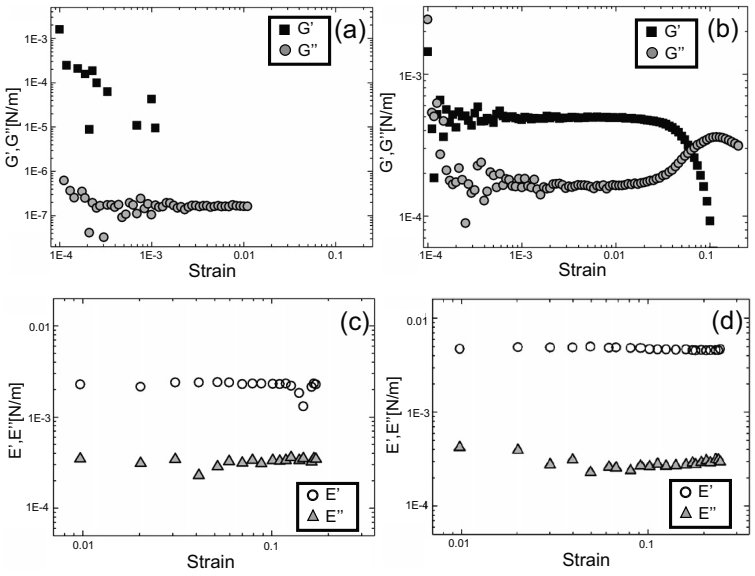

Figure 2.5: The visocleastic moduli of PNIPAM-co-MAA microgel layers at heptane-water interface. Viscoelastic shear moduli as a function of strain amplitude at (a)pH 3 and (b)pH 9. Viscoelastic dilatational moduli as a function of strain amplitude at (c)pH 2.8 and (d)pH 9.2. Figures taken from[144] with permission from RSC.

to study layers of PNIPAM-co-MAA microgel particles at a heptane-water interface. They evaluated the effect of both pH and temperature on the dilatational viscoelastic moduli. At low temperature and high pH, the interface was found to be predominantly elastic. Addition of acid reduced the Coulombic repulsion and consequently the storage modulus also decreased. Increasing the temperature above the VPTT caused a dramatic increase in the loss modulus. This work was complemented by considering the effect of pH on shear rheology, dilation rheology and compression behaviour for a similar system. The effect of the pH on the interfacial rheological properties was substantiated by the cryo-SEM images of the interfacial layer taken at different pH. At high pH where the particles are

charged, the interface exhibited a soft gel-like structure that gave rise to an elastic response to mechanical deformation. However at low pH where the charge on the particles is lower, the resultant layer was compact and brittle (i.e. breaking easily upon deformation). Recently Cohin *et al.*[39] looked at the interfacial dynamics of microgels using particle tracking. They found that the motion of particles at the interface was arrested even at very low bulk concentrations of PNIPAM particles.

It is clear that many insights are still lacking regarding interfacial rheology of PNIPAM microgel layers. Clearly, the stimuli responsive nature of these particles results in a rich behaviour with morphological transformations that can have interesting consequences for the interfacial rheology. Also the non-aqueous phase, whether it is air or oil (and in case of oil: polar or non-polar) has an effect on the interfacial rheology[34]. However, the details of the interplay between electrostatic, elastic and hydrophilic/hydrophobic interactions still have to be resolved. The mathematical modelling of these interactions and their relation to the macroscopic interfacial rheological properties is also still missing. Interfacial micro-rheological investigations supported by appropriate theoretical analysis could provide some interesting insights in this regard.

2.5 Interfacial assembly and emulsion stabilization

Ultimately, the acquired insights on the interfacial adsorption, the particle interactions (in bulk and at the interface) and the rheology of the layer, have to be combined to understand the stability of particle-stabilized emulsions. The most common explanation for the stability of Pickering emulsions is the steric hindrance provided by the particulate layer. However, some studies have also attributed emulsion stability to the slow thinning of liquid films between the drops[101], or the interfacial rheological properties of the particle layer[147–150]. Several excellent scientific studies on isolated mechanisms have appeared in the past 15 years[6, 12, 64, 151–156]. However, due to the variability of the systems,

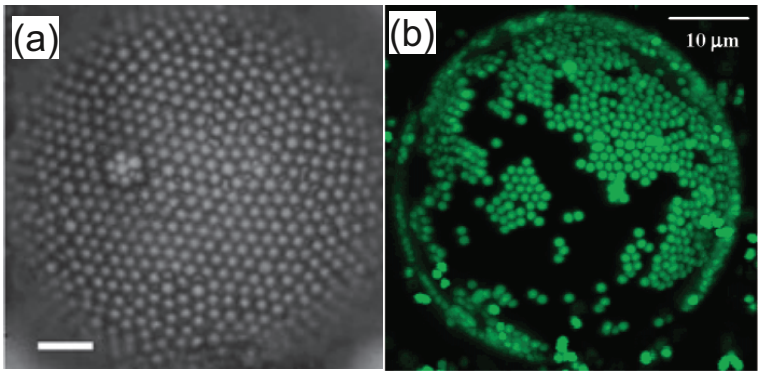

Figure 2.6: (a)Drop of hexadecane in 1M aqueous NaCl solution stabilized by densely packed layer of 3.2μm diameter carboxyl-coated PS latex particles. Image taken from Binks *et al.*[145] with permission from Wiley and (b)Drop of poly(dimethylsiloxane) in water stabilized by 1μm PS latex particles. Image reprinted from Tarimala and Dai[146] (scale bars for both images =10μm)

mechanistic explanations of the stability of Pickering emulsions may still differ from system to system.

For this reason, many formulations are still empirical in nature, or make use of just some basic principles. For example, using the fact that particles adsorb irreversibly to a liquid-liquid interface, emulsions with very narrow droplet size distribution have been obtained, utilizing the phenomenon called limited coalescence[157, 158]. Here a very large oil-water interfacial area is produced by shaking a mixture of oil, water and particles vigorously. When the shaking stops, insufficiently covered drops coalesce until the drops are sufficiently covered with particles. The final drop diameter (D) was found to be related to the total number of particles in the system (n) and their coverage (C) by the following relation:

$$\frac{1}{D} = \frac{n\pi d_p^2}{24CV_d} \tag{2.17}$$

Where d_p is the particle diameter and V_d is the dispersed phase volume. The coverage C, defined as the ratio of surface covered by particles to the

total interfacial area, thus contains some information about the packing of the (hard) particles at the interface. For an ideal case when the droplet is covered by a uniform densely packed layer of particles as shown in fig 6(a)[145], C is close to 0.9. On the other hand in other studies on hard particles it has been found that sparsely covered droplets can be stable too (as shown in fig 6(b)[[146] where $C < 0.9$), indicating that interactions other than excluded volume type could play a role and even dominate. The stability of the sparsely droplets could be explained by a possible formation of network structure at the interface or due to the formation of single or double layered bridge at the droplet contact area[159]. Another possible explanation is that the stability of these sparsely covered droplets is governed by electrostatics and is due to preferential localisation of particles at the droplet junctions[160].

Microgel particles differ fundamentally from hard particles, regarding their interfacial assembly. They are inherently surface active, and they readily adsorb to the interface. As a consequence, dense layers are formed very easily. This was first noticed by Ngai *et al.*[36] in their freeze-fracture SEM images of PNIPAM-co-MAA stabilized toluene-water emulsions. Using cryo-Field Emission Scanning Electron Microscopy (Cryo-FESEM), Schmidt *et al.*[34] showed that it was not electrostatic interactions but the soft, deformable nature of the microgel particles that was responsible for the stability of emulsions. Destribats *et al.*[161, 162] used cryo-SEM to show that the microgels were substantially deformed at the interface. (Also see fig 7)

They formed hexagonally packed ordered layers at the interface and adopted a unique structure with a protruding core and a flat shell made out of long ramified digitations that covered the remaining part of the interface. The authors attributed this "fried egg-like" morphology to the uneven distribution of crosslinker within the microgels. The same authors also studied water in oil emulsions[162] and showed that inverse emulsions were stabilized by multilayers of undeformed microgels located inside the aqueous phase. First attempts at revealing the conformations of particles in 3D were made by Geisel *et al.*[94] using freeze-fracture shadow-casting cryo SEM (FreSCa). They reported the particles to be substantially flat-

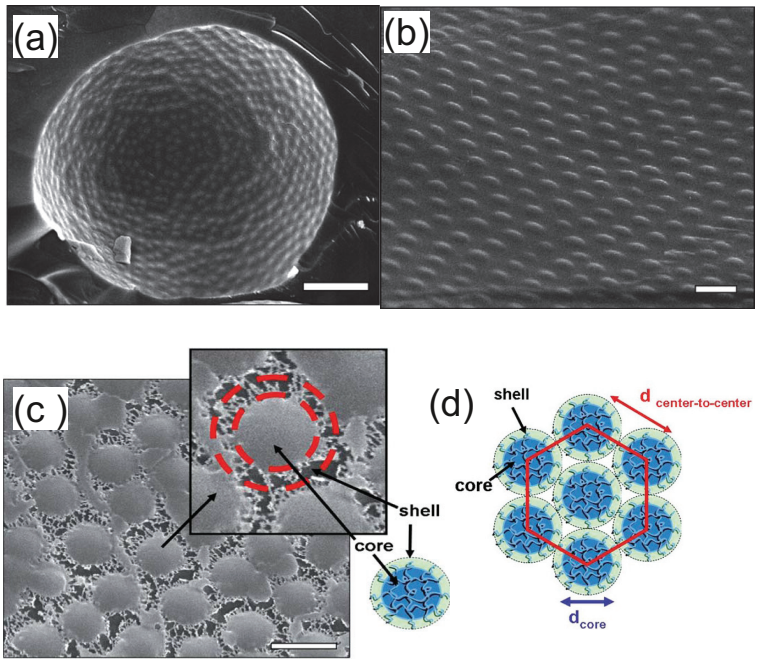

Figure 2.7: Cryo-SEM images of dodecane drops covered with microgel particles (a) large view of the drop (scale bar =5μm) (b) Close up view of the same droplet showing the lens shaped flattened morphology of the particles. (scale bar =1μm) (c) Close packed hexagonal structure formed by microgel particles at heptane-water interface and (scale bar =1μm) (d) Schematic of the structure and arrangement of particles at the interface. Images reprinted from Destribats *et al.*[161] with permission from RSC.

tened with an internal core that protruded slightly into the oil phase. Surprisingly this protrusion height was independent of pH. In summary, particle self-assembly at interface is an important factor that governs the stability of emulsions. Both in case of hard and soft particles, the resistance to coalescence arise due to the presence of a continuous elastic layer of closely packed particles at the interface. For microgel particles, the deformation of these particles at the interface gives rise to interesting

mesostructures that ultimately help in stabilizing these emulsions.

2.6 Conclusion and Outlook

The stability of Pickering emulsions is caused by the permanent adsorption of solid particles onto a fluid-fluid interface. Soft microgels represent a class of its own in the area of colloidal particles. Their ability to swell and shrink upon thermal or chemical triggers and the incorporation of functional co-monomers makes them very well suited for a variety of applications. In the past 5 years their high potential as stabilizers for emulsions and foams has been picked up by researchers worldwide. Their practical efficacy as stabilizers has been demonstrated, and some major steps have already been made in understanding their adsorption behaviour, interactions, assembly and mechanical properties. The adsorption of soft polymeric microgels (at air-water or oil-water interfaces) is clearly distinguished from that of hard colloidal particles. Owing to their polymer character, microgels can adsorb in small steps, without the need to overcome high adsorption barriers as found for hard particles. Yet in the end, also the adsorption of the microgels is irreversible.

An important deficiency in the adsorption kinetics studies, that was hitherto unnoticed, is the improper usage of the equation of state to relate the surface pressure and adsorption. Latest studies in this regard indicate a need to revisit the previous studies with a new perspective.

The interactions between adsorbed microgels are fundamentally different from that of hard particles: whereas for the latter, the (sometimes complex) electrostatic contributions are often dominant, for many microgel systems they appear to play a more modest role. Often both the Van der Waals attractions and the electrostatic repulsions are weak for microgel particles, making their deformability more important.

The ability of interfacial microgels to either stretch or compress itself, depending on the chemical environment and external mechanical load, has only been modestly explored. This probably will be an important direction for further research into interfacial microgels in the coming years.

The ongoing and future effort should strongly benefit also from (the latest developments in) optical and rheological techniques such as Cryo-scanning electron microscopy and ellipsometry. Interfacial micro-rheology will be an indispensable tool to increase our understanding of how interfacial microgels deform under different conditions: from the stretch or compression of individual particles during adsorption, to the viscoelastic response of an entire layer under different dynamic conditions (time scale, strain amplitude), including those that pertain to potential coalescence events. Interfacial rheology on particle layers can involve delicate experiments, and interpretation may provide issues, especially for some micro-rheological techniques (which are still under development). Combination of different interfacial rheological experiments, with some overlap between measuring regimes, is therefore recommended.

The way particles adsorb and arrange at the interface directly impacts the mechanical strength of the interfacial layers and consequently the stability of emulsions. Microgel stabilized emulsions are a result of an intricate interplay between various parameters. A small change in any one of the parameters can lead to drastically different end results in terms of interfacial properties and/or emulsion stability. This makes it rather difficult to characterize them in a generalized framework. But on the positive side, it also enables formulation of systems that can be tailor-made to suit very specific applications.

Bibliography

[1] P. Becher. *Encyclopedia of Emulsion Technology*, volume 1. Marcel Dekker, New York, 1983.

[2] J. Sjoblom. *Encyclopedic Handbook of Emulsion Technology*. Marcel Dekker, New York, 2001.

[3] J. Bibette, F. L. Calderon, and P. Poulin. Emulsions: basic principles. *Reports on Progress in Physics*, 62(6):969–1033, 1999.

[4] T. N. Hunter, R. J. Pugh, G. V. Franks, and G. J. Jameson. The role of particles in stabilising foams and emulsions. *Advances in Colloid and Interface Science*, 137(2):57–81, 2008.

[5] T. G. Mason. New fundamental concepts in emulsion rheology. *Current Opinion in Colloid & Interface Science*, 4(3):231–238, 1999.

[6] S. Sacanna, W. K. Kegel, and A. P. Philipse. Thermodynamically stable pickering emulsions. *Physical Review Letters*, 98(15), 2007.

[7] C. Stubenrauch and R. von Klitzing. Disjoining pressure in thin liquid foam and emulsion films - new concepts and perspectives. *Journal of Physics-Condensed Matter*, 15(27):R1197–R1232, 2003.

[8] Spencer Umfreville Pickering. Cxcvi.-emulsions. *Journal of the Chemical Society, Transactions*, 91(0):2001–2021, 1907.

[9] W. Ramsden. Separation of solids in the surface-layers of solutions and 'suspensions' (observations on surface-membranes, bubbles, emulsions, and mechanical coagulation). – preliminary account. *Proceedings of the Royal Society of London*, 72(477-486):156–164, 1903.

[10] Bernard P. Binks. Particles as surfactants—similarities and differences. *Current Opinion in Colloid & Interface Science*, 7(1–2):21–41, 2002.

[11] Stéphane Arditty, Véronique Schmitt, Joanna Giermanska-Kahn, and Fernando Leal-Calderon. Materials based on solid-stabilized emulsions. *Journal of Colloid and Interface Science*, 275(2):659–664, 2004.

[12] R. Aveyard, B. P. Binks, and J. H. Clint. Emulsions stabilised solely by colloidal particles. *Advances in Colloid and Interface Science*, 100:503–546, 2003.

[13] Eric Dickinson. Faraday research article. structure and composition of adsorbed protein layers and the relationship to emulsion stability. *Journal of the Chemical Society, Faraday Transactions*, 88(20):2973–2983, 1992.

[14] Eric Dickinson. Hydrocolloids as emulsifiers and emulsion stabilizers. *Food Hydrocolloids*, 23(6):1473–1482, 2009.

[15] Peter Wilde, Alan Mackie, Fiona Husband, Patrick Gunning, and Victor Morris. Proteins and emulsifiers at liquid interfaces. *Advances in Colloid and Interface Science*, 108–109(0):63–71, 2004.

[16] Bernard Binks and Tommy Hozorov. *Colloidal Particles at Liquid Interfaces*. Cambridge University Press, New York, 2006.

[17] K. Du, E. Glogowski, T. Emrick, T. P. Russell, and A. D. Dinsmore. Adsorption energy of nano- and microparticles at liquid-liquid interfaces. *Langmuir*, 26(15):12518–12522, 2010.

[18] A. Stocco, W. Drenckhan, E. Rio, D. Langevin, and B. P. Binks. Particle-stabilised foams: an interfacial study. *Soft Matter*, 5(11):2215–2222, 2009.

[19] D. Y. Zang, A. Stocco, D. Langevin, B. B. Wei, and B. P. Binks. An ellipsometry study of silica nanoparticle layers at the water surface. *Physical Chemistry Chemical Physics*, 11(41):9522–9529, 2009.

[20] B. J. Park, J. Vermant, and E. M. Furst. Heterogeneity of the electrostatic repulsion between colloids at the oil-water interface. *Soft Matter*, 6(21):5327–5333, 2010.

[21] R. Aveyard, B. P. Binks, J. H. Clint, P. D. I. Fletcher, T. S. Horozov, B. Neumann, V. N. Paunov, J. Annesley, S. W. Botchway, D. Nees, A. W. Parker, A. D. Ward, and A. N. Burgess. Measurement of long-range repulsive forces between charged particles at an oil-water interface. *Physical Review Letters*, 88(24), 2002.

[22] K. Masschaele, B. J. Park, E. M. Furst, J. Fransaer, and J. Vermant. Finite ion-size effects dominate the interaction between charged colloidal particles at an oil-water interface. *Physical Review Letters*, 105(4):4, 2010.

[23] R. McGorty, J. Fung, D. Kaz, and V. N. Manoharan. Colloidal self-assembly at an interface. *Materials Today*, 13(6):34–42, 2010.

[24] D. Ershov, J. Sprakel, J. Appel, M. A. C. Stuart, and J. van der Gucht. Capillarity-induced ordering of spherical colloids on an interface with anisotropic curvature. *Proceedings of the National Academy of Sciences of the United States of America*, 110(23):9220–9224, 2013.

[25] P. A. Kralchevsky, I. B. Ivanov, K. P. Ananthapadmanabhan, and A. Lips. On the thermodynamics of particle-stabilized emulsions: Curvature effects and catastrophic phase inversion. *Langmuir*, 21(1):50–63, 2005.

[26] D. M. Kaz, R. McGorty, M. Mani, M. P. Brenner, and V. N. Manoharan. Physical ageing of the contact line on colloidal particles at liquid interfaces. *Nature Materials*, 11(2):138–142, 2012.

[27] M. G. Nikolaides, A. R. Bausch, M. F. Hsu, A. D. Dinsmore, M. P. Brenner, D. A. Weitz, and C. Gay. Electric-field-induced capillary attraction between like-charged particles at liquid interfaces. *Nature*, 420(6913):299–301, 2002.

[28] Brian R. Saunders and Brian Vincent. Microgel particles as model colloids: theory, properties and applications. *Advances in Colloid and Interface Science*, 80(1):1–25, 1999.

[29] H. Senff and W. Richtering. Influence of cross-link density on rheological properties of temperature-sensitive microgel suspensions. *Colloid and Polymer Science*, 278(9):830–840, 2000.

[30] Ying Guan and Yongjun Zhang. Pnipam microgels for biomedical applications: from dispersed particles to 3d assemblies. *Soft Matter*, 7(14):6375–6384, 2011.

[31] Christine Schwall and Ipsita Banerjee. Micro- and nanoscale hydrogel systems for drug delivery and tissue engineering. *Materials*, 2(2):577–612, 2009.

[32] Justin D. Debord and L. Andrew Lyon. Synthesis and characterization of ph-responsive copolymer microgels with tunable volume phase transition temperatures. *Langmuir*, 19(18):7662–7664, 2003.

[33] L. Andrew Lyon and Alberto Fernandez-Nieves. The polymer/colloid duality of microgel suspensions. *Annual Review of Physical Chemistry*, 63(1):25–43, 2012.

[34] Sabrina Schmidt, Tingting Liu, Stephan Rutten, Kim-Ho Phan, Martin Moller, and Walter Richtering. Influence of microgel architecture and oil polarity on stabilization of emulsions by stimuli-sensitive core–shell poly(n-isopropylacrylamide-co-methacrylic acid) microgels: Mickering versus pickering behavior? *Langmuir*, 27(16):9801–9806, 2011.

[35] Zifu Li, Karen Geisel, Walter Richtering, and To Ngai. Poly(n-isopropylacrylamide) microgels at the oil-water interface: adsorption kinetics. *Soft Matter*, 9(41):9939–9946, 2013.

[36] To Ngai, Sven Holger Behrens, and Helmut Auweter. Novel emulsions stabilized by ph and temperature sensitive microgels. *Chemical Communications*, (3):331–333, 2005.

[37] To Ngai, Helmut Auweter, and Sven Holger Behrens. Environmental responsiveness of microgel particles and particle-stabilized emulsions. *Macromolecules*, 39(23):8171–8177, 2006.

[38] S. Tsuji and H. Kawaguchi. Thermosensitive pickering emulsion stabilized by poly(n-isopropylacrylamide)-carrying particles. *Langmuir*, 24(7):3300–3305, 2008.

[39] Yann Cohin, Maelle Fisson, Kévin Jourde, Gerald G Fuller, Nicolas Sanson, Laurence Talini, and Cécile Monteux. Tracking the interfacial dynamics of pnipam soft microgels particles adsorbed at the air–water interface and in thin liquid films. *Rheologica Acta*, 52(5):445–454, 2013.

[40] R. Miller and L. Liggieri. *Interfacial Rheology*. CRC Press, 2009.

[41] Sultana Ferdous, MariosA Ioannidis, and Dale Henneke. Adsorption kinetics of alkanethiol-capped gold nanoparticles at the hexane–water interface. *Journal of Nanoparticle Research*, 13(12):6579–6589, 2011.

[42] Sultana Ferdous, MariosA Ioannidis, and DaleE Henneke. Effects of temperature, ph, and ionic strength on the adsorption of nanoparticles at liquid–liquid interfaces. *Journal of Nanoparticle Research*, 14(5):1–12, 2012.

[43] M. Jeribi, B. Almir-Assad, D. Langevin, I. Hénaut, and J. F. Argillier. Adsorption kinetics of asphaltenes at liquid interfaces. *Journal of Colloid and Interface Science*, 256(2):268–272, 2002.

[44] S. Kutuzov, J. He, R. Tangirala, T. Emrick, T. P. Russell, and A. Boker. On the kinetics of nanoparticle self-assembly at liquid/liquid interfaces. *Physical Chemistry Chemical Physics*, 9(48):6351–6358, 2007.

[45] Jayant P. Rane, David Harbottle, Vincent Pauchard, Alexander Couzis, and Sanjoy Banerjee. Adsorption kinetics of asphaltenes at

the oil–water interface and nanoaggregation in the bulk. *Langmuir*, 28(26):9986–9995, 2012.

[46] Omkar S. Deshmukh, Armando Maestro, Michel H. G. Duits, Dirk van den Ende, Martien Cohen Stuart, and Frieder Mugele. Equation of state and adsorption dynamics of soft microgel particles at an air-water interface. *Soft Matter*, 10:7045–7050, 2014.

[47] J. K. Beattie and A. Gray-Weale. Oil/water interface charged by hydroxide ions and deprotonated fatty acids: A comment. *Angewandte Chemie-International Edition*, 51(52):12941–12942, 2012.

[48] K. C. Jena, R. Scheu, and S. Roke. Surface impurities are not responsible for the charge on the oil/water interface: A comment. *Angewandte Chemie-International Edition*, 51(52):12938–12940, 2012.

[49] K. Roger and B. Cabane. Why are hydrophobic/water interfaces negatively charged? *Angewandte Chemie-International Edition*, 51(23):5625–5628, 2012.

[50] Sarah L. Kettlewell, Andreas Schmid, Syuji Fujii, Damien Dupin, and Steven P. Armes. Is latex surface charge an important parameter for foam stabilization? *Langmuir*, 23(23):11381–11386, 2007.

[51] Huan Ma, Mingxiang Luo, and Lenore L. Dai. Influences of surfactant and nanoparticle assembly on effective interfacial tensions. *Physical Chemistry Chemical Physics*, 10(16):2207–2213, 2008.

[52] Armando Maestro, Emmanuelle Rio, Wiebke Drenckhan, Dominique Langevin, and Anniina Salonen. Foams stabilised by mixtures of nanoparticles and oppositely charged surfactants: relationship between bubble shrinkage and foam coarsening. *Soft Matter*, 2014.

[53] Francesca Ravera, Eva Santini, Giuseppe Loglio, Michele Ferrari, and Libero Liggieri. Effect of nanoparticles on the interfacial properties of liquid/liquid and liquid/air surface layers. *The Journal of Physical Chemistry B*, 110(39):19543–19551, 2006.

[54] A. N. Wang, D. M. Kaz, R. McGorty, and V. N. Manoharan. Relaxation dynamics of colloidal particles at liquid interfaces. In Dynam Res Trans-disciplinary Flow and Inst Fluid Sci Gcoe Tohoku Univ, editors, *4th International Symposium on Slow Dynamics in Complex Systems*, volume 1518 of *AIP Conference Proceedings*, pages 336–343, 2013.

[55] A. F. H. Ward and L. Tordai. Timedependence of boundary tensions of solutions i. the role of diffusion in timeeffects. *The Journal of Chemical Physics*, 14(7):453–461, 1946.

[56] Hernán Ritacco, Dominique Langevin, Haim Diamant, and David Andelman. Dynamic surface tension of aqueous solutions of ionic surfactants: Role of electrostatics. *Langmuir*, 27(3):1009–1014, 2011.

[57] Z. Adamczyk and P. Warszynski. Role of electrostatic interactions in particle adsorption. *Advances in Colloid and Interface Science*, 63:41–149, 1996.

[58] Z. Adamczyk. Particle adsorption and deposition: role of electrostatic interactions. *Advances in Colloid and Interface Science*, 100:267–347, 2003.

[59] N. Bizmark, M. A. Ioannidis, and D. E. Henneke. Irreversible adsorption-driven assembly of nanoparticles at fluid interfaces revealed by a dynamic surface tension probe. *Langmuir*, 30(3):710–717, 2014.

[60] Robert Aveyard, John H. Clint, Dieter Nees, and Vesselin N. Paunov. Compression and structure of monolayers of charged la-

tex particles at air/water and octane/water interfaces. *Langmuir*, 16(4):1969–1979, 2000.

[61] Plamen V. Petkov, Krassimir D. Danov, and Peter A. Kralchevsky. Surface pressure isotherm for a monolayer of charged colloidal particles at a water/nonpolar-fluid interface: Experiment and theoretical model. *Langmuir*, 30(10):2768–2778, 2014.

[62] J. Lyklema. *Fundamentals of Interface and Colloid Science: Particulate Colloids*, volume IV. Academic Press, 2005.

[63] W.B. Russel, D.A. Saville, and W.R. Schowalter. *Colloidal Dispersions*. Cambridge University Press, 1989.

[64] M. E. Leunissen, J. Zwanikken, R. van Roij, P. M. Chaikin, and A. van Blaaderen. Ion partitioning at the oil-water interface as a source of tunable electrostatic effects in emulsions with colloids. *Physical Chemistry Chemical Physics*, 9(48):6405–6414, 2007.

[65] Adam Daniel Law. *Structure and interactions of colloidal particles at fluid interfaces*. PhD thesis, Department of Physics, University of Hull, 2011.

[66] J. Bleibel, A. Domínguez, and M. Oettel. Colloidal particles at fluid interfaces: Effective interactions, dynamics and a gravitation–like instability. *The European Physical Journal Special Topics*, 222(11):3071–3087, 2013.

[67] Alvaro Domínguez, Martin Oettel, and S. Dietrich. Force balance of particles trapped at fluid interfaces. *The Journal of Chemical Physics*, 128(11):–, 2008.

[68] Derek Frydel and Martin Oettel. Charged particles at fluid interfaces as a probe into structural details of a double layer. *Physical Chemistry Chemical Physics*, 13(9):4109–4118, 2011.

[69] Frank H. Stillinger. Interfacial solutions of the poissonboltzmann equation. *The Journal of Chemical Physics*, 35(5):1584–1589, 1961.

[70] A. J. Hurd. The electrostatic interaction between interfacial colloidal particles. *Journal of Physics a-Mathematical and General*, 18(16):1055–1060, 1985.

[71] P. Pieranski. Two-dimensional interfacial colloidal crystals. *Physical Review Letters*, 45(7):569–572, 1980.

[72] Bum Jun Park and Eric M. Furst. Optical trapping forces for colloids at the oilwater interface. *Langmuir*, 24(23):13383–13392, 2008.

[73] Michael Maas, Chin C. Ooi, and Gerald G. Fuller. Thin film formation of silica nanoparticle/lipid composite films at the fluidfluid interface. *Langmuir*, 26(23):17867–17873, 2010.

[74] Sebastian Uppapalli and Hui Zhao. The influence of particle size and residual charge on electrostatic interactions between charged colloidal particles at an oil-water interface. *Soft Matter*, 10:4555–4560, 2014.

[75] J. Mahanty and B.W. Ninham. *Dispersion forces.* Academic Press, 1976.

[76] Dominic Vella and L. Mahadevan. The "cheerios effect". *American Journal of Physics*, 73(9):817–825, 2005.

[77] Nikolina D. Vassileva, Dirk van den Ende, Frieder Mugele, and Jorrit Mellema. Capillary forces between spherical particles floating at a liquidliquid interface. *Langmuir*, 21(24):11190–11200, 2005. PMID: 16285790.

[78] Marie-Julie Dalbe, Darija Cosic, Michael Berhanu, and Arshad Kudrolli. Aggregation of frictional particles due to capillary attraction. *Phys. Rev. E*, 83:051403, May 2011.

[79] Peter A. Kralchevsky and Kuniaki Nagayama. Capillary interactions between particles bound to interfaces, liquid films and biomembranes. *Advances in Colloid and Interface Science*, 85(2–3):145 – 192, 2000.

[80] Dimitris Stamou, Claus Duschl, and Diethelm Johannsmann. Long-range attraction between colloidal spheres at the air-water interface: The consequence of an irregular meniscus. *Phys. Rev. E*, 62:5263–5272, Oct 2000.

[81] Peter A. Kralchevsky, Nikolai D. Denkov, and Krassimir D. Danov. Particles with an undulated contact line at a fluid interface: interaction between capillary quadrupoles and rheology of particulate monolayers. *Langmuir*, 17(24):7694–7705, 2001.

[82] Krassimir D. Danov, Peter A. Kralchevsky, Boris N. Naydenov, and Günter Brenn. Interactions between particles with an undulated contact line at a fluid interface: Capillary multipoles of arbitrary order. *Journal of Colloid and Interface Science*, 287(1):121 – 134, 2005.

[83] J. C. Loudet, A. M. Alsayed, J. Zhang, and A. G. Yodh. Capillary interactions between anisotropic colloidal particles. *Phys. Rev. Lett.*, 94:018301, Jan 2005.

[84] J. C. Loudet, A. G. Yodh, and B. Pouligny. Wetting and contact lines of micrometer-sized ellipsoids. *Phys. Rev. Lett.*, 97:018304, Jul 2006.

[85] Krassimir D. Danov and Peter A. Kralchevsky. Capillary forces between particles at a liquid interface: General theoretical approach and interactions between capillary multipoles. *Advances in Colloid and Interface Science*, 154(1–2):91 – 103, 2010.

[86] Alvaro Domínguez, Martin Oettel, and S. Dietrich. Dynamics of colloidal particles with capillary interactions. *Phys. Rev. E*, 82:011402, Jul 2010.

[87] M. Karg and T. Hellweg. New "smart" poly(nipam) microgels and nanoparticle microgel hybrids: Properties and advances in characterisation. *Current Opinion in Colloid & Interface Science*, 14(6):438–450, 2009.

[88] M. Stieger, J. S. Pedersen, P. Lindner, and W. Richtering. Are thermoresponsive microgels model systems for concentrated colloidal suspensions? a rheology and small-angle neutron scattering study. *Langmuir*, 20(17):7283–7292, 2004.

[89] M. Stieger, W. Richtering, J. S. Pedersen, and P. Lindner. Small-angle neutron scattering study of structural changes in temperature sensitive microgel colloids. *Journal of Chemical Physics*, 120(13):6197–6206, 2004.

[90] H. Senff and W. Richtering. Temperature sensitive microgel suspensions: Colloidal phase behavior and rheology of soft spheres. *Journal of Chemical Physics*, 111(4):1705–1711, 1999.

[91] D. van den Ende, E. H. Purnomo, M. H. G. Duits, W. Richtering, and F. Mugele. Aging in dense suspensions of soft thermosensitive microgel particles studied with particle-tracking microrheology. *Physical Review E*, 81(1), 2010.

[92] Bastian Brugger and Walter Richtering. Emulsions stabilized by stimuli-sensitive poly(n-isopropylacrylamide)-co-methacrylic acid polymers: Microgels versus low molecular weight polymers. *Langmuir*, 24(15):7769–7777, 2008.

[93] Bastian Brugger, Brian A. Rosen, and Walter Richtering. Microgels as stimuli-responsive stabilizers for emulsions. *Langmuir*, 24(21):12202–12208, 2008.

[94] Karen Geisel, Lucio Isa, and Walter Richtering. Unraveling the 3d localization and deformation of responsive microgels at oil/water interfaces: A step forward in understanding soft emulsion stabilizers. *Langmuir*, 28(45):15770–15776, 2012.

[95] Walter Richtering. Responsive emulsions stabilized by stimuli-sensitive microgels: Emulsions with special non-pickering properties. *Langmuir*, 28(50):17218–17229, 2012.

[96] D. M. Heyes and A. C. Branka. Interactions between microgel particles. *Soft Matter*, 5(14):2681–2685, 2009.

[97] Karen Geisel, Lucio Isa, and Walter Richtering. The compressibility of ph-sensitive microgels at the oil–water interface: Higher charge leads to less repulsion. *Angewandte Chemie International Edition*, 53(19):4905–4909, 2014.

[98] Hans-Jürgen Butt. Capillary forces: influence of roughness and heterogeneity. *Langmuir*, 24(9):4715–4721, 2008.

[99] Hans-Jurgen Butt, W. Jon P. Barnes, Aranzazu del Campo, Michael Kappl, and Friedhelm Schonfeld. Capillary forces between soft, elastic spheres. *Soft Matter*, 6:5930–5936, 2010.

[100] J. Mewis and N.J. Wagner. *Colloidal Suspension Rheology*. Cambridge University Press, 2012.

[101] D. E. Tambe and M. M. Sharma. The effect of colloidal particles on fluid-fluid interfacial properties and emulsion stability. *Advances in Colloid and Interface Science*, 52:1–63, 1994.

[102] D. Langevin. Influence of interfacial rheology on foam and emulsion properties. *Advances in Colloid and Interface Science*, 88(1–2):209–222, 2000.

[103] Alma J. Mendoza, Eduardo Guzmán, Fernando Martínez-Pedrero, Hernán Ritacco, Ramón G. Rubio, Francisco Ortega, Victor M. Starov, and Reinhard Miller. Particle laden fluid interfaces: Dynamics and interfacial rheology. *Advances in Colloid and Interface Science*, 206(0):303–319, 2014.

[104] Hani Hilles, Francisco Monroy, Laura J. Bonales, Francisco Ortega, and Ramón G. Rubio. Fourier-transform rheology of polymer langmuir monolayers: Analysis of the non-linear and plastic behaviors. *Advances in Colloid and Interface Science*, 122(1–3):67–77, 2006.

[105] A. Javadi, J. Kragel, A. V. Makievski, V. I. Kovalchuk, N. M. Kovalchuk, N. Mucic, G. Loglio, P. Pandolfini, M. Karbaschi, and R. Miller. Fast dynamic interfacial tension measurements and dilational rheology of interfacial layers by using the capillary pressure technique. *Colloids and Surfaces a-Physicochemical and Engineering Aspects*, 407:159–168, 2012.

[106] F. Ortega, H. Ritacco, and R. G. Rubio. Interfacial microrheology: Particle tracking and related techniques. *Current Opinion in Colloid & Interface Science*, 15(4):237–245, 2010.

[107] Carlton F. Brooks, Gerald G. Fuller, Curtis W. Frank, and Channing R. Robertson. An interfacial stress rheometer to study rheological transitions in monolayers at the airwater interface. *Langmuir*, 15(7):2450–2459, 1999.

[108] R. Miller, R. Wustneck, J. Kragel, and G. Kretzschmar. Dilational and shear rheology of adsorption layers at liquid interfaces. *Colloids and Surfaces a-Physicochemical and Engineering Aspects*, 111(1-2):75–118, 1996.

[109] A. Maestro, F. Ortega, F. Monroy, J. Krägel, and R. Miller. Molecular weight dependence of the shear rheology of poly(methyl methacrylate) langmuir films: A comparison between two different rheometry techniques. *Langmuir*, 25(13):7393–7400, 2009.

[110] P. Cicuta and A. M. Donald. Microrheology: a review of the method and applications. *Soft Matter*, 3(12):1449–1455, 2007.

[111] F. C. MacKintosh and C. F. Schmidt. Microrheology. *Current Opinion in Colloid & Interface Science*, 4(4):300–307, 1999.

[112] D. T. Chen, E. R. Weeks, J. C. Crocker, M. F. Islam, R. Verma, J. Gruber, A. J. Levine, T. C. Lubensky, and A. G. Yodh. Rheological microscopy: Local mechanical properties from microrheology. *Physical Review Letters*, 90(10), 2003.

[113] T. Gisler and D. A. Weitz. Tracer microrheology in complex fluids. *Current Opinion in Colloid & Interface Science*, 3(6):586–592, 1998.

[114] D. Weihs, T. G. Mason, and M. A. Teitell. Bio-microrheology: A frontier in microrheology. *Biophysical Journal*, 91(11):4296–4305, 2006.

[115] T. A. Waigh. Microrheology of complex fluids. *Reports on Progress in Physics*, 68(3):685–742, 2005.

[116] A. K. Kandar, R. Bhattacharya, and J. K. Basu. Interfacial microrheology as a tool to study viscoelastic transitions in nanoconfined soft matter. *Physical Review E*, 81(4):041504, 2010.

[117] M. H. Lee, C. P. Lapointe, D. H. Reich, K. J. Stebe, and R. L. Leheny. Interfacial hydrodynamic drag on nanowires embedded in thin oil films and protein layers. *Langmuir*, 25(14):7976–7982, 2009.

[118] KyuHan Kim, Siyoung Q. Choi, Joseph A. Zasadzinski, and Todd M. Squires. Interfacial microrheology of dppc monolayers at the air-water interface. *Soft Matter*, 7(17):7782–7789, 2011.

[119] Binhua Lin, Stuart A. Rice, and D. A. Weitz. Static and dynamic evanescent wave light scattering studies of diblock copolymers adsorbed at the air/water interface. *The Journal of Chemical Physics*, 99(10):8308–8324, 1993.

[120] Andrew H. Marcus, Binhua Lin, and Stuart A. Rice. Self-diffusion in dilute quasi-two-dimensional hard sphere suspensions: Evanescent wave light scattering and video microscopy studies. *Physical Review E*, 53(2):1765–1776, 1996.

[121] T. Cherdhirankorn, V. Harmandaris, A. Juhari, P. Voudouris, G. Fytas, K. Kremer, and K. Koynov. Fluorescence correlation spectroscopy study of molecular probe diffusion in polymer melts. *Macromolecules*, 42(13):4858–4866, 2009.

[122] Prajnaparamita Dhar, Vikram Prasad, Eric R. Weeks, Thomas Bohlein, and Thomas M. Fischer. Immersion of charged nanoparticles in a salt solution/air interface. *The Journal of Physical Chemistry B*, 112(32):9565–9567, 2008.

[123] J. C. Crocker and D. G. Grier. Methods of digital video microscopy for colloidal studies. *Journal of Colloid and Interface Science*, 179(1):298–310, 1996.

[124] C. L. Wirth, E. M. Furst, and J. Vermant. Weak electrolyte dependence in the repulsion of colloids at an oil-water interface. *Langmuir*, 30(10):2670–2675, 2014.

[125] Armando Maestro, Laura J. Bonales, Hernan Ritacco, Thomas M. Fischer, Ramon G. Rubio, and Francisco Ortega. Surface rheology: macro- and microrheology of poly(tert-butyl acrylate) monolayers. *Soft Matter*, 7(17):7761–7771, 2011.

[126] Joseph Reese Samaniuk and Jan Vermant. Micro and macrorheology at fluid-fluid interfaces. *Soft Matter*, 2014.

[127] V. Prasad and E. R. Weeks. Two-dimensional to three-dimensional transition in soap films demonstrated by microrheology. *Physical Review Letters*, 102(17), 2009.

[128] R. Shlomovitz, A. A. Evans, T. Boatwright, M. Dennin, and A. J. Levine. Measurement of monolayer viscosity using noncontact microrheology. *Physical Review Letters*, 110(13), 2013.

[129] Yanmei Song and Lenore L. Dai. Two-particle interfacial microrheology at polymerpolymer interfaces. *Langmuir*, 26(16):13044–13047, 2010.

[130] R. Miller, V. B. Fainerman, V. I. Kovalchuk, D. O. Grigoriev, M. E. Leser, and M. Michel. Composite interfacial layers containing microsize and nano-size particles. *Advances in Colloid and Interface Science*, 128:17–26, 2006.

[131] Francesca Ravera, Michele Ferrari, Libero Liggieri, Giuseppe Loglio, Eva Santini, and Alessandra Zanobini. Liquid–liquid interfacial properties of mixed nanoparticle–surfactant systems. *Colloids and Surfaces A: Physicochemical and Engineering Aspects*, 323(1–3):99–108, 2008.

[132] L. Liggieri, E. Santini, E. Guzman, A. Maestro, and F. Ravera. Wide-frequency dilational rheology investigation of mixed silica nanoparticle-ctab interfacial layers. *Soft Matter*, 7(17):7699–7709, 2011.

[133] M. Safouane, D. Langevin, and B. P. Binks. Effect of particle hydrophobicity on the properties of silica particle layers at the airwater interface. *Langmuir*, 23(23):11546–11553, 2007.

[134] L. J. Bonales, J. E. F. Rubio, H. Ritacco, C. Vega, R. G. Rubio, and F. Ortega. Freezing transition and interaction potential in monolayers of microparticles at fluid interfaces. *Langmuir*, 27(7):3391–3400, 2011.

[135] Toshio Kobayashi and Masami Kawaguchi. Surface dilational moduli of latex-particle monolayers spread at air–water interface. *Journal of Colloid and Interface Science*, 390(1):147–150, 2013.

[136] A. G. Bykov, B. A. Noskov, G. Loglio, V. V. Lyadinskaya, and R. Miller. Dilational surface elasticity of spread monolayers of polystyrene microparticles. *Soft Matter*, 10:6499–6505, 2014.

[137] D. Y. Zang, E. Rio, G. Delon, D. Langevin, B. Wei, and B. P. Binks. Influence of the contact angle of silica nanoparticles at the air–water interface on the mechanical properties of the layers composed of these particles. *Molecular Physics*, 109(7-10):1057–1066, 2011.

[138] D. Y. Zang, E. Rio, D. Langevin, B. Wei, and B. P. Binks. Viscoelastic properties of silica nanoparticle monolayers at the air-water interface. *The European Physical Journal E*, 31(2):125–134, 2010.

[139] Hans M. Wyss, Kunimasa Miyazaki, Johan Mattsson, Zhibing Hu, David R. Reichman, and David A. Weitz. Strain-rate frequency superposition: A rheological probe of structural relaxation in soft materials. *Physical Review Letters*, 98(23):238303, 2007.

[140] Rema Krishnaswamy, Sayantan Majumdar, Rajesh Ganapathy, Ved Varun Agarwal, A. K. Sood, and C. N. R. Rao. Interfacial rheology of an ultrathin nanocrystalline film formed at the liquid/liquid interface. *Langmuir*, 23(6):3084–3087, 2007.

[141] Davide Orsi, Giacomo Baldi, Pietro Cicuta, and Luigi Cristofolini. On the relation between hierarchical morphology and mechanical properties of a colloidal 2d gel system. *Colloids and Surfaces A: Physicochemical and Engineering Aspects*, 413(0):71–77, 2012.

[142] Pietro Cicuta, Edward J. Stancik, and Gerald G. Fuller. Shearing or compressing a soft glass in 2d: Time-concentration superposition. *Physical Review Letters*, 90(23):236101, 2003.

[143] Sourav Barman and Gordon F. Christopher. Simultaneous interfacial rheology and microstructure measurement of densely aggregated particle laden interfaces using a modified double wall ring interfacial rheometer. *Langmuir*, 0(0):null, 0.

[144] Bastian Brugger, Jan Vermant, and Walter Richtering. Interfacial layers of stimuli-responsive poly-(n-isopropylacrylamide-co-methacrylicacid) (pnipam-co-maa) microgels characterized by interfacial rheology and compression isotherms. *Physical Chemistry Chemical Physics*, 12(43):14573–14578, 2010.

[145] Bernard P. Binks and Jhonny A. Rodrigues. Inversion of emulsions stabilized solely by ionizable nanoparticles. *Angewandte Chemie International Edition*, 44(3):441–444, 2005.

[146] Sowmitri Tarimala and Lenore L. Dai. Structure of microparticles in solid-stabilized emulsions. *Langmuir*, 20(9):3492–3494, 2003.

[147] David E. Tambe and Mukul M. Sharma. Factors controlling the stability of colloid-stabilized emulsions: I. an experimental investigation. *Journal of Colloid and Interface Science*, 157(1):244–253, 1993.

[148] David E. Tambe and Mukul M. Sharma. Factors controlling the stability of colloid-stabilized emulsions: Ii. a model for the rheological properties of colloid-laden interfaces. *Journal of Colloid and Interface Science*, 162(1):1–10, 1994.

[149] David E. Tambe and Mukul M. Sharma. Factors controlling the stability of colloid-stabilized emulsions: Iii. measurement of the rheological properties of colloid-laden interfaces. *Journal of Colloid and Interface Science*, 171(2):456–462, 1995.

[150] David Tambe, Janaka Paulis, and Mukul M. Sharma. Factors controlling the stability of colloid-stabilized emulsions: Iv. evaluating the effectiveness of demulsifiers. *Journal of Colloid and Interface Science*, 171(2):463–469, 1995.

[151] B. P. Binks and S. O. Lumsdon. Stability of oil-in-water emulsions stabilised by silica particles. *Physical Chemistry Chemical Physics*, 1(12):3007–3016, 1999.

[152] B. P. Binks and S. O. Lumsdon. Influence of particle wettability on the type and stability of surfactant-free emulsions. *Langmuir*, 16(23):8622–8631, 2000.

[153] B. P. Binks and S. O. Lumsdon. Pickering emulsions stabilized by monodisperse latex particles: Effects of particle size. *Langmuir*, 17(15):4540–4547, 2001.

[154] K. Golemanov, S. Tcholakova, P. A. Kralchevsky, K. P. Ananthapadmanabhan, and A. Lips. Latex-particle-stabilized emulsions of anti-bancroft type. *Langmuir*, 22(11):4968–4977, 2006.

[155] S. Melle, M. Lask, and G. G. Fuller. Pickering emulsions with controllable stability. *Langmuir*, 21(6):2158–2162, 2005.

[156] L. G. Torres, R. Iturbe, M. J. Snowden, B. Z. Chowdhry, and S. A. Leharne. Preparation of o/w emulsions stabilized by solid particles and their characterization by oscillatory rheology. *Colloids and Surfaces a-Physicochemical and Engineering Aspects*, 302(1-3):439–448, 2007.

[157] S. Arditty, C. P. Whitby, B. P. Binks, V. Schmitt, and F. Leal-Calderon. Some general features of limited coalescence in solid-stabilized emulsions. *The European Physical Journal E*, 11(3):273–281, 2003.

[158] Thomas H. Whitesides and David S. Ross. Experimental and theoretical analysis of the limited coalescence process: Stepwise limited coalescence. *Journal of Colloid and Interface Science*, 169(1):48 – 59, 1995.

[159] Emanuele Vignati, Roberto Piazza, and Thomas P. Lockhart. Pickering emulsions: interfacial tension, colloidal layer morphology, and trapped-particle motion. *Langmuir*, 19(17):6650–6656, 2003.

[160] Mathieu Destribats, Stéphane Gineste, Eric Laurichesse, Hugo Tanner, Fernando Leal-Calderon, Valérie Héroguez, and Véronique Schmitt. Pickering emulsions: What are the main parameters determining the emulsion type and interfacial properties? *Langmuir*, 30(31):9313–9326, 2014.

[161] Mathieu Destribats, Veronique Lapeyre, Melanie Wolfs, Elisabeth Sellier, Fernando Leal-Calderon, Valerie Ravaine, and Veronique Schmitt. Soft microgels as pickering emulsion stabilisers: role of particle deformability. *Soft Matter*, 7(17):7689–7698, 2011.

[162] Mathieu Destribats, Véronique Lapeyre, Elisabeth Sellier, Fernando Leal-Calderon, Véronique Schmitt, and Valérie Ravaine.

Water-in-oil emulsions stabilized by water-dispersible poly(n-isopropylacrylamide) microgels: Understanding anti-finkle behavior. *Langmuir*, 27(23):14096–14107, 2011.

3 Materials & Experimental Methods

Abstract In this chapter, the systems, instruments and experimental methods used in this thesis are described. As we investigate interfaces laden with thermoresponsive microparticles, I firstly describe the synthesis and characterisation of these thermoresponsive microparticles. Next the techniques used to investigate particle laden interfaces, i.e. the pendant drop technique and the Langmuir trough technique, are discussed.

3.1 Introduction

The experimental methods evoked in the course of the thesis are described in this chapter. PNIPAM particles used in this research are synthesized in house. We begin with describing the procedure used for the sysnthesis of these microgel particles. We then characterise these particles using Static and Dynamic Light scattering. We also measure the electrophoretic mobility and the zeta-potential of the particles.

The main experimental techniques used in this thesis are dynamic interfacial tension measurement using the pendant drop method and the measurement of surface pressure- area isotherms using a Langmuir film balance. I present the working principle for both these methods and explain in detail, the experimental protocol that was followed.

3.2 PNIPAM microgel sysnthesis

The sysnthesis of PNIPAM microgel particles was carried out using batch suspension polymerisation as described previously in the literature[1, 2]. The exact recipe was finalised after some discussions and a few iterations.

3.2.1 Chemicals

N-Isopropylacrylamide monomer (Acros organics), N,N-Methylene bis(acrylamide) (Sigma Aldrich), Acylic acid (Sigma Aldrich), Potassium persulfate (Acros organics) are used as received. Sodium dodecyl sulfate (SDS) is used from the stock already available in the lab in purified form. Glycerol (Merck) is used as a heating medium. N-Isopropylacrylamide is the monomer. N,N'-Methylenebis(acrylamide) (BIS) is used as the cross-linker in the polymerisation reaction of the N-Isopropylacrylamide monomer. Addition of acrylic acid(AA) made the particles sensitive to pH. Potassium persulfate (KPS) is used as an initiator and Sodium dodecyl sulfate (SDS) as a surfactant to facilitate emulsion polymerisation. The concentration of the surfactant gives us a handle on the size of the particles.

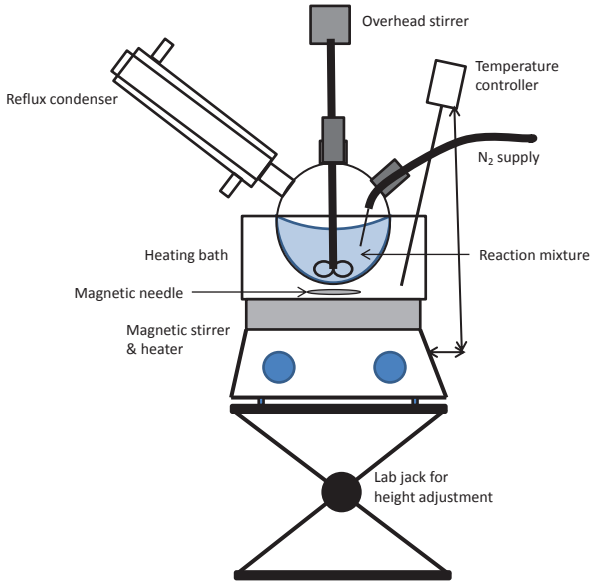

Figure 3.1: Experimental setup

3.2.2 Experimental setup

The setup consists of a 500 ml three neck round bottom flask (RBF). The rotary blade, made of Teflon, is connected to an overhead stirrer through the central neck. One of the remaining two outlets is connected to a water cooled reflux condensor, the other is used to add chemicals or as an inlet for nitrogen supply. This entire assembly is immersed in a heating bath with glycerol as the heating liquid. Gylcerol is chosen over silicon oil because it is easy to clean the exterior of the flask by simply washing it with water. The heating liquid is stirred for uniform heating using a teflon coated magnetic bar. The temperature of the liquid is kept constant at 80°C using a temperature measurement and control unit that is connected to the heater/stirrer. The entire setup was placed in a fume hood. Figure 3.1 shows a schematic of the experimental setup.

3.2.3 Synthesis protocol

200 ml MilliQ water is degassed by sonicating it at 60 – 70°C for about 30 minutes and introduced into the reaction vessel (RBF). Nitrogen is bubbled through it for another 30 minutes to get rid of any dissolved oxygen. 100 ml MilliQ water is degassed separately using a similar procedure in a glass bottle. 6.35 gm of monomer (NIPA), 0.425 gm of cross-linker (BIS), and 8.6 mg SDS are weighed and transferred to the glass bottle. Once the content in the bottle has dissolved completely, it is transferred to the RBF. 10 ml water in a glass tube is degassed using the above mentioned procedure. 140 mg of KPS is dissolved in the tube. The temperature of the bath is set at 80°C. I wait till the temperature has stabilized within a margin of ±0.2°C from the set temperature. Once the temperature is stable, I transfer the contents of the tube into the RBF. Nitrogen is continuously bubbled through the reaction mixture. The reaction mixture is stirred continuously at a speed of approximately 500 rpm. Within a few minutes after adding the initiator, the reaction mixture turns translucent indicating the start of the polymerisation reaction. The reaction mixture soon turns milky. The reaction conditions are maintained for 2 hours from the start of the reaction. After 2 hours, I stop the heating and let the RBF cool down in air for about 15 minutes. After that I remove the RBF from the setup and cleaned any glycerol sticking to the exterior of the RBF by washing it with cold water. This cools the reaction mixture further. Following this, the reaction mixture is filtered twice. First with a crude filter paper to separate any agglomerates and then followed by filtering through a Whatmann filter paper with a mesh size of 3 micron, which ensures that only particles less than that size are present in the filtrate. The unreacted monomers and the surfactants are separated by centrifugation at 18000g in an ultracentrifuge. After each centrifugation step, the supernatant is thrown away and the particles are resuspended in MilliQ water. This procedure is repeated at least 5 times. Finally the particles are flash-frozen and freeze dried in a lyophilizer to yield dry flakes of particles. These particles can be resuspended in water to get the desired concentration of particles.

3.3 Particle characterisation

3.3.1 Dynamic Light Scattering

The hydrodynamic diameter of the particles is measured by dynamic light scattering (DLS)[3] using a Malvern Zeta-sizer Nano ZS instrument. The instrument measures the intensity fluctuations of the scattered light at a fixed angle (173°). The intensity fluctuations are used to construct a correlation function.

$$G(\tau) = \langle I(t).I(t+\tau)\rangle \tag{3.1}$$

Here the brackets denote time averaging. For large particles performing Brownian motion, this correlation function decays exponentially with the decay time τ as:

$$G(\tau) = A\left[1 + B\exp(-2\Gamma\tau)\right] \tag{3.2}$$

In the above expression, A and B are the baseline and intercept of the correlation function respectively. The term Γ is given by:

$$\Gamma = Dq^2 \tag{3.3}$$

Here, D is the diffusion coefficient of the particles and q is the wave vector which is expressed as:

$$q = \frac{4\pi n_{solv}}{\lambda_0}\sin\left(\frac{\theta}{2}\right) \tag{3.4}$$

Where, n_{solv} is the refractive index of the solvent, λ_0 the wavelength of the laser and θ the scattering angle. Thus, if our sample is fairly monodisperse, we can fit a single exponential to the correlation function and extract the mean size D_H(hydrodynamic diameter). Figure 3.3(a) shows how the hydrodynamic diameter of the microgel particles varies with temperature.

3.3.2 Static Light Scattering

To get further information about the microgel particles, we studied them using Static Light Scattering (SLS)[4]. This enabled us to measure the

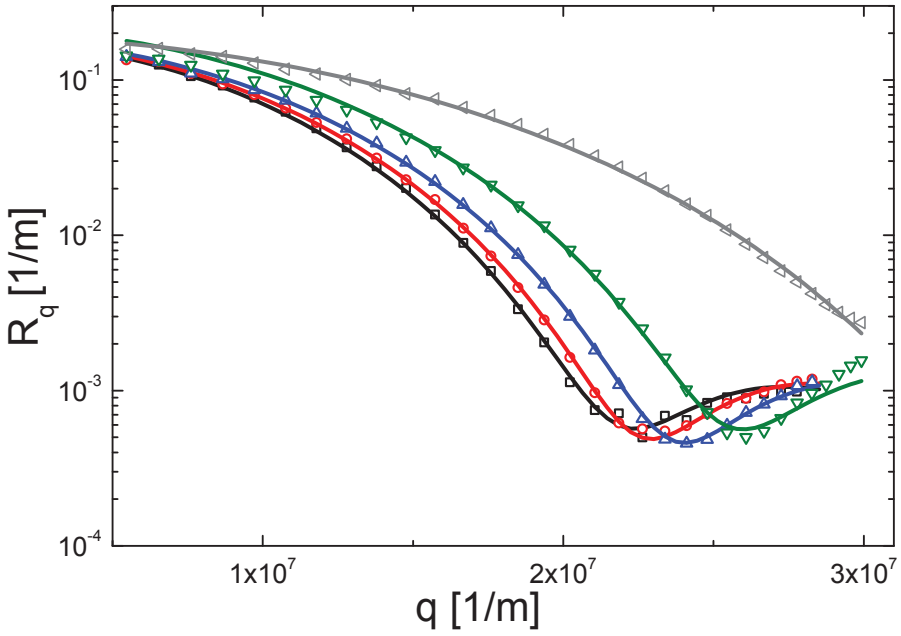

Figure 3.2: Scan of Raleigh ratio R_q measured for angles between 20° and 130° detection angles. The different symbols and colours denote the measurements for various temperatures namely: (□) 20°C, (○) 24°C, (△) 28°C, (▽) 32°C, (◁) 36°C. The solid lines are the fits to the experimental measurements.

molar mass (M) of the particles and the size (R_{SLS}) equivalent to a homogeneous spherical particle. We can quantify the scattering intensity at each angle θ using the Excess Rayleigh Scattering (R_θ) as:

$$R_\theta = \frac{I(\theta)_{sample} - I(\theta)_{solv}}{I(\theta)_{ref}} R_{ref} \frac{n^2_{solv}}{n^2_{ref}} \tag{3.5}$$

For our experiments we use Toluene as a reference since it is known from the literature that $n_{toluene} = 1.494$ and $R_{toluene} = 2.10 \times 10^{-3} m^{-1}$ for $\lambda_0 = 532nm$. The excess rayleigh scattering can also be expressed as a function of wave vector q (defined above in eqn.3.4) as:

$$R_q = K_r C M P(qR) S(q) \tag{3.6}$$

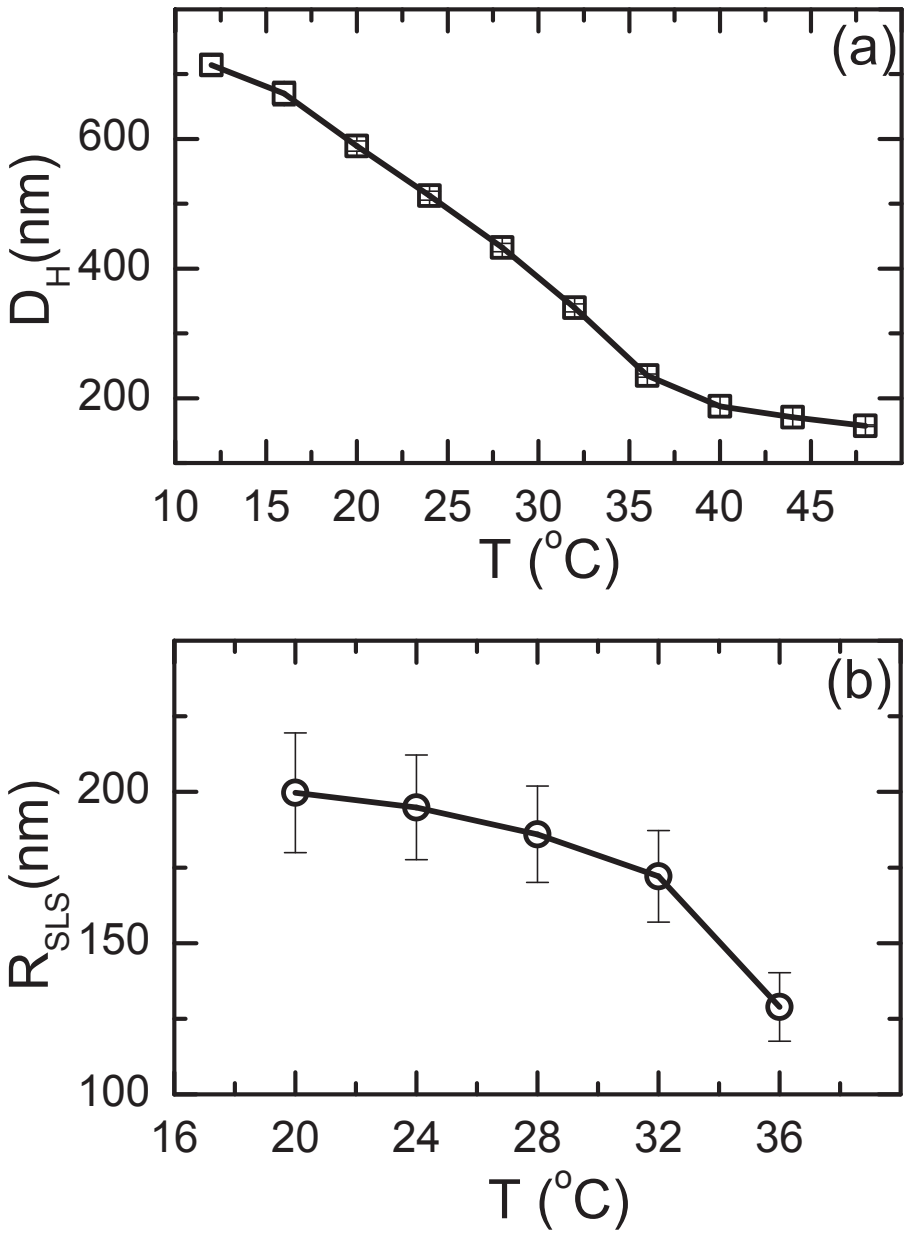

Figure 3.3: (a) The hydrodynamic diameter D_H as a function of temperature measured by DLS, (b) The size R_{SLS} as it varies with temperature as measured by SLS.

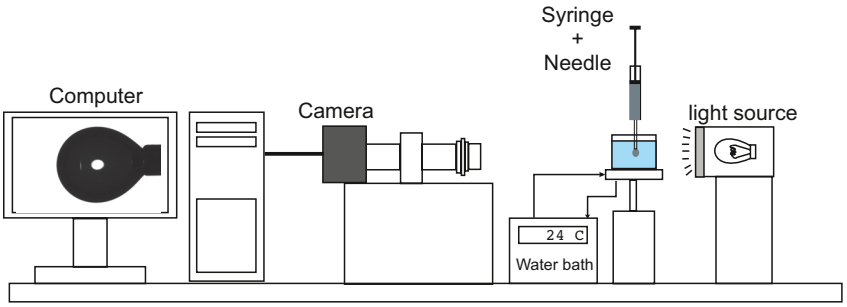

Figure 3.4: Schematic of the pendant drop shape analysis setup.

Where, K_r is a constant that depends on physical properties of the particle like refractive index (n) and (dn/dC), $S(q)$ is the structure factor, which for low particle concentrations is unity, C is the particle concentration, M is the molar mass and $P(qR)$ is the form factor, which for homogeneous spherical particles is expressed as:

$$P(qR) = 9\left(\frac{sin(qR) - qRcos(qR)}{(qR)^3}\right)^2 \tag{3.7}$$

We plot R_q as a function of q for various temperatures as shown in figure 3.2. From this we can extract the size and the molar mass by using them as fit parameters. In our case the molar mass of the particles was found to be 1.82×10^6 kg/mol. The equivalent radius (R_{SLS}) has been plotted as a function of temperature in figure. 3.3(b).

3.4 Pendant drop measurements

The dynamic interfacial tension of particle laden drop interfaces is measured on a Dataphysics OCA 20L device as shown in the figure 3.4. The device consists of a pendant drop or a bubble created at the tip of a needle. The drop is illuminated from behind and the shape of the drop

is recorded by a camera capable of capturing images at 30 frames per second. The drop shape for each individual image is then analysed using SCA 22 software provided by the manufacturer from which the interfacial tension is determined using the Axisymmetric Drop Shape Analysis method .

3.4.1 Axisymmetric Drop Shape Analysis (ADSA)

The basic principle behind the ADSA method is described as follows[5]:

The pressure difference (ΔP) across a very thin film separating two bulk phases is given by the classical Laplace equation.

$$\Delta P = \gamma \left(\frac{1}{R_1} + \frac{1}{R_2} \right) \tag{3.8}$$

Where, γ is the interfacial tension and R_1 is the radius of curvature in the image plane and R_2 is the radius of curvature in a plane perpendicular to the image plane.

In absence of any external force other than gravity, the hydrostatic pressure head at a given point can be given by:

$$\Delta P = \Delta P_0 + \Delta \rho g z \tag{3.9}$$

Where, ΔP_0 is the pressure difference at the selected datum plane. If we select the datum to be at the base of the drop, then at the origin $R_1 = R_2 = R_0$. Also R_2 can be expressed as $R_2 = x / \sin\phi$, where ϕ is the angle measured between the tangent to the interface at point (x, z) and the datum plane.

Thus from equations 3.8 and 3.9 we get:

$$\gamma \left(\frac{1}{R_1} + \frac{\sin\phi}{x} \right) = \frac{2\gamma}{R_0} + \Delta \rho g z \tag{3.10}$$

Mathematically, the interface is completely described as $u(x, y, z) = 0$. But given the axisymmetric nature of the drop, one only needs to describe

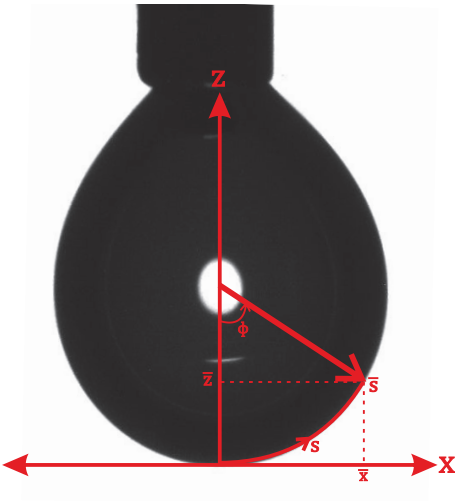

Figure 3.5: Co-ordinate system for a profile of a pendant drop.

the meridian section of the drop. The system can be further simplified by expressing the curve in parametric form as:

$$x = x(s) \text{ and } z = z(s) \tag{3.11}$$

Where, s is the arc length measured from the origin. Thus, both x and z are reduced to being single valued functions of s and we have:

$$\frac{dx}{ds} = \cos\phi \tag{3.12}$$

$$\frac{dz}{ds} = \sin\phi \tag{3.13}$$

Also, the curvature $1/R_1$ can be defined by geometry as:

$$\frac{1}{R_1} = \frac{d\phi}{ds} \tag{3.14}$$

Substituting eqn. 3.14 in eqn. 3.10 and rearranging, we get:

$$\frac{d\phi}{ds} = \frac{2}{R_0} + \frac{\Delta\rho g z}{\gamma} - \frac{\sin\phi}{x} \tag{3.15}$$

Equations 3.12, 3.13 and 3.15 together with the boundary conditions:

$$x(0) = z(0) = \phi(0) = 0 \tag{3.16}$$

form a set of first-order differential equations. For a given R_0 and $\Delta\rho g/\gamma$, we can obtain the complete shape of the drop by simultaneously integrating these equations. Conversely, if the shape of the drop is known, we can fit it to the theoretical expression and extract the value of $\Delta\rho g/\gamma$ as a fit parameter.

3.4.2 Dilatational Rheology

Dilatational rheology of adsorbed layers of PNIPAM microgel particles is carried out on the Dataphysics OCA 20L instrument using an additional accessory called Oscillating Drop Generator (ODG). The ODG basically consists of a small peizo element attached to the setup which can be used to periodically dispense very small volumes of liquid in a controlled fashion to generate a systematic variation of the interfacial area. The response of the system to these perturbations in the interfacial area is reflected in the interfacial tension values[6, 7]. The dilatational surface modulus E is thus defined as[8]:

$$E = \frac{d\gamma}{dlnA} \tag{3.17}$$

However, in most practical cases, the response of the system is not perfectly elastic. The interfacial tension response often lags behind the oscillations in the interfacial area. In such scenario, the system is described by a complex dilatational modulus (E^*) as:

$$E^* = E' + iE'' \tag{3.18}$$

Where, $E' = |E|cos\phi$ is the dilatational storage modulus, $E'' = |E|sin\phi$ is the dilatational loss modulus and $|E| = \Delta\gamma/(\Delta A/A)$.

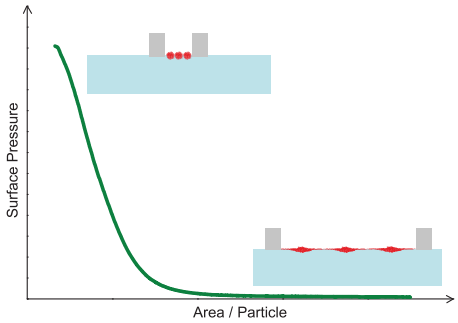

Figure 3.6: A typical Pressure-Area isotherm for PNIPAM particles spread on an air-water interface. Insets show schematic picture of the morphology and interactions of particles as they are compressed.

3.5 Langmuir Film Balance measurements

A Langmuir film is defined as a monolayer of insoluble species spread on a flat subphase[9, 10]. A langmuir monolayer can be compressed or expanded by modifying the area by means of movable barriers in a Langmuir film balance (LB). The surface tension (or surface pressure) is measured by Wilhelmy plate method as the area of the monolayer is compressed. A typical Pressure-Area isotherm for PNIPAM particles spread on an air-water interface is shown in figure 3.6. The isotherm helps us to understand the morphology of particles at the interface and also the nature of interactions between them as they are compressed. Since the number of particles that we spread on the interface is known, and because these particles, due to the high energy barrier, never leave the interface, the Pressure - Area isotherm can be represented as a Pressure - Surface concentration curve. This is just the equation of state (EOS) for the PNIPAM particles at an air-water interface.

For my experiments, I have used two Langmuir trough setups. In Chapter 4, for the experiments at room temperature, I used the KSV NIMA trough. The trough and the barriers are both made out of Teflon. The maximum and minimum possible area available in the trough is 500 cm^2 and 40 cm^2 respectively. The surface pressure is measured using a stan-

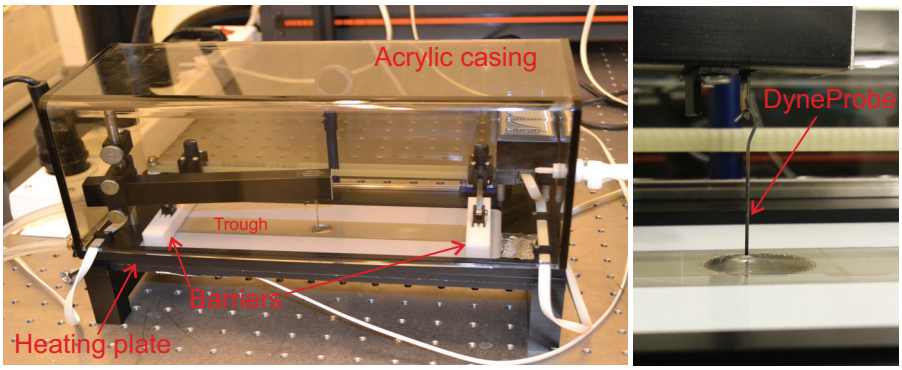

Figure 3.7: A photograph of the Kibron μ-trough setup.

dard paper Wilhelmy plate connected to a Mini PS4 sensor capable of measuring minimum surface pressure variations of 0.1 mN/m. Follow-up measurements for Chapter 4 and the measurements with temperature control are performed on a Kibron μ-trough. Figure 3.7 shows a photograph of the apparatus. The Kibron trough is much smaller as compared to the NIMA trough. The maximum and minimum possible area available in the Kibron μ-trough is 51.50 cm^2 and 3.25 cm^2 respectively. The surface pressure is measured using a platinum Wilhelmy plate (DyneProbe) connected to a sensor capable of measuring surface pressure with a resolution of 0.01 mN/m. The temperature of the trough is controlled by means of a heating plate placed beneath the trough. The heating plate is connected to a LAUDA RE306 water bath fitted with a temperature controller. The temperature on the surface of the trough is separately monitored using a thermocouple.

The experimental protocol is similar for both setups. Prior to the experiments, I clean the trough with choloroform to remove any impurities. Then I create a bare air-water interface. The interface is thoroughly cleaned by aspirating and removing any impurities floating on the interface. This is done until the pressure-area compression cycle shows a perfectly horizontal line and the pressure at maximum compression is < 0.1 mN/m. Next, I spread a known amount of particles on a clean air-water

interface, wait for at least 30 minutes for the system to equilibrate and then systematically reduce the area of the interface. The reproducibility of the experiments is checked by repeating the experiment under the same conditions. We also check for hysteresis between the compression and the expansion cycles. The observed hysteresis in the pressure in all cases is less than 2mN/m.

Acknowledgements

I thank Prof. Peter Schall and his student Dr. Yasser Rahmani (UvA, Amsterdam) for sharing their experimental protocol for synthesis of PNIPAM particles. I would also like to acknowledge the insights given by Dr. Samruddhi Kamble(NCL, Pune) in the systhesis of particles. I thank Marc Ankone (CDD group, U Twente) for letting me use the freeze dryer and Kirsten van Leijenhorst-Groener (NBP, U Twente) for the use of their ultracentrifuge. I thank Remko Fokkink (Wageningen University) for his help with the SLS measurements and Sry Dewi (CDD group, U Twente) for help with the Malvern Zeta-sizer.

Bibliography

[1] Roberta Acciaro, Tibor Gilanyi, and Imre Varga. Preparation of monodisperse poly(n-isopropylacrylamide) microgel particles with homogenous cross-link density distribution. *Langmuir*, 27(12):7917–7925, 2011.

[2] X. Wu, R. H. Pelton, A. E. Hamielec, D. R. Woods, and W. McPhee. The kinetics of poly(n-isopropylacrylamide) microgel latex formation. *Colloid and Polymer Science*, 272(4):467–477, 1994.

[3] B.J. Berne and R. Pecora. *Dynamic Light Scattering: With Applications to Chemistry, Biology, and Physics*. Dover Books on Physics Series. Dover Publications, 2000.

[4] Remco Fokkink. Introduction to static light scattering. Lecture Notes on Research Methods Soft Matter, 2013.

[5] Y Rotenberg, L Boruvka, and A.W Neumann. Determination of surface tension and contact angle from the shapes of axisymmetric fluid interfaces. *Journal of Colloid and Interface Science*, 93(1):169 – 183, 1983.

[6] Stoyan C. Russev, Nikola Alexandrov, Krastanka G. Marinova, Krassimir D. Danov, Nikolai D. Denkov, Lyudmil Lyutov, Vassil Vulchev, and Christine Bilke-Krause. Instrument and methods for surface dilatational rheology measurements. *Review of Scientific Instruments*, 79(10):–, 2008.

[7] Francesca Ravera, Giuseppe Loglio, and Volodymyr I. Kovalchuk. Interfacial dilational rheology by oscillating bubble/drop methods. *Current Opinion in Colloid & Interface Science*, 15(4):217 – 228, 2010.

[8] R. Miller and L. Liggieri. *Interfacial Rheology*. CRC Press, 2009.

[9] A.W. Adamson and A.P. Gast. *Physical chemistry of surfaces*. Wiley, 1997.

[10] D.J. Shaw. *Introduction to Colloid and Surface Chemistry*. Chemical, Petrochemical & Process. Butterworth-Heinemann, 1992.

4 Equation of state and adsorption dynamics of soft microgel particles at an air-water interface

Abstract In this study I experimentally determine an equation of state (EOS) for Poly (N-isopropylacrylamide) (PNIPAM) microgel particles adsorbed onto an air-water interface using a Langmuir film balance. I detect a finite surface pressure at very low surface concentration of particles, for which standard theories based on hard disk models predict negligible pressures, implying that the particles must deform strongly upon adsorption to the interface. Furthermore, I study the evolution of the surface pressure due to the adsorption of PNIPAM particles as a function of time using pendant drop tensiometry. The equation of state determined in the equilibrium measurements allows us to extract the adsorbed amount as a function of time. I find a mixed-kinetic adsorption that is initially controlled by the diffusion of particles towards the interface and at longer times by a coverage-dependent adsorption barrier related to crowding of particles at the interface

This chapter has been published as Deshmukh OS, *et al.*, Equation of state and adsorption dynamics of soft microgel particles at an air - water interface, Soft Matter (2014), http://dx.doi.org/10.1039/C4SM00566J

4.1 Introduction

Microgel particles (swollen colloidal particles consisting of cross-linked soluble polymers) show great promise as Pickering stabilizers of emulsions and foams[1–3]. This has two reasons. First, the fact that they are particles makes them adsorb very strongly to the interface with adsorption energies in order of hundreds of k_BT or more[4]. Second, their swollen polymeric character facilitates attachment from solution to fluid interfaces in comparison to solid particles[4, 5]. Understanding how these particles stabilize the interface, what shape they take and what surface pressures they generate are the important questions that need to be addressed in the context of knowledge based design of particles for these specific applications. Although various studies of adsorbed microgel layers have appeared[6–11], none of them has precisely established the equation of state for these adsorbed soft microgel particles. There also exists a dearth of experiments regarding the adsorption dynamics of these particles onto fluid interfaces. Yet, the processes controlling adsorption are at present not well understood. For example, it has been found that the adsorption of hard colloidal particles is strongly affected by the electrostatic interactions between the particles and the air-water interface[12]. Negative particles are repelled and adsorb slowly or not at all (depending on the ionic strength and dynamic conditions) whereas positive particles adsorb readily, possibly following a diffusion based rate law. It is not yet known whether the adsorption of soft particles is governed by similar processes. Even the equilibrium surface pressure as a function of the amount of adsorbed soft particles, *i.e.* the equation of state (EOS) is poorly known, let alone the physical mechanism giving rise to surface pressure. It is well-known that a 2D ideal gas model of adsorbed colloidal particles will not lead to a measurable pressure due to the large size of the particles[8]. Hence a simple 2D hard disk model will predict measurable pressures only for adsorbed layers extremely close to the hexagonal close packing limit. Groot and Stoyanov[13] carried out dissipative particle dynamics (DPD) simulations of soft particles at fluid interfaces and proposed to rescale the density by introducing an effective length scale, which is two orders

of magnitude smaller than the particle size. This leads to more realistic values of the surface pressure, yet the physical meaning of this effective length is not very clear.

Finally it is important to realize that such soft microgel particles deform strongly upon adsorption to both solid - liquid[14] and liquid - liquid[3, 7, 15, 16] interfaces resulting in 'sombrero' or 'fried egg-like' morphologies. In the case of fluid - fluid interfaces, this deformation is usually attributed to the tendency of the polymer strands to maximize their contact with the interface counteracted by the particle elasticity. The extent of deformation is then controlled by $\Delta\gamma/\epsilon$, where $\Delta\gamma$ is the net interfacial tension acting on the particle and ϵ is the Young's modulus of the particles. For swollen particles at the air-water interface one typically finds such deformations to be of the order of 10^{-6} m which is comparable to the size of the particle. Hence such particles undergo substantial deformation at the interface, an aspect that has not been taken into account in the simulations of Groot and Stoyanov.

It is the purpose of this chapter to address these issues by first determining the (equilibrium) equation of state (EOS) for PNIPAM microgel particles adsorbed onto an air-water interface using a Langmuir balance(LB). Second, I follow the time-dependent evolution of surface pressure in a separate experiment as PNIPAM particles adsorb from an aqueous bulk solution to the interface of newly formed air bubble using pendant drop (c.q. 'bubble') tensiometry. From these two measurements it is possible to obtain the kinetics of adsorption $\Gamma(t)$, revealing important aspects of the mechanisms controlling the adsorption kinetics.

4.2 Materials

The PNIPAM particles are synthesized by a batch suspension polymerization using a recipe that has been described in literature[17, 18]. I used N-isopropyl acrylamide (NIPAM) as monomer with N, N'-methylenebisacrylamide as the cross linker (2 mol%) and potassium persulfate as the initiator for the polymerization reaction. I expect the particles to carry a small amount of charge due to the potassium persulfate

used in the initiation step. The particles are purified by repeatedly centrifuging at 18000 g and replacing the supernatant with fresh Milli-Q water. The process was repeated at least 5 times. The particles are then freeze dried and stored. The suspension is prepared by weighing a calculated amount of the freeze dried particles and simply adding them to Milli-Q water to get the desired concentration and stirring for at least 24 hours before use. I prepare a stock solution of 0.5 g/l concentration. Suspensions of lower concentration are prepared by diluting this stock solution.

4.3 Methods

4.3.1 Particle Characterisation

The size of the microgels is measured by Dynamic Light Scattering on a Malvern Zeta Sizer. The hydrodynamic diameter of the particles at 20 °C is 589 ± 5 nm which, using the Stokes-Einstein relation, corresponds to a diffusion coefficient of 7.29×10^{-13} m^2/s. Calibrated Static Light Scattering is used to find the molar mass and the radius of gyration of these particles by fitting the form factor assuming the particle to be spherical. I use dn/dC = 0.167 ml/g as reported in literature[19]. The molar mass is 1.82×10^6 kg/mol and the radius of gyration (R_g) at 20 °C is 200 ± 19 nm. A small value of R_g / R_h indicates existence of long dangling chains on the periphery of a stiffer cross-linked core[20].

4.3.2 LB pressure-area isotherms

The equation of state (Pressure v/s Adsorbed mass relationship) is determined using a Langmuir trough. All the experiments are carried out at room temperature. Firstly I carefully clean the air water interface until a point where the pressure – area compression cycle shows a perfectly horizontal line and the pressure at maximum compression is < 0.1 mN/m. I then spread a known amount of particles on a clean air-water interface and systematically reduce the area of the interface. The resultant change

in pressure is recorded by a pressure sensor using a Wilhelmy plate. I perform 3 different sets of experiments: Two of these sets are performed on a NIMA Langmuir trough with a Mini PS4 pressure sensor using a paper Wilhelmy plate. The maximum and minimum possible areas available on the NIMA trough are 500 cm^2 and 40 cm^2 respectively. In the first set I study the particles at high initial loading. I spread 100 μl of a suspension of 0.5 g/l concentration. I carefully place the drops of the suspension on the interface using a 10 μl syringe with a sharp tip by holding the needle very close and parallel to the interface. I try to evenly deposit the drops over the initial spreading area and wait for at least 30 minutes for the system to stabilize before I begin my measurements. For the second set of experiments I use the same NIMA trough but this time I study the system at lower initial loading. I spread 40 μl of the 0.5 g/l concentration suspension. I carry out one more set of experiments on a Kibron μ-trough. The maximum and minimum possible areas in the Kibron μ-trough are 51.50 cm^2 and 3.25 cm^2, respectively. I spread 100 μl of 0.035 g/l particle solution on an initially clean air-water interface. These loading conditions are similar to the loading conditions for NIMA for high loading. The compression rate was kept low (10 cm^2/min for NIMA trough and 5 cm^2/min for Kibron μ-trough). The reproducibility of the experiments is checked by repeating the experiment under the same conditions. I also check for hysteresis between the compression and the expansion cycles. I find the hysteresis in the values of pressure to be < 2 mN/m. Compression-expansion cycles are repeated and no evidence for particle detachment is found in any experiment.

4.3.3 Interfacial tension measurements

I use a Dataphysics OCA apparatus to measure the surface tension of microgel particle laden interfaces. I create an air bubble in the suspensions of varying concentrations using an inverted needle. The interfacial tension (γ) is calculated with a resolution $\pm$ 0.01 mN/m by image analysis from the shape of the bubble using the well-known Laplace equation. I convert the values of interfacial tension into surface pressure by using the

correlation $\Pi(t) = \gamma_0 - \gamma(t)$. Where γ_0 = 72 mN/m is the value of bare air-water interfacial tension. For the interfacial tension measurements to be accurate, I make sure that the bubble is big enough so that it is substantially deformed by the buoyancy forces. The Bond number is defined as $Bo = \Delta\rho g R^2/\gamma$, where, $\Delta\rho$ is the density difference between the fluids, R is the radius of the drop and γ is the interfacial tension. It is a measure of the interplay between the gravity/buoyancy and surface forces. For accurate measurements, it is advised that Bo should always lie between 0.1 and 1[21]; I check this to be the case in all my measurements. Like the surface pressure experiments, all tensiometry measurements are carried out at room temperature.

4.4 Results and Discussion

The pressure-area isotherms are obtained from compression of spread monolayers on a Langmuir trough for 3 different set of experiments. The area coordinates in these isotherms are scaled by the number of particles adsorbed on the interface. All the curves collapse on to a single plot as shown in figure 4.1. At increasing compression, the pressure initially varies a little, but below 2 μm^2/particle, there is a steep increase in the pressure. The slope of the curve first increases, but reaches a maximum at ~ 27 mN/m where there is an inflection point followed by a somewhat weaker slope. The value of area per particle (A_c) that corresponds to this inflection point turns out to be 0.545 μm^2 as shown by the dotted line in figure 4.1. Assuming the particles are closely packed, this corresponds to an inter-particle distance of ~ 835 nm, which is much larger than the hydrodynamic diameter of the particles measured in the bulk solution (590 nm) suggesting that the particles are indeed substantially deformed. As the inset of figure 4.1 shows, finite surface pressures of order 0.5 mN/m (i.e. well above our detection limit of 0.1 mN/m) can in fact be measured already at areas per particle of around 4 μm^2. The inset also shows that the absolute values of Π are reproducible to within 0.3 mN/m between different experiments on the two different Langmuir troughs.

In figure 4.2 I present the same data as in figure 4.1, but converted into

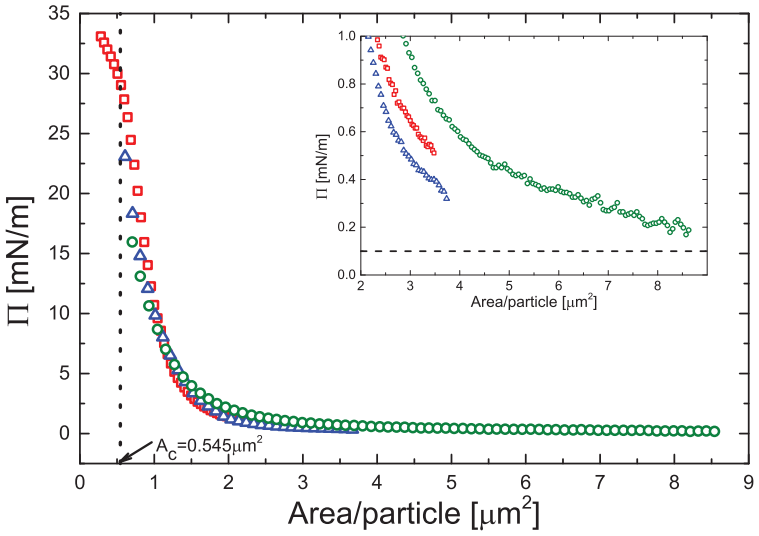

Figure 4.1: Pressure area isotherm for PNIPAM particles at air-water interface. The open symbols denote experimental data points corresponding to three different sets of experiments namely: (□) NIMA trough with high initial particle loading, (◯) NIMA trough with low initial particle loading and (△) Kibron μ-trough with high initial particle loading. Inset shows expanded view of the pressure area curve at low loadings. The dashed line in the inset denotes the detection limit of the pressure sensor.

a Pressure v/s adsorbed amount curve using $\Gamma = 1/(A \times N_{Av})$ where A is the area/particle from figure 4.1 and N_{Av} is the Avogadro number. This curve represents the 2D Equation of State (EOS) of the present system. At relatively low densities ($< 5 \times 10^{-13}$mol/m^2) the pressure is extremely low ($\approx$ 1mN/m) but quite well detectable. It follows that even at low densities where the inter-particle distance is much larger than the particle size in solution, the particles still somehow interact. As the particles hardly have any electrophoretic mobility[22, 23], electrostatic repulsion is unlikely to be the cause. The only other option is particle-particle contact. Hence the particles must be strongly deformed upon their adsorption onto the interface, which qualitatively agrees with the findings by other

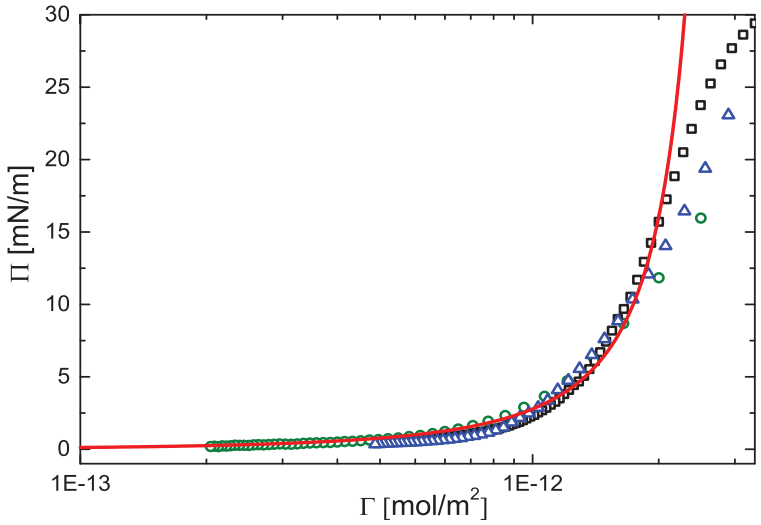

Figure 4.2: Surface pressure(Π) v/s amount of PNIPAM particles adsorbed (Γ) on an air - water interface. The open symbols denote experimental data points corresponding to three different sets of experiments namely: (□) NIMA trough with high initial particle loading, (◯) NIMA trough with low initial particle loading and (△) Kibron μ-trough with high initial particle loading. The solid red line denotes the predictions made using the Groot and Stoyanov model.

authors[2, 3, 7, 8, 15, 24]. I can make a rough estimate the extent of deformation using the ansatz $\Delta r \approx \Delta\gamma/\varepsilon$. Using typical values of $\varepsilon \approx$ 50 kPa from the literature[25, 26] along with $\Delta\gamma$ = 70 mN/m, I find Δr = 1.7μm which is consistent with the distances of ~ 3 μm between close-packed and fully deformed particles. I base my analysis on the assumption that the particles that I spread on the interface do not desorb. But even if I accounted for desorption of particles, it would only mean that the finite pressures detected would in fact correspond to even lower surface concentrations. figure 4.3 shows a schematic explanation of the mechanism of deformation of the particles at the interface. It should be noted that in case of LB experiments, the particles are spread on the

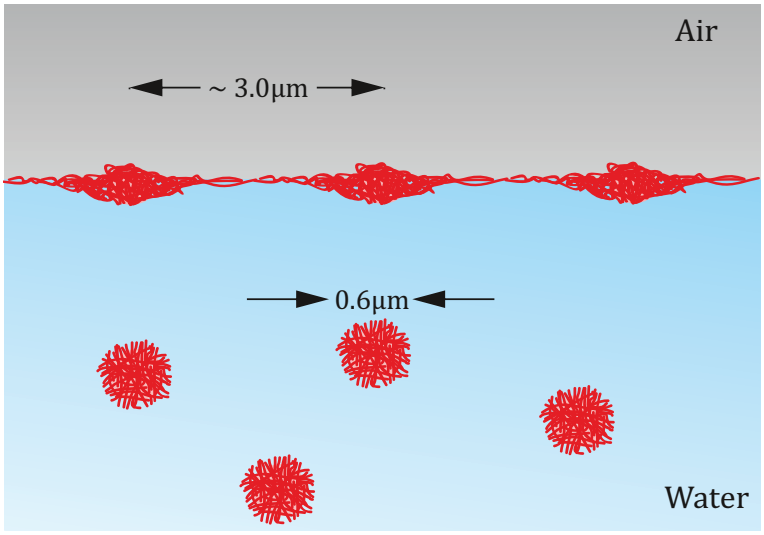

Figure 4.3: Schematic representation of the deformation of microgel particles upon adsorption to the interface at very low loading conditions.

interface and I do not have any particles in the bulk. In case of the interfacial tension measurements, the particles diffuse from the bulk to the interface.

Particles adsorbing to a fluid-fluid interface interact with each other and give rise to the surface pressure (Π), which is the 2D analogue of pressure in 3D systems. By extending this analogy further, it is also possible to relate this surface pressure to other state parameters like the number density and temperature via an equation of state. For colloidal particles adsorbing on a fluid-fluid interface, the simplest approximation could be that of 2D hard disks. The equation of state (EOS) for a one component system is given in terms of density dependence of the compressibility factor Z. The literature is replete with multiple approaches towards providing an expression for an EOS for 2D hard disk fluid. Mulero et.al.[27, 28] provide a succinct review and comparison of all these equations of state.

I find that at very low densities the surface pressure measured is at least 5-6 orders of magnitude higher than predictions of surface pressures as-

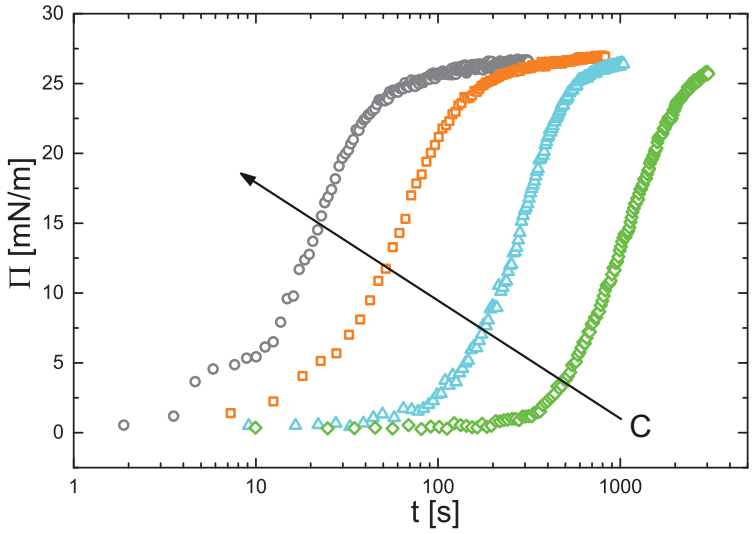

Figure 4.4: Evolution of Surface pressure (Π) as a function of time. The open symbols are experimental data points. Different symbols and colors denote various bulk concentration of particles: (◇)0.10 g/l, (△)0.20 g/l, (□)0.50 g/l, (○)1.00 g/l. Arrow denotes the direction of increasing concentration.

suming an ideal gas of non-interacting particles at these densities. Groot and Stoyanov[13] do not explicitly consider the deformation of these particles due to surface tension. They simply postulate that the pressure depends predominantly on the micro-structure and composition of polymers within the colloidal particles, and introduce a new length scale d_{eff} which is meant to reflect the particle micro-structure, and which up scales the pressure to experimental values. However, realizing that the particles spread out to a large extent, I can also see the measured pressure as reflecting the internal elasticity of the particles. Since this is given by a 2D density of crosslinks, it is not surprising that I find a microscopic length.

Groot and Stoyanov propose an expression for surface pressure(Π) that takes into account the size of these smaller correlated domains within the

particle given by:

$$\Pi = \frac{4k_B T}{\pi {d_{eff}}^2}\left(\frac{b\eta Z(\lambda\eta)}{\lambda} - b_2\eta^2\right) \tag{4.1}$$

where, d_{eff} is the size of the correlated domains within the particle. The compressibility factor (Z) can be expressed by using any of the equations of state available in literature. In my case, I use the modified Henderson equation[29] given by:

$$Z_{HM} = \frac{1+\eta^2/8}{(1-\eta)^2} - \frac{0.043\eta^4}{(1-\eta)^3} \tag{4.2}$$

where η is the surface packing fraction which can in turn be expressed in terms of the number density of particles (ρ) and the bulk diameter of individual particle (d) as $\eta = (\pi/4)\rho d^2$. For my experiments, η lies between 0 and 0.91. The corresponding values of Z_{HM} lie between 1 and 96.

I fit the scaling relation given by Groot and Stoyanov to my data in figure 4.2(red curve). The fitting gives $d_{eff} = 1.25$ nm as the characteristic length scale. To provide a physical picture, this d_{eff} can be viewed as the average distance between cross-links within the microgel particle. This is in agreement with previous studies[30, 31] that report a mesh size in the range of 1 - 10 nm. The parameters b and λ used in the model denote repulsive interactions due to the elastic nature of disks. For my system, the values for b and λ can be taken as unity[13]. The parameter b_2 denotes short range attractive interactions. I checked the effect of short range attraction interaction by incorporating the parameter b_2 as a fit parameter, but the analysis yields extremely small values of b_2 ($\sim 1\times10^{-4}$). Hence I conclude that I have purely repulsive particles. The deviations of the actual data from the model at high loading are possibly because at high compressions, the surface no longer remains flat but undergoes out-of-plane deformations i.e., buckles. Also, these particles have a lot of loose, un-cross-linked polymer chain segments along the periphery of these particles. At high compressions, it is energetically favourable for these segments to leave the interface rather than inter-penetrate. Such

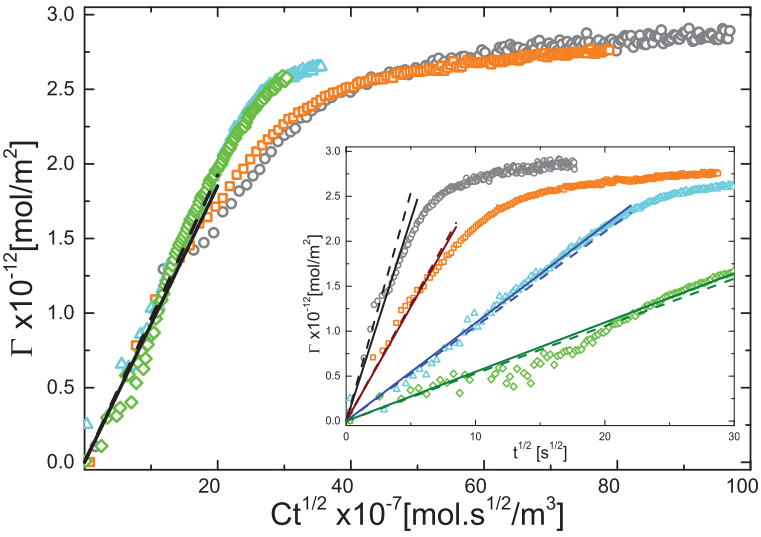

Figure 4.5: Adsorbed amount(Γ)as a function of the product $Ct^{1/2}$. The inset shows the individual curves of Γ v/s $t^{1/2}$ for various bulk concentration of microgel particles: (◇)0.10 g/l, (△)0.20 g/l, (□)0.50 g/l, (○)1.00 g/l. Solid lines are straight line fits and dashed lines are drawn with slopes calculated using $D=D_{DLS}$.

partial desorption also may result in deviations from the predictions of hard disk like model.

Having established an equation of state to correlate the surface pressure and the adsorbed amount, I now proceed to study the adsorption dynamics of the particles. For this I monitor the evolution of the interfacial tension of a freshly prepared air bubble in a suspension of PNIPAM particles as a function of time. I convert the values of interfacial tension into surface pressure. The results are as shown in figure 4.4. The values of surface pressure initially increase rapidly and then relax to a final equilibrium value. The dynamics can be clearly separated into two separate time scales: An initial rapid dynamics denoted by the increase in the surface pressure values, and a slow part as the system relaxes towards the final equilibrium state. This distinction between rapid kinetics at short

Table 4.1: Values of diffusion co-efficient D (m^2/s) for various concentrations calculated from the experimental Γ v/s $t^{1/2}$ curves compared to ones measured using DLS.

Conc(g/l)	Conc(mol/m^3)	$D_{exp}(m^2/s)$	$D_{DLS}(m^2/s)$
0.10	5.495×10^{-8}	7.57×10^{-13}	7.26×10^{-13}
0.20	1.099×10^{-7}	7.73×10^{-13}	7.20×10^{-13}
0.50	2.747×10^{-7}	6.72×10^{-13}	7.01×10^{-13}
1.00	5.495×10^{-7}	6.48×10^{-13}	6.72×10^{-13}

times and much slower kinetics at longer times is characteristic for the adsorption behaviour of many surface active materials[32, 33].

At short time scales, the increase in Π is limited by the transport of the particles from the bulk to the interface. I expect the transport to be governed by the diffusion of particles. Since my particles are fairly large, the energy of adsorption for these particles is 3-4 orders of magnitude higher than $k_B T$. Hence it is safe to assume that the particles never leave the interface once they are adsorbed. Under these conditions, the Ward and Tordai model[34] gives:

$$\Gamma = 2C\sqrt{\frac{Dt}{\pi}} \tag{4.3}$$

where, Γ is the adsorbed molar mass, C is the bulk concentration and D is the diffusion co-efficient of the particles.

Using the experimental Π v/s Γ curves obtained in figure 4.2, I convert the $\Pi(t)$ data into $\Gamma(t)$ data and then plot Γ v/s C $t^{1/2}$ as shown in figure 4.5. I scale the time axis with concentration expecting the curves to collapse onto a single curve. What I observe is that the initial growth of Γ follows the $t^{1/2}$ dependence quite well. This is followed by a concentration dependent slowing down in the relaxation of Γ at long times as the system

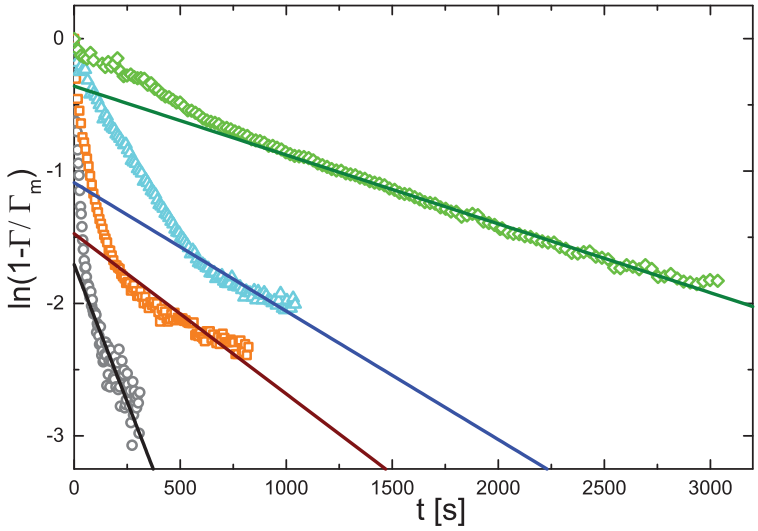

Figure 4.6: ln(1 - Γ/Γ_m) as a function of time for various bulk concentration of microgel particles: (◇)0.10 g/l, (△)0.20 g/l, (□)0.50 g/l, (○)1.00 g/l. Solid lines are straight line fits.

approaches saturation. The inset in figure 4.5 shows the individual Γ v/s $t^{1/2}$ curves for different bulk concentration of particles. The solid lines are straight line fits to the initial part of the experimental data (open symbols). The initial slope of each curve yields a value for the diffusion coefficient D. For comparison, the dashed lines are drawn with slopes calculated using D obtained from Dynamic Light Scattering (DLS) ($D_{DLS} = 7.29 \times 10^{-13} m^2/s$). As can be seen, they do not deviate very much from the experimental curves. Alternatively, I can determine D from best fits to the data. Table 1 gives the values of D as obtained by fitting straight lines (solid lines) to the experimental results for different bulk concentration and compares them to the value obtained from DLS. The values so obtained do not deviate by more than 10% from the ones measured by DLS.

As the system approaches saturation, the fall in $\Gamma(t)$ must slow down as the surface gets crowded. The concentration of the adsorbate just below

Table 4.2: Values of rate constant $k(1/s)$ for various concentrations calculated from the experimental curves in Fig 6.

Conc(g/l)	Conc(mol/m^3)	$k(1/s)$
0.10	5.495×10^{-8}	5.21×10^{-4}
0.20	1.099×10^{-7}	9.70×10^{-4}
0.50	2.747×10^{-7}	1.21×10^{-3}
1.00	5.495×10^{-7}	4.13×10^{-3}

the surface then falls out of equilibrium with the adsorbed species and the kinetics becomes limited by an adsorption barrier. A first order kinetic process then leads to:

$$\frac{d\Gamma}{dt} \sim k\,(\Gamma_{\max} - \Gamma) \tag{4.4}$$

where, k is the rate constant that is related to the adsorption barrier. Ideally, k should be proportional to the local solute concentration below the interface. This leads to an exponential relaxation:

$$\Gamma = \Gamma_{\max}\left(1 - e^{-kt}\right) \tag{4.5}$$

Figure 4.6 shows that such a barrier controlled regime does indeed exist at long times. The open symbols are the experimental values for $ln(1 - \Gamma/\Gamma_{\max})$. At long times, the curves fit a straight line as denoted by the solid lines. The slopes of the solid lines can be identified to the inverse of a kinetic relaxation time which is $1/k$.

As shown in Table 2, the rate constant depends on the bulk concentration of the microgel particles. But the dependence is not linear. This presumably indicates that the adsorption process itself is rather complex and depends on details of the configuration of the particles at the interface. A deeper analysis of these aspects is beyond the scope of the present work.

4.5 Conclusions

PNIPAM microgels adsorb readily to an air-water interface owing to their polymeric nature. I have experimentally established a 2D equation of state for such soft microgel particles adsorbed onto an air water interface. The pressure area isotherms give a measurable pressure even at average inter-particle distances much larger than their hydrodynamic diameter in the bulk. This confirms the fact that the particles deform substantially at the interface. Using a simple scaling argument I show that the deformation of particles is of the same order as the inter-particle distance at very low loadings resulting in a very small yet measurable pressure. This pressure at low loadings indirectly probes the internal elasticity of the particles, which is related to the internal cross link density. Experimental observations of an EOS match the scaling relation proposed by Groot and Stoyanov. The length scale $d_{eff} = 1.25$ nm that arises out of this scaling relation can be seen as an effective distance between the cross-links. The deviations from the scaling relation at very high loadings may be attributed to buckling of the interfacial layer or to partial desorption of the peripheral polymeric chain segments due to compression.

Using the experimental EOS, I study the adsorption dynamics of these microgel particles on to air-water interface. I find that the adsorption process can be clearly separated into two regimes. At short times, the adsorption process is controlled by the diffusion of the particles from bulk to the interface. At long times, the interface gets filled with particles thereby creating a barrier for newer particles to adsorb onto the interface. This leads to an exponential relaxation of Γ.

4.6 Acknowledgements

I would like to thank Prof. Vinod Subramaniam for letting me use the Kibron μ-trough and Mr. Aditya Iyer with his help in the experiments on the Kibron μ-trough. I also thank Dr. Arun Banpurkar for his ideas and discussions.

Bibliography

[1] Bastian Brugger and Walter Richtering. Emulsions stabilized by stimuli-sensitive poly(n-isopropylacrylamide)-co-methacrylic acid polymers: Microgels versus low molecular weight polymers. *Langmuir*, 24(15):7769–7777, 2008.

[2] Bastian Brugger, Brian A. Rosen, and Walter Richtering. Microgels as stimuli-responsive stabilizers for emulsions. *Langmuir*, 24(21):12202–12208, 2008.

[3] Mathieu Destribats, Veronique Lapeyre, Melanie Wolfs, Elisabeth Sellier, Fernando Leal-Calderon, Valerie Ravaine, and Veronique Schmitt. Soft microgels as pickering emulsion stabilisers: role of particle deformability. *Soft Matter*, 7(17):7689–7698, 2011.

[4] Bernard P. Binks. Particles as surfactants—similarities and differences. *Current Opinion in Colloid & Interface Science*, 7(1–2):21–41, 2002.

[5] L. Andrew Lyon and Alberto Fernandez-Nieves. The polymer/colloid duality of microgel suspensions. *Annual Review of Physical Chemistry*, 63(1):25–43, 2012.

[6] Bastian Brugger, Jan Vermant, and Walter Richtering. Interfacial layers of stimuli-responsive poly-(n-isopropylacrylamide-co-methacrylicacid) (pnipam-co-maa) microgels characterized by interfacial rheology and compression isotherms. *Physical Chemistry Chemical Physics*, 12(43):14573–14578, 2010.

[7] Mathieu Destribats, Véronique Lapeyre, Elisabeth Sellier, Fernando Leal-Calderon, Valérie Ravaine, and Véronique Schmitt. Origin and control of adhesion between emulsion drops stabilized by thermally sensitive soft colloidal particles. *Langmuir*, 28(8):3744–3755, 2012.

[8] Karen Geisel, Lucio Isa, and Walter Richtering. Unraveling the 3d localization and deformation of responsive microgels at oil/water in-

terfaces: A step forward in understanding soft emulsion stabilizers. *Langmuir*, 28(45):15770–15776, 2012.

[9] Zifu Li, Karen Geisel, Walter Richtering, and To Ngai. Poly(n-isopropylacrylamide) microgels at the oil-water interface: adsorption kinetics. *Soft Matter*, 9(41):9939–9946, 2013.

[10] To Ngai, Sven Holger Behrens, and Helmut Auweter. Novel emulsions stabilized by ph and temperature sensitive microgels. *Chemical Communications*, (3):331–333, 2005.

[11] Yann Cohin, Maelle Fisson, Kévin Jourde, GeraldG Fuller, Nicolas Sanson, Laurence Talini, and Cécile Monteux. Tracking the interfacial dynamics of pnipam soft microgels particles adsorbed at the air–water interface and in thin liquid films. *Rheologica Acta*, 52(5):445–454, 2013.

[12] Sarah L. Kettlewell, Andreas Schmid, Syuji Fujii, Damien Dupin, and Steven P. Armes. Is latex surface charge an important parameter for foam stabilization? *Langmuir*, 23(23):11381–11386, 2007.

[13] Robert D. Groot and Simeon D. Stoyanov. Equation of state of surface-adsorbing colloids. *Soft Matter*, 6(8):1682–1692, 2010.

[14] Sarah Höfl, Lothar Zitzler, Thomas Hellweg, Stephan Herminghaus, and Frieder Mugele. Volume phase transition of "smart" microgels in bulk solution and adsorbed at an interface: A combined afm, dynamic light, and small angle neutron scattering study. *Polymer*, 48(1):245 – 254, 2007.

[15] Mathieu Destribats, Mayalen Eyharts, Véronique Lapeyre, Elisabeth Sellier, Imre Varga, Valérie Ravaine, and Véronique Schmitt. Impact of pnipam microgel size on its ability to stabilize pickering emulsions. *Langmuir*, 30(7):1768–1777, 2014.

[16] Marta Horecha, Volodymyr Senkovskyy, Alla Synytska, Manfred Stamm, Alexander I. Chervanyov, and Anton Kiriy. Ordered surface structures from pnipam-based loosely packed microgel particles. *Soft Matter*, 6(23):5980–5992, 2010.

[17] Roberta Acciaro, Tibor Gilanyi, and Imre Varga. Preparation of monodisperse poly(n-isopropylacrylamide) microgel particles with homogenous cross-link density distribution. *Langmuir*, 27(12):7917–7925, 2011.

[18] X. Wu, R. H. Pelton, A. E. Hamielec, D. R. Woods, and W. McPhee. The kinetics of poly(n-isopropylacrylamide) microgel latex formation. *Colloid and Polymer Science*, 272(4):467–477, 1994.

[19] Shuiqin Zhou, Shiyan Fan, Steve C. F. Au-yeung, and Chi Wu. Light-scattering studies of poly(n-isopropylacrylamide) in tetrahydrofuran and aqueous solution. *Polymer*, 36(7):1341–1346, 1995.

[20] Imre Varga, Tibor Gilányi, Róbert Mészáros, Genoveva Filipcsei, and Miklós Zrínyi. Effect of cross-link density on the internal structure of poly(n-isopropylacrylamide) microgels. *The Journal of Physical Chemistry B*, 105(38):9071–9076, 2001.

[21] Rielle de Ruiter, R. Willem Tjerkstra, Michel H. G. Duits, and Frieder Mugele. Influence of cationic composition and ph on the formation of metal stearates at oil–water interfaces. *Langmuir*, 27(14):8738–8747, 2011.

[22] M.J. Garcia-Salinas, M.S. Romero-Cano, and F.J. de las Nieves. Electrokinetic characterization of poly(n-isopropylacrylamide) microgel particles: Effect of electrolyte concentration and temperature. *Journal of Colloid and Interface Science*, 241(1):280 – 285, 2001.

[23] Omkar S. Deshmukh, Armando Maestro, Michel H. G. Duits, Dirk van den Ende, Martien Cohen Stuart, and Frieder Mugele. Adsorption and interactions of soft microgel particles at oil-water interfaces. Manuscript in preparation, 2014.

[24] Walter Richtering. Responsive emulsions stabilized by stimuli-sensitive microgels: Emulsions with special non-pickering properties. *Langmuir*, 28(50):17218–17229, 2012.

[25] Anna Burmistrova, Marcel Richter, Michael Eisele, Cagri Üzüm, and Regine von Klitzing. The effect of co-monomer content on the swelling/shrinking and mechanical behaviour of individually adsorbed pnipam microgel particles. *Polymers*, 3(4):1575–1590, 2011.

[26] Eko H. Purnomo, Dirk van den Ende, Siva A. Vanapalli, and Frieder Mugele. Glass transition and aging in dense suspensions of thermosensitive microgel particles. *Phys. Rev. Lett.*, 101:238301, Dec 2008.

[27] A. Mulero, editor. *Theory and Simulation of Hard-Sphere Fluids and Related Systems*. Lecture Notes in Physics. Springer, Berlin, 2008.

[28] A. Mulero, I. Cachadiña, and J. R. Solana. The equation of state of the hard-disc fluid revisited. *Molecular Physics*, 107(14):1457–1465, 2009.

[29] Douglas Henderson. Monte carlo and perturbation theory studies of the equation of state of the two-dimensional lennard-jones fluid. *Molecular Physics*, 34(2):301–315, 1977.

[30] Christian Fänger, Holger Wack, and Mathias Ulbricht. Macroporous poly(n-isopropylacrylamide) hydrogels with adjustable size "cut-off" for the efficient and reversible immobilization of biomacromolecules. *Macromolecular Bioscience*, 6(6):393–402, 2006.

[31] Shengtong Sun and Peiyi Wu. A one-step strategy for thermal- and ph-responsive graphene oxide interpenetrating polymer hydrogel networks. *J. Mater. Chem.*, 21:4095–4097, 2011.

[32] Chien Hsiang Chang and Elias I. Franses. Adsorption dynamics of surfactants at the air/water interface: a critical review of mathematical models, data, and mechanisms. *Colloids and Surfaces A: Physicochemical and Engineering Aspects*, 100(0):1 – 45, 1995.

[33] Hernan Ritacco, Dominique Langevin, Haim Diamant, and David Andelman. Dynamic surface tension of aqueous solutions of ionic surfactants: Role of electrostatics. *Langmuir*, 27(3):1009–1014, 2011.

[34] A. F. H. Ward and L. Tordai. Timedependence of boundary tensions of solutions i. the role of diffusion in timeeffects. *The Journal of Chemical Physics*, 14(7):453–461, 1946.

5 Effect of temperature on equation of state and adsorption dynamics of soft microgel particles on an air-water interface.

Abstract In the previous chapter, an equation of state (EOS) was experimentally determined for PNIPAM microgel particles spread on an air-water interface at room temperature.This EOS was used to study the adsorption dynamics of microgel particles. In this chapter I extend the work carried out in the previous chapter to study the effect of temperature on the EOS and consequently on the adsorption dynamics. It is observed that the interfacial layer appears to become softer with increasing temperature. This softness is a combined result of long range electrostatic repulsion and short range attraction between microgel particles induced by the hydrophobic interactions of the polymer segments which leads to formation of an open network of particles. The complete adsorption process can be explained using a simple model that assumes diffusion limited adsorption at the beginning and at long times limited by an adsorption barrier. The model was fitted to the experimental data to extract parameters like the diffusion co-efficient (D), adsorption rate constant (K) and the equilibrium surface concentration (Γ_∞).

5.1 Introduction

Emulsions are thermodynamically metastable systems. Their unstable nature is a critical issue in a variety of well-established industrial applications ranging from pharmaceutical, food and cosmetics to oil-recovery [1, 2]. Colloidal particles can attach to oil/water interfaces achieving the stabilization of oil droplets to achieve surfactant-free emulsions. Such particle-stabilized emulsions are known as (Ramsden)-Pickering emulsions[3, 4]. The efficiency of partially hydrophobic particles in the stabilization of emulsions is related to their ability to irreversibly adsorb at fluid interfaces[5]. Furthermore, the stability of Pickering emulsions also comes from the strong repulsion produced by steric interactions and long-range electrostatic forces between layers of colloidal particles sitting at the interface of droplets.

Lately, microgel particles (swollen colloidal particles consisting of cross-linked soluble polymers) have shown great promise as Pickering stabilizers of emulsions and foams[6–9]. The fact that they are particles makes them adsorb very strongly to the interface with adsorption energies in order of hundreds of k_BT or more[5]. Having said that, their swollen polymeric character facilitates attachment from solution to fluid interfaces in comparison to solid particles[5, 10]. What makes these systems really interesting is the possibility of tuning the stability of such emulsions by exploiting the stimuli responsive behaviour of the polymer microgels. A deeper understanding of the adsorption mechanism and the interactions between these particles on fluid interfaces and how these change with external stimuli is vital in the context of design of smart particles for specific applications.

Microgels based on thermosensitive polymer Poly N-Isopropyl acrylamide (PNIPAM) undergo volume phase transition at temperatures around the body temperature and therefore are considered promising for applications such as thermo-stimulated drug delivery and smart emulsions. Given the interest these systems have generated in the scientific community, there have been various studies of adsorbed microgel layers[11–16]. Yet the precise knowledge of the adsorption dynamics and

the nature of interparticle interactions is still lacking. Especially the effect of external stimuli such as temperature on the adsorption, particle morphology and interactions at an interface and their relation to the stability/instability of emulsions is yet unexplored.

It is well known that the microgel particles deform substantially upon adsorption on to both solid - liquid[17] and liquid - liquid[8, 12, 18, 19] interfaces resulting in 'sombrero' or 'fried egg-like' morphologies. In our previous work[20], I experimentally measured the equation of state for a layer of particles spread on an air-water interface. I show that the deformation of microgels results in a measurable surface pressure at very low concentrations whereas standard hard-disk models predict pressures that are orders of magnitude lower than the observed pressures. In this chapter I extend our previous work to probe the effect of temperature on the equation of state and consequently on the adsorption kinetics of microgel particles on an air-water interface.

5.2 Materials

The PNIPAM particles are synthesized by a batch suspension polymerization using a recipe that has been described in literature[21, 22]. We used N-isopropyl acrylamide (NIPAM) as monomer with N, N'-methylenebisacrylamide as the cross linker (2 mol%) and potassium persulfate as the initiator for the polymerization reaction. We expect the particles to carry a small amount of charge due to the potassium persulfate used in the initiation step. The particles are purified by repeatedly centrifuging at 18000 g and replacing the supernatant with fresh Milli-Q water. The process is repeated at least 5 times. The particles are then freeze dried and stored. The suspension is prepared by weighing a calculated amount of the freeze dried particles and simply adding them to Milli-Q water to get the desired concentration. The suspension is stirred for at least 24 hours before use. Doing so, we prepare a stock solution of 0.5 g/l concentration. Samples of lower concentration are prepared by diluting this stock solution.

5.3 Experimental methods

5.3.1 Particle Characterisation

The temperature dependent size of the microgel particles is determined by both Dynamic Light Scattering (DLS) and Static Light Scatering (SLS). The DLS measurements are performed using a Malvern Zeta Sizer. The Stokes-Einstein relation ($D = k_B T/6\pi\eta R_H$, where k_B is the Boltzmann constant, T is the absolute temperature and η is the viscosity of the solvent) is used to calculate the hydrodynamic diameter (D_H) from the measured diffusion coefficient (D) of the particles measured with DLS. The variation of D_H with temperature was shown previously in Chapter 3 (figure 3.2(a)). With SLS the molar mass and the light scattering radius (R_{SLS}) (for an equivalent homogeneous sphere) of these particles are determined by fitting the form factor to the recorded data. R_{SLS} is given in figure 3.2(b). The molar mass of the particles is The molar mass of the particles is 1.82×10^6 kg/mol.

5.3.2 LB Pressure-Area isotherms

The equation of state (Pressure versus Adsorbed mass relationship) is determined using a Langmuir trough. All the experiments are carried out on a Kibron μ-trough Langmuir apparatus. The temperature of the trough is controlled by means of a heating plate placed beneath the trough. The heating plate is connected to a LAUDA RE306 water bath fitted with a temperature controller. The temperature on the surface of the trough is separately monitored using a thermocouple. The entire trough is covered by an acrylic casing to prevent any disturbances from ambient air currents. I place a wet paper inside the casing to ensure that the evaporation losses at higher temperatures are minimised. I also recalibrate the pressure sensor at each temperature taking into account the changes in the value of bare air-water interfacial tension with temperature[23]. Firstly the air water interface is carefully cleaned until a point where the pressure – area compression cycle shows a perfectly horizontal line and the pressure at maximum compression is < 0.1 mN/m. Then a known amount of parti-

cles is spread on the clean air-water interface and the area of the interface is systematically reduced. The resultant change in pressure is recorded by a pressure sensor using a DyneProbe. The maximum and minimum possible areas in the Kibron μ-trough are 51.50 cm^2 and 3.25 cm^2, respectively. I spread 100 μl of a suspension of 0.025 g/l concentration.The drops are carefully placed on the interface using a 10 μl syringe with a sharp tip by holding the needle very close and parallel to the interface. It is ensured that the drops are evenly deposited over the initial spreading area and a waiting time of at least 30 minutes is allowed for the system to stabilize before starting the measurements. The compression rate is kept low (5 cm^2/min). The reproducibility of the experiments is checked by repeating them under the same conditions. I also check for hysteresis between the compression and the expansion cycles. The hysteresis in the pressure is < 2 mN/m. Compression-expansion cycles are repeated and no evidence for particle detachment is found in any experiment. Each cycle is repeated atleast 3 times to ensure reproducibility of experiments.

5.3.3 Interfacial tension measurements

I use a Dataphysics OCA 20L apparatus to measure the surface tension of microgel particle laden interfaces. I create an air bubble in the suspensions of varying concentrations using an inverted needle. The interfacial tension (γ) is calculated with a resolution ± 0.01 mN/m by image analysis from the shape of the bubble using the well-known Laplace equation (See chapter 3). We convert the values of interfacial tension into surface pressure(Π) by using the correlation $\Pi(t) = \gamma_0 - \gamma(t)$. Where γ_0 is the value of bare air-water interfacial tension. For the interfacial tension measurements to be accurate, we make sure that the bubble is big enough to deform substantially under the buoyancy forces. The Bond number is defined as $Bo = \Delta\rho g R^2/\gamma$, where, $\Delta\rho$ is the density difference between the fluids, g is the acceleration due to gravity, R is the radius of the drop and γ is the interfacial tension. It is a measure of the interplay between the gravity/buoyancy and surface forces. For accurate measurements, it is advised that Bo should always lie between 0.1 and 1[24]; we check this to be

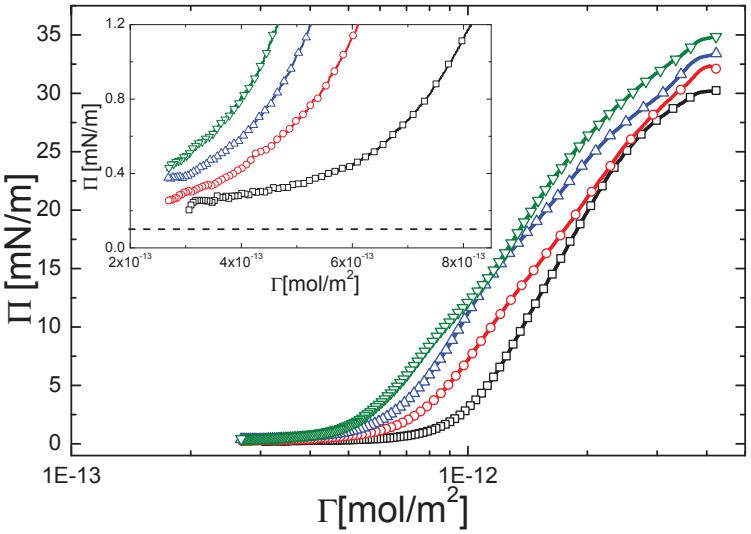

Figure 5.1: Surface pressure(Π) versus amount of PNIPAM particles adsorbed (Γ) on an air-water interface. The open symbols denote experimental data points corresponding to different temperatures : (□) 24°C, (◯) 28°C, (△) 32°C and (▽) 36°C. Inset shows expanded view of the pressure versus adsorbed amount curves at low loadings. The dashed line in the inset denotes the detection limit of the pressure sensor.

the case in all our measurements. Like the surface pressure experiments, all tensiometry measurements are carried out at room temperature.

5.4 Results

The pressure-area isotherms for 4 different temperatures are obtained from compression of spread monolayers on a Langmuir trough. The Pressure versus area per molecule data, as obtained from the LB experiments is converted into Pressure versus adsorbed amount curves as shown in figure 5.1, using the relation $\Gamma = 1/(A \times N_{Av})$ where A is the area/particle and N_{Av} is the Avogadro's number. These curves represent the 2D equation of state (EOS) for the given temperatures. The pressure versus adsorbed

amount curves as shown in figure 5.1 show low, yet finite surface pressures at very low loadings. The curves seem to be touching each other at low loadings. However, when we blow up the graph and look closely at the data for very low loadings we observe that the surface pressure at low loadings also is apparently affected by increasing the temperature. It must however be noted that owing to sensitivity issues, the pressure readings below 1 mNm may not be very accurate. The error bars for pressure values 1 mN/m are of the order of 0.5 mN/m. Even if we consider only the pressure values from 1 mN/m onwards, the corresponding effective area per particle at 1 mN/m increases approximately by a factor of 2 with increasing temperature. Pinaud *et al.*[25] perform similar compression experiments of microgel particles at an air-water interface. They are able to scan a much wider range of areas. They propose that the increase in pressure is due to the peripheral brush like polymer segments coming in contact with each other. Upon further compression, the pressure reaches a plateau. Our experiments are carried out in a range where only the onset to this plateau is visible.

In their recent work, Geisel *et al.*[26] show that the microgel layers produced by compression of spread monolayers and the ones formed by spontaneous adsorption are very similar. Hence the EOS can thus be safely used in the study of adsorption kinetics of these particles at an air water interface. For this we monitor the interfacial tension of a freshly prepared air bubble in a suspension of PNIPAM microgel particles as a function of time using the pendant drop method. I measure the decay in the interfacial tension as a function of time for 2 concentrations 1.0 g/l and 0.5 g/l as shown in figure 5.2(a). For each concentration measurements are performed at 4 different temperatures namely 24°C, 28°C, 32°C, 36°C as shown in figure 5.2(b). Each measurement at a given temperature and concentration is repeated atleast 3 times to ensure consistency. Since the values of bare air-water interfacial tension as a function of temperature are known[23], the interfacial tension can also be expressed as surface pressure. The increase in pressure is as expected slower for lower concentrations as seen in figure 5.2(a). A quick rough calculation indicates that the pressure scales as square of concentration which is indicative of

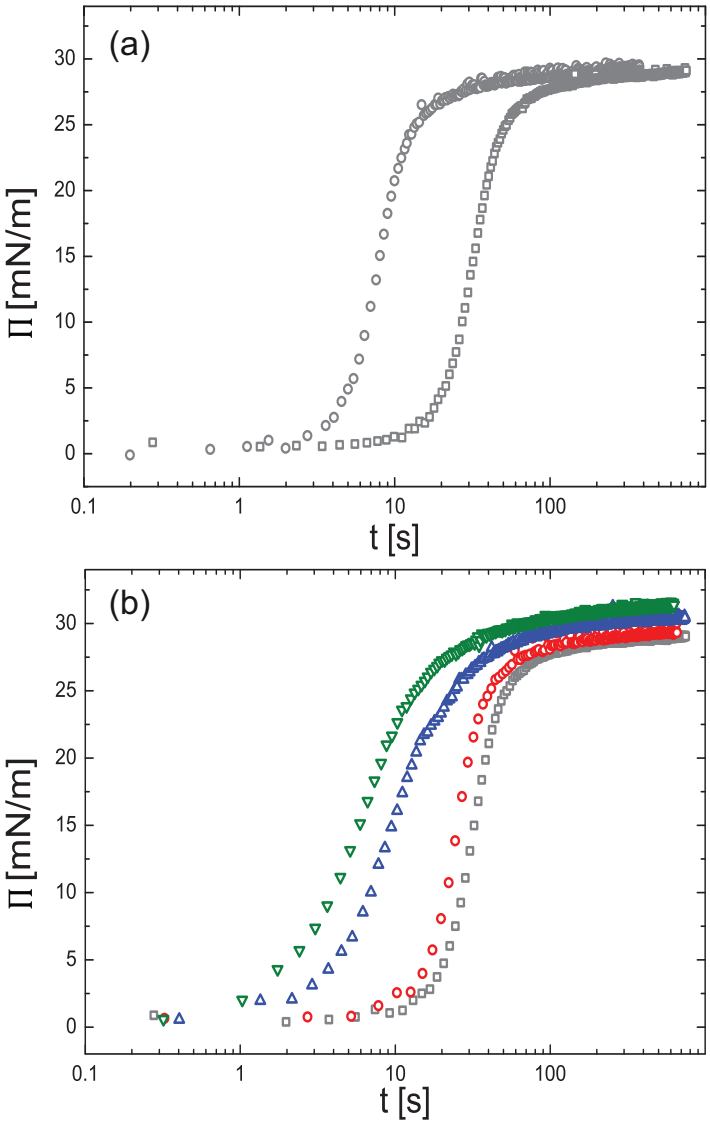

Figure 5.2: Measurement of surface pressure over time. (a)Surface pressure as a function of time for various concentrations: (□)0.5g/l and (○)1.0g/l measured at 24°C. (b) Surface pressure as a function of time for 0.5g/l for various temperatures: (□) 24°C, (○) 28°C, (△) 32°C and (▽) 36°C.

diffusive transport of particles. The particles shrink with increasing temperature. This means that they will diffuse faster at higher temperatures. This is reflected in a faster increase in the surface pressure as seen in figure 5.2(b).

Now coming back to my EOS measurements. I express the surface concentration as a function of surface pressure by fitting the EOS data with a smoothing spline in MATLAB. I use the fit results to convert the $\Pi(t)$ data obtained using the pendant drop measurements into $\Gamma(t)$ data.

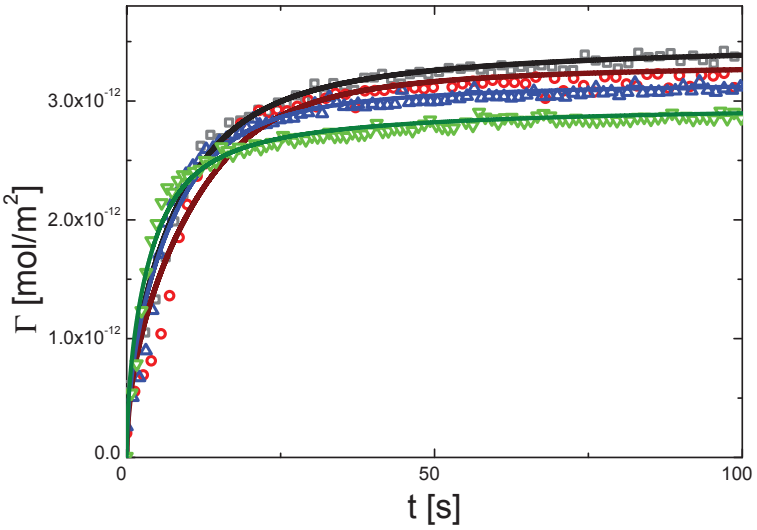

Figure 5.3: Evolution of surface concentration as a function of time for 1.0g/l PNIPAM suspension for various temperatures, (□) 24°C, (◯) 28°C, (△) 32°C and (▽) 36°C. Solid lines are the fit to the experimental data generated using the model described in section 5.4.1

5.4.1 Adsorption process: Mathematical model

For modelling the adsorption process, the classical approach involves separating the physical process into two steps. (i) The transport of particles

from the bulk to a thin sublayer just beneath the interface and (ii) adsorption from the sublayer onto the interface. For particles adsorbing onto a initially bare interface in absence of any external flow fields, the transport of particles is governed by Fickian diffusion described as:

$$\frac{\partial c}{\partial t} = D\frac{\partial^2 c}{\partial x^2} \tag{5.1}$$

The drop provides a finite interfacial area for the particles to adsorb. Since these particles are irreversibly adsorbed on the interface, each adsorbing particle reduces the possible number of adsorption sites for the subsequent particles. This kinetic process can be described as:

$$\frac{\partial \Gamma}{\partial t} = kc_0(\Gamma_\infty - \Gamma)^q \tag{5.2}$$

Where k is the rate constant, c_0 is the concentration of particles in the sublayer and Γ_∞ is the equilibrium surface concentration.

Assuming that the interface is initially bare and that there are no concentration gradients within the drop, the initial conditions can be given as:

$$\Gamma(0) = 0 \tag{5.3}$$

$$c(x,0) = c_\infty \tag{5.4}$$

Similarly, the boundary conditions are:

$$D\left(\frac{\partial c}{\partial x}\right)_{x=0} = \frac{\partial \Gamma}{\partial t} \tag{5.5}$$

$$c(\infty,t) = c_\infty \tag{5.6}$$

Equations 5.1 and 5.2 can be solved numerically to predict the evolution of $\Gamma(t)$. The details of the numerical calculations and the algorithm are provided as an appendix to this chapter. A MATLAB routine fits the numerical solution to the experimental data as shown in figure 5.3. The fit parameters are defined as:

$$Q = \sqrt{\frac{K\Gamma_\infty^2}{Dc_\infty}}, \qquad t_* = \frac{1}{Kc_\infty} \tag{5.7}$$

Q and t_* can be used to calculate more tangible physical parameters such as the diffusion co-efficient(D), rate constant(K) and equilibrium surface concentration(Γ_∞). The pendant drop measurement technique is not very accurate is measurement of surface pressures below 1mN/m. Hence the Π(t) data contains a lot of scatter especially within the first few seconds after creation of the drop. This scatter also transcends into the Γ(t) data. Hence for our fit, we ignore the data points for the first few seconds.

5.5 Discussion

The pressure versus surface loading curves presented in figure 5.1 provide many interesting insights into the inter-particle interactions and morphology of these soft particles at an interface. I observe detectable surface pressures even at very low loadings for all temperatures. I have previously established that this finite pressure is a result of deformation of the particles upon adsorption to the air-water interface. This explanation seems plausible when the particles are in a swollen state. But at higher temperatures the particles are collapsed in the bulk. So the hypothesis that these particles also deform upon adsorption to the interface on the outset, is counter-intuitive.

The collapse of particles in the bulk at higher temperatures is entropically driven. However when these particles arrive at the interface, they experience a deforming force which is countered by the elasticity of the particles. This deformation causes an additional gain in the free energy. In short, upon reaching the interface, the particles may lose some free energy by losing their collapsed state, but they gain more energy by spreading out along the interface. So the scenario that the particles deform at the interface irrespective of whether they are swollen or collapsed in the bulk does seem plausible. Another interesting observation is that as the temperature increases, the surface pressure, even at low loadings is slightly higher as shown in the inset in figure 5.1. This suggests that at higher temperatures, the origin of surface pressure does not simply lie in the steric interactions between particles. At temperatures above the VPTT, the shrinking of the particles cause an increase in the charge density and

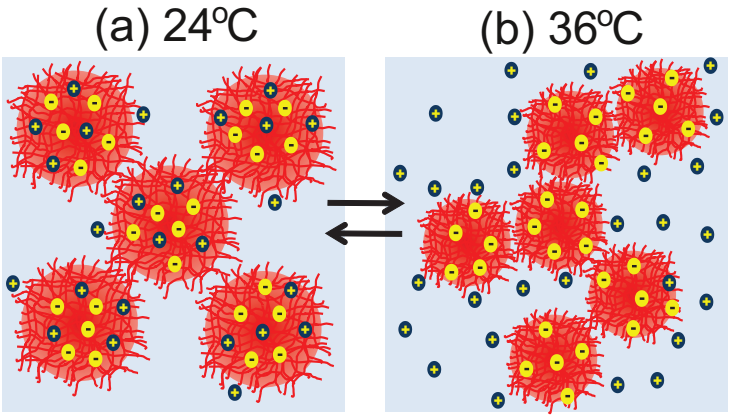

Figure 5.4: Schematic description of the conformational changes in the particles at interface as a function of temperature.

thereby an increase in the electrostatic interactions between the particles. The asymmetry in the charge dissociation at the interface causes the particles to act like dipoles which increases the range as well as the strength of the electrostatic repulsion. But the shrinking of these particles also induce short range attractive forces due to the interactions between hydrophobic polymer segments. These findings of increased electrostatic repulsion are exactly opposite to the findings of Geisel *et al.*[27], who report that higher charge in the microgel particles leads to reduced replusion amongst particles at the interface. Thus a combination of long range electrostatic repulsion and short range attractions leads the microgels to form a percolating network at the interface. Thus the morphology of the microgel monolayer at the interface changes from ordered, dense layer of particles to an open network consisting of clusters of particles as shown in figure 5.4. This transformation is evident from the change in the compression isotherms. At temperatures above the VPTT, the compression isotherms show an increasingly softer response. Such a transformation in the interfacial microstructure from a dense and ordered structure to a clustered network of particles has been previously reported[8, 11, 28].

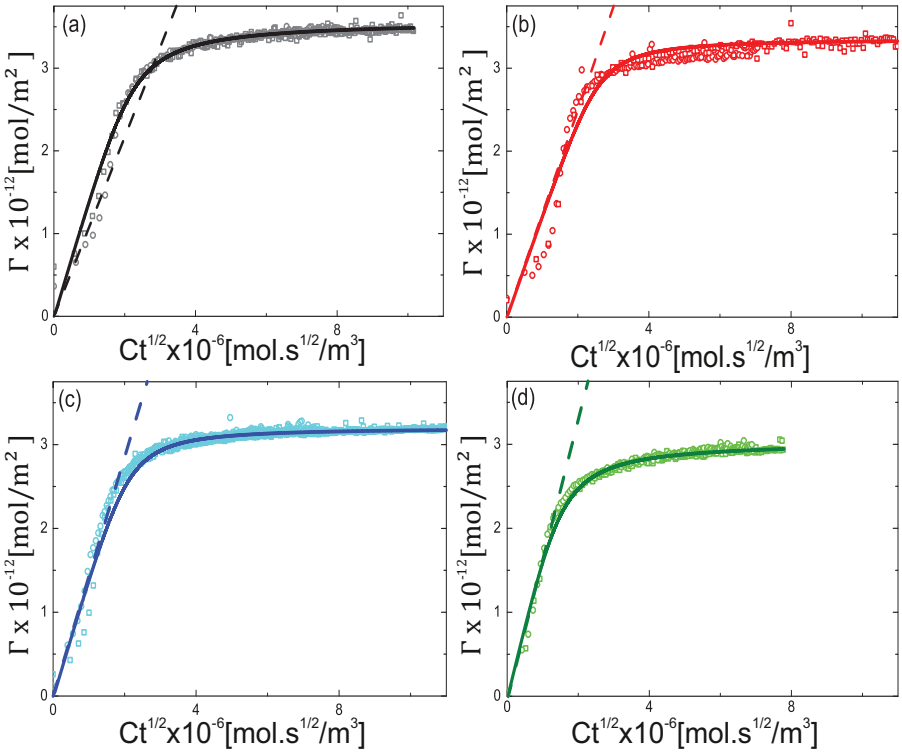

Figure 5.5: Adsorbed amount (Γ) as a function of product $Ct^{1/2}$ for various temperatures: (a)24°C, (b)28°C, (c)32°C and (d)36°C. The dashed lines denote a slope $2\sqrt{D/\pi}$, where D is the diffusion co-efficient measured using DLS. The solid lines denote the fits of the model to the experimental data.

However, these findings are for pH responsive microgels as a response to a change in pH. Whether similar underlying mechanisms also play a role in case of thermoresponsive microgel particles is unclear. The electrostatic interactions are discussed in greater detail in the next chapter.

At short times the adsorption is governed by the diffusion of particles from bulk to the interface. In this case, the evolution of surface concentration with time can be predicted by the well known Ward & Tordai

Table 5.1: Values of diffusion co-efficient D (m^2/s) for various temperatures calculated from fitting the adsorption model to the experimental $\Gamma(t)$ curves and values of D measured using DLS.

Temperature(°C)	$D_{fit}(m^2/s)$	$D_{DLS}(m^2/s)$
24	$1.51 \pm 0.14 \times 10^{-12}$	9.22×10^{-13}
28	$1.29 \pm 0.05 \times 10^{-12}$	1.22×10^{-12}
32	$1.74 \pm 0.35 \times 10^{-12}$	1.71×10^{-12}
36	$2.61 \pm 0.32 \times 10^{-12}$	2.75×10^{-12}

equation[29]:

$$\Gamma = 2c_\infty \sqrt{\frac{Dt}{\pi}} \tag{5.8}$$

For each temperature, the data is plotted as Γ versus $Ct^{1/2}$ as shown in figure 5.5. The surface concentration data collapses nicely. For all temperatures, the initial part of the $\Gamma(t)$ curve scales as $t^{1/2}$. However since the study is limited to relatively high bulk concentrations of PNIPAM microgels, this diffusive regime is later taken over by a regime where the adsorption is controlled by a barrier created due to crowding of particles at the interface. Such a crossover from diffusion limited to barrier limited adsorption has been previously observed for other surface active materials as well[30, 31]. Fitting the adsorption model described in section 5.4.1, it is possible to calculate the value of diffusion co-efficient D from the fit parameters Q and t_*. Alternatively, D can also be measured by DLS using the Stokes-Einstein relation. Values of D calculated by both the above methods are listed in table 5.1 and are found to be in fair agreement.

As the system approaches saturation, the rate of surface adsorption also slows down considerably. This happens due to crowding of the particles at the interface. In such a scenario, the concentration of the particles in the sub layer just beneath the interface falls out of equilibrium with the

Table 5.2: Values of adsorption rate constant K (m^3/mol.s) and equilibrium surface concentration Γ_∞ (mol/m^2) for various temperatures calculated by fitting the adsorption model to the experimental $\Gamma(t)$ curves.

Temperature(°C)	K(m^3/mol.s)	Γ_∞(mol/m^2)
24	$3.23 \pm 2.37 \times 10^6$	$3.48 \pm 0.08 \times 10^{-12}$
28	$8.64 \pm 4.06 \times 10^6$	$3.33 \pm 0.06 \times 10^{-12}$
32	$6.83 \pm 3.92 \times 10^6$	$3.20 \pm 0.04 \times 10^{-12}$
36	$4.88 \pm 1.04 \times 10^6$	$3.05 \pm 0.05 \times 10^{-12}$

particle already adsorbed and the kinetics become limited by an adsorption barrier. This process can be described by a general q^{th} order kinetic process as described in equation 5.2. It is possible to also include the order q as one of the fit parameters. But the fit results always yield values close to 2. Hence to improve the efficiency, we fix the value to q = 2.The fitting also yields other relevant physical parameters like the adsorption rate constant K and the final equilibrium concentration Γ_∞ the values of which are provided in table 5.2. As described in the appendix, the value of fit parameter Q determines whether the adsorption is limited by diffusion or by the adsorption barrier. For the range of temperatures and concentrations investigated in this study, the values of Q lie between 5 and 10. These values are high enough so that we can say that the adsorption process is predominantly diffusion limited. This in addition to the scatter in the $\Gamma(t)$ data results in the fitting to be relatively insensitive to the values of K. Thus we observe a very large scatter in the values of K.

The values of Γ_∞ however show a clear trend. The surface saturates at a lower surface concentration with increasing temperature. Thus, lesser amount of particles at the interface still result in higher surface pressures. These findings agree very well to our hypothesis of dense ordered monolayers at lower temperatures and open network consisting of clusters of

particles combined with higher electrostatic repulsion at higher temperatures, that we had put forth earlier.

5.6 Conclusions

Even at temperatures above the VPTT, PNIPAM microgel particles adsorb readily to an air-water interface. A temperature dependent experimental equation of state was established. The pressure-loading curves suggest that even if the particles are in a collapsed state in the bulk, they deform upon adsorption to the interface. Above the VPTT, the particles experience a long range interaction, which is most possibly electrostatic repulsion. This in addition to the short range attraction between polymer segments leads to formations of lose open networks consisting of clusters of particles at the interface. This results in a soft response to lateral compression of the monolayers.

This experimental EOS is used to study the adsorption dynamics of these microgel particles at an air-water interface. A simple model taking into account diffusion limited adsorption at short times followed by barrier limited adsorption created by particles filling the interface, describes the adsorption process fairly well. The full solution to this model is fitted to the experimental $\Gamma(t)$ values to extract values of diffusion coefficient (D). The values thus obtained are in good agreement with ones measured using DLS.

For the range of concentrations investigated, the adsorption process is predominantly governed by diffusion. Hence the fitting is insensitive to the values of K. The reduction in the equilibrium surface concentration Γ_∞ with increasing temperatures corroborates the hypothesis of formation of network of particles consisting of particle clusters as the temperature increases beyond VPTT.

5.7 Acknowledgements

I thank Prof. Vinod Subramaniam (AMOLF, Amsterdam) for letting me use the Kibron μ-trough for the LB experiments. I also thank Mr. Aditya Iyer for introducing me to the Kibron μ-trough and hosting me during my visit to AMOLF. I also thank Mariska van der Weide for her help with the IFT measurements.

Bibliography

[1] P. Becher. *Encyclopedia of Emulsion Technology*, volume 1. Marcel Dekker, New York, 1983.

[2] J. Sjoblom. *Encyclopedic Handbook of Emulsion Technology*. Marcel Dekker, New York, 2001.

[3] Spencer Umfreville Pickering. Cxcvi.-emulsions. *Journal of the Chemical Society, Transactions*, 91(0):2001–2021, 1907.

[4] W. Ramsden. Separation of solids in the surface-layers of solutions and 'suspensions' (observations on surface-membranes, bubbles, emulsions, and mechanical coagulation). – preliminary account. *Proceedings of the Royal Society of London*, 72(477-486):156–164, 1903.

[5] Bernard P. Binks. Particles as surfactants—similarities and differences. *Current Opinion in Colloid & Interface Science*, 7(1–2):21–41, 2002.

[6] Bastian Brugger and Walter Richtering. Emulsions stabilized by stimuli-sensitive poly(n-isopropylacrylamide)-co-methacrylic acid polymers: Microgels versus low molecular weight polymers. *Langmuir*, 24(15):7769–7777, 2008.

[7] Bastian Brugger, Brian A. Rosen, and Walter Richtering. Microgels as stimuli-responsive stabilizers for emulsions. *Langmuir*, 24(21):12202–12208, 2008.

[8] Mathieu Destribats, Veronique Lapeyre, Melanie Wolfs, Elisabeth Sellier, Fernando Leal-Calderon, Valerie Ravaine, and Veronique Schmitt. Soft microgels as pickering emulsion stabilisers: role of particle deformability. *Soft Matter*, 7(17):7689–7698, 2011.

[9] Véronique Schmitt, Mathieu Destribats, and Rénal Backov. Colloidal particles as liquid dispersion stabilizer: Pickering emulsions and materials thereof. *Comptes Rendus Physique*, (0):–, 2014.

[10] L. Andrew Lyon and Alberto Fernandez-Nieves. The polymer/colloid duality of microgel suspensions. *Annual Review of Physical Chemistry*, 63(1):25–43, 2012.

[11] Bastian Brugger, Jan Vermant, and Walter Richtering. Interfacial layers of stimuli-responsive poly-(n-isopropylacrylamide-co-methacrylicacid) (pnipam-co-maa) microgels characterized by interfacial rheology and compression isotherms. *Physical Chemistry Chemical Physics*, 12(43):14573–14578, 2010.

[12] Mathieu Destribats, Véronique Lapeyre, Elisabeth Sellier, Fernando Leal-Calderon, Valérie Ravaine, and Véronique Schmitt. Origin and control of adhesion between emulsion drops stabilized by thermally sensitive soft colloidal particles. *Langmuir*, 28(8):3744–3755, 2012.

[13] Karen Geisel, Lucio Isa, and Walter Richtering. Unraveling the 3d localization and deformation of responsive microgels at oil/water interfaces: A step forward in understanding soft emulsion stabilizers. *Langmuir*, 28(45):15770–15776, 2012.

[14] Zifu Li, Karen Geisel, Walter Richtering, and To Ngai. Poly(n-isopropylacrylamide) microgels at the oil-water interface: adsorption kinetics. *Soft Matter*, 9(41):9939–9946, 2013.

[15] To Ngai, Sven Holger Behrens, and Helmut Auweter. Novel emulsions stabilized by ph and temperature sensitive microgels. *Chemical Communications*, (3):331–333, 2005.

[16] Yann Cohin, Maelle Fisson, Kévin Jourde, GeraldG Fuller, Nicolas Sanson, Laurence Talini, and Cécile Monteux. Tracking the interfacial dynamics of pnipam soft microgels particles adsorbed at the air–water interface and in thin liquid films. *Rheologica Acta*, 52(5):445–454, 2013.

[17] Sarah Höfl, Lothar Zitzler, Thomas Hellweg, Stephan Herminghaus, and Frieder Mugele. Volume phase transition of “smart” microgels

in bulk solution and adsorbed at an interface: A combined afm, dynamic light, and small angle neutron scattering study. *Polymer*, 48(1):245 – 254, 2007.

[18] Mathieu Destribats, Mayalen Eyharts, Véronique Lapeyre, Elisabeth Sellier, Imre Varga, Valérie Ravaine, and Véronique Schmitt. Impact of pnipam microgel size on its ability to stabilize pickering emulsions. *Langmuir*, 2014.

[19] Marta Horecha, Volodymyr Senkovskyy, Alla Synytska, Manfred Stamm, Alexander I. Chervanyov, and Anton Kiriy. Ordered surface structures from pnipam-based loosely packed microgel particles. *Soft Matter*, 6(23):5980–5992, 2010.

[20] Omkar S. Deshmukh, Armando Maestro, Michel H. G. Duits, Dirk van den Ende, Martien Cohen Stuart, and Frieder Mugele. Equation of state and adsorption dynamics of soft microgel particles at an air-water interface. *Soft Matter*, 10:7045–7050, 2014.

[21] Roberta Acciaro, Tibor Gilanyi, and Imre Varga. Preparation of monodisperse poly(n-isopropylacrylamide) microgel particles with homogenous cross-link density distribution. *Langmuir*, 27(12):7917–7925, 2011.

[22] X. Wu, R. H. Pelton, A. E. Hamielec, D. R. Woods, and W. McPhee. The kinetics of poly(n-isopropylacrylamide) microgel latex formation. *Colloid and Polymer Science*, 272(4):467–477, 1994.

[23] N. B. Vargaftik, B. N. Volkov, and L. D. Voljak. International tables of the surface tension of water. *Journal of Physical and Chemical Reference Data*, 12(3):817–820, 1983.

[24] Rielle de Ruiter, R. Willem Tjerkstra, Michel H. G. Duits, and Frieder Mugele. Influence of cationic composition and ph on the formation of metal stearates at oil–water interfaces. *Langmuir*, 27(14):8738–8747, 2011.

[25] Florent Pinaud, Karen Geisel, Pascal Masse, Bogdan Catargi, Lucio Isa, Walter Richtering, Valerie Ravaine, and Veronique Schmitt. Adsorption of microgels at an oil-water interface: correlation between packing and 2d elasticity. *Soft Matter*, 10:6963–6974, 2014.

[26] Karen Geisel, Walter Richtering, and Lucio Isa. Highly ordered 2d microgel arrays: compression versus self-assembly. *Soft Matter*, 10:7968–7976, 2014.

[27] Karen Geisel, Lucio Isa, and Walter Richtering. The compressibility of ph-sensitive microgels at the oil–water interface: Higher charge leads to less repulsion. *Angewandte Chemie*, 126(19):5005–5009, 2014.

[28] Mathieu Destribats, Véronique Lapeyre, Elisabeth Sellier, Fernando Leal-Calderon, Véronique Schmitt, and Valérie Ravaine. Water-in-oil emulsions stabilized by water-dispersible poly(n-isopropylacrylamide) microgels: Understanding anti-finkle behavior. *Langmuir*, 27(23):14096–14107, 2011.

[29] A. F. H. Ward and L. Tordai. Timedependence of boundary tensions of solutions i. the role of diffusion in timeeffects. *The Journal of Chemical Physics*, 14(7):453–461, 1946.

[30] Chien Hsiang Chang and Elias I. Franses. Adsorption dynamics of surfactants at the air/water interface: a critical review of mathematical models, data, and mechanisms. *Colloids and Surfaces A: Physicochemical and Engineering Aspects*, 100(0):1 – 45, 1995.

[31] Hernan Ritacco, Dominique Langevin, Haim Diamant, and David Andelman. Dynamic surface tension of aqueous solutions of ionic surfactants: Role of electrostatics. *Langmuir*, 27(3):1009–1014, 2011.

5.8 Appendix

5.8.1 Introduction

We consider the adsorption of particles on an initially clean interface from a liquid reservoir. Due to the adsorption process, the particle concentration in the liquid near the interface, $c_0 = c(x = 0, t)$, is initially depleted. But it is soon re-established at its original value c_∞, by diffusion. In these notes we will investigate this process numerically.

5.8.2 Governing equations

The equations governing this process are given by:[1]

$$\frac{\partial c}{\partial t} = D\frac{\partial^2 c}{\partial x^2} \tag{5.9}$$

$$\frac{\partial \Gamma}{\partial t} = k c_0(\Gamma_\infty - \Gamma)^q \tag{5.10}$$

The initial and boundary conditions are given by:

$$\Gamma(0) = 0 \tag{5.11}$$

$$c(x, 0) = c_\infty \tag{5.12}$$

$$D\left(\frac{\partial c}{\partial x}\right)_{x=0} = \frac{\partial \Gamma}{\partial t} \tag{5.13}$$

$$c(\infty, t) = c_\infty \tag{5.14}$$

These expressions are made dimensionless by substituting:

$$x = L_*\ \xi, \qquad t = t_*\ \tau, \qquad c = c_\infty\ n, \qquad \Gamma = \Gamma_\infty\ \theta$$

which results in:

$$\frac{\partial n}{\partial \tau} = A\ \frac{\partial^2 n}{\partial \xi^2}\ , \qquad \frac{\partial \theta}{\partial \tau} = B\ n_0(1-\theta)^q\ , \qquad \left(\frac{\partial n}{\partial \xi}\right)_{\xi=0} = Q\ n_0(1-\theta)^q \tag{5.15}$$

[1] The expressions were formulated by Prof. Martien Cohen Stuart and Dr. Dirk van den Ende. DvdE formulated the numerical solving algorithm and wrote a MATLAB routine for fitting the solution to the experimental data.

where $n_0 = n(\xi = 0, \tau)$ and the dimensionless constants A, B and Q are given by:

$$A = \frac{D\, t_*}{L_*^2} \ , \qquad B = K c_\infty t_* \ , \qquad Q = \frac{K \Gamma_\infty L_*}{D} \ , \qquad K = k \Gamma_\infty^{q-1} \tag{5.16}$$

The other bc's are now given by:

$$\theta(0) = 0 \ , \qquad n(\xi, 0) = 1 \ , \qquad n(\infty, \tau) = 1 \tag{5.17}$$

Here L_* and t_* are not yet defined. They can be defined in such a way that 2 of the constants A, B, Q are one. In case $A_1 = B_1 = 1$ (case 1) the scaling factors L_*, t_* and Q_1 are equal to:

$$L_* = \sqrt{\frac{D}{K c_\infty}} \ , \qquad t_* = \frac{1}{K c_\infty} \ , \qquad Q_1 = \sqrt{\frac{K \Gamma_\infty^2}{D c_\infty}} \tag{5.18}$$

Let's look for the meaning of Q_1. The time t_* is the characteristic adsorption time in case $c_0 \simeq c_\infty$. In this time the particles in the fluid diffuse over the scaling distance $L_* = (D t_*)^{1/2}$. There is second length scale in this process, which is the distance over which the liquid will be depleted due to the adsorption, $L = \Gamma_\infty / c_\infty$. Q_1 is just the ratio of these length scales, i.e. $Q_1 = L / L_*$. Another option (case 2) is to define $L_* = L$. Defining $A_2 = 1$, we obtain now:

$$L_* = \frac{\Gamma_\infty}{c_\infty} \ , \qquad t_* = \frac{\Gamma_\infty^2}{D c_\infty^2} \ , \qquad B_2 = Q_2 = \frac{K \Gamma_\infty^2}{D c_\infty} \tag{5.19}$$

The set of Eqs. (5.15) can be solved numerically. But before we do so we first consider the asymptotic behavior of the process.

5.8.3 Asymptotic behavior

Fast diffusion

In case of fast diffusion, i.e. $Q \ll 1$, the concentration in the liquid near the interface (in the sublayer) remains constant, $c_0 \simeq c_\infty$. In that case the

problem reduces to solving, see Eq. (5.15):

$$\frac{d\theta}{d\tau} = B(1-\theta)^q$$

which results for $q = 1$ in:

$$\theta = 1 - \exp(-B\tau) \tag{5.20}$$

and for $q \neq 1$ in:

$$\theta = 1 - \left(1 + (q-1)B\tau\right)^{-1/(q-1)} \tag{5.21}$$

where $\theta = \Gamma/\Gamma_\infty$ and $B\tau = Kc_\infty t$.

Fast adsorption

In case of fast adsorption, i.e. $Q \gg 1$, the concentration in the sublayer is fully depleted to $n_0 \ll 1$. We suppose n_0 is constant, so the equations (5.15) are now decoupled. First we have to solve the concentration distribution $n(\xi, \tau)$ and from that the surface density $\theta(\tau) = BQ^{-1} \int dn/d\xi \, d\tau$. Suppose the liquid is confined between $\xi = 0$ and $\xi = L$, where $L \gg 1$. We express the concentration profile as the sum of its equilibrium profile and a Fourier series:

$$n(\xi, \tau) = \frac{\xi}{L} + n_0 \frac{L-\xi}{L} + \sum_1^\infty a_m(\tau) \sin\left(\frac{m\pi\xi}{L}\right) \tag{5.22}$$

As $n(\xi, 0) = 1$ except at $\xi = 0$ where it is n_0, i.e.

$$\sum_1^\infty a_m(0) \sin\left(\frac{m\pi\xi}{L}\right) = (1-n_0)\left(1 - \frac{\xi}{L}\right) \tag{5.23}$$

the coefficients at $t = 0$ are given by:

$$a_m(0) = (1-n_0)\frac{2}{m\pi} \tag{5.24}$$

To obey the diffusion equation these coefficients develop in time according:

$$\frac{da_m}{d\tau} = -A\left(\frac{m\pi}{L}\right)^2 a_m \tag{5.25}$$

or

$$a_m(\tau) = (1-n_0)\frac{2}{m\pi}\exp(-\left(\frac{m\pi}{L}\right)^2 A\tau) \tag{5.26}$$

Substituting this relation in Eq. (5.22) we get for the derivative at zero:

$$\begin{aligned}\left(\frac{\partial n}{\partial \xi}\right)_{\xi=0} &= \frac{1-n_0}{L} + \frac{2(1-n_0)}{L}\sum_1^\infty \exp(-\left(\frac{m\pi}{L}\right)^2 A\tau) \\ &= \frac{2(1-n_0)}{L}\left(\sum_1^\infty \exp(-\left(\frac{m\pi}{L}\right)^2 A\tau) + \frac{1}{2}\right)\end{aligned} \tag{5.27}$$

To evaluate the summation we consider the integral:

$$\begin{aligned}\int_0^\infty e^{-z^2}\,dz &= \lim_{\delta z\to 0}\sum_0^\infty \int_{m\delta z}^{(m+1)\delta z} e^{-z^2}\,dz \\ &= \lim_{\delta z\to 0}\frac{\delta z}{2}\sum_0^\infty \left(e^{-(m\delta z)^2} + e^{-((m+1)\delta z)^2}\right) \\ &= \lim_{\delta z\to 0}\delta z\left(\sum_1^\infty e^{-(m\delta z)^2} + \frac{1}{2}\right) = \tfrac{1}{2}\sqrt{\pi}\end{aligned} \tag{5.28}$$

Hence, for $\pi(A\tau)^{1/2}/L \ll 1$ we obtain:

$$\sum_1^\infty \exp(-\left(\frac{m\pi}{L}\right)^2 A\tau) + \frac{1}{2} = \frac{L}{2\sqrt{\pi A\tau}} \tag{5.29}$$

and so:

$$\left(\frac{\partial n}{\partial \xi}\right)_{\xi=0} = \frac{1-n_0}{\sqrt{\pi A\tau}} \tag{5.30}$$

The rate $d\theta/d\tau$ is

$$\frac{d\theta}{d\tau} = \frac{B}{Q}\left(\frac{\partial n}{\partial \xi}\right)_{\xi=0} = \frac{B(1-n_0)}{Q\sqrt{\pi A\tau}} \tag{5.31}$$

Integrating this expression yields:

$$\theta = (1-n_0)\frac{2B}{Q}\sqrt{\frac{\tau}{\pi A}} \tag{5.32}$$

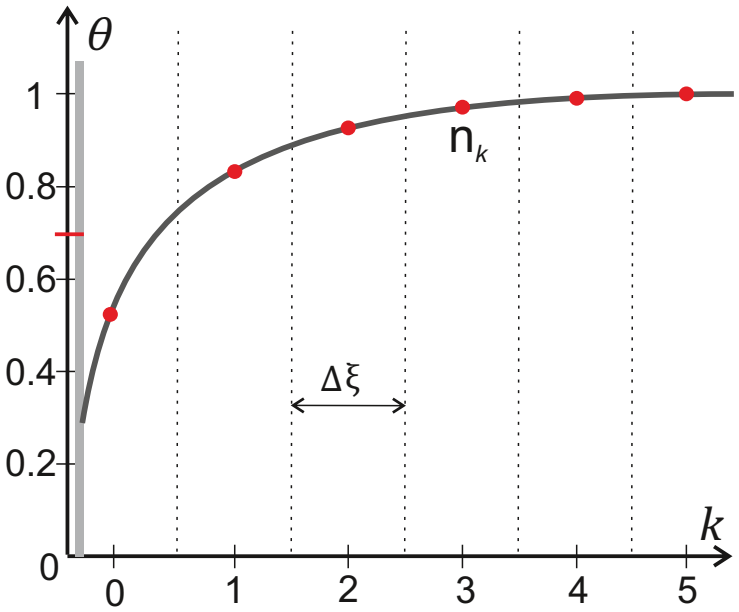

Figure 5.6: Sketch of the substrate with surface density θ and the sublayers with concentration n_k.

or in dimensional form:

$$\Gamma = 2(c_\infty - c_0)\sqrt{\frac{D\,t}{\pi}} \tag{5.33}$$

with $c_0 \ll c_\infty$.

5.8.4 Numerical approach

To solve the set of equations:

$$\frac{\partial n}{\partial \tau} = \frac{\partial^2 n}{\partial \xi^2}\,, \qquad \frac{\partial \theta}{\partial \tau} = n_0(1-\theta)\,, \qquad \left(\frac{\partial n}{\partial \xi}\right)_{\xi=0} = Q\; n_0(1-\theta) \tag{5.34}$$

numerically, we discretize the time derivative as:

$$\frac{dn}{d\tau} = \frac{n(\tau+\delta\tau) - n(\tau)}{\delta\tau} \tag{5.35}$$

and integrate the diffusion equation over small distance $\delta\xi$:

$$\int_{\xi-\delta\xi/2}^{\xi+\delta\xi/2} \frac{\partial n}{\partial \tau}\, d\xi = \int_{\xi-\delta\xi/2}^{\xi+\delta\xi/2} \frac{\partial^2 n}{\partial \xi^2}\, d\xi \tag{5.36}$$

or for sufficiently small $\delta\xi$:

$$\begin{aligned} \frac{\partial n}{\partial \tau}\, \delta\xi &= \left(\frac{\partial n}{\partial \xi}\right)_{\xi+\delta\xi/2} - \left(\frac{\partial n}{\partial \xi}\right)_{\xi-\delta\xi/2} \\ &= \frac{n(\xi+\delta\xi) - n(\xi)}{\delta\xi} - \frac{n(\xi) - n(\xi-\delta\xi)}{\delta\xi} \end{aligned} \tag{5.37}$$

Combining Eq. (5.35) with Eq. (5.37) we get the update scheme for $n(\xi, \tau)$:

$$\frac{n(\xi, \tau+\delta\tau) - n(\xi,\tau)}{\delta\tau} = \frac{n(\xi+\delta\xi,\tau) + n(\xi-\delta\xi,\tau) - 2n(\xi,\tau)}{\delta\xi^2} \tag{5.38}$$

Defining $n_k^m = n(\xi_k, \tau_m)$ we can write this as:

$$n_k^{m+1} = n_k^m + \left(n_{k+1}^m + n_{k-1}^m - 2n_k^m\right) \frac{\delta\tau}{\delta\xi^2} \tag{5.39}$$

where $\xi_k = (k + 1/2)\delta\xi$ and $\tau_m = m\delta\tau$. The time derivative of the surface density is given by:

$$\left(\frac{\partial\theta}{\partial\tau}\right)^m = n_0^m(1-\theta^m) = Q^{-1}\left(\frac{\partial n}{\partial\xi}\right)_{1/2}^m \tag{5.40}$$

So the update step for the surface density becomes:

$$\theta^{m+1} = \theta^m + \left(\frac{\partial\theta}{\partial\tau}\right)^m \delta\tau = \theta^m + \left(n_0^m(1-\theta^m)\right)\delta\tau \tag{5.41}$$

and for n_0 we get:

$$n_0^{m+1} = n_0^m + \left(n_1^m - n_0^m\right) \frac{\delta\tau}{\delta\xi^2} - Q\, n_0^m(1-\theta^m)\, \frac{\delta\tau}{\delta\xi} \tag{5.42}$$

Hence, the complete algorithm becomes:

$$n_k^{m+1} = n_k^m + \left(n_{k+1}^m + n_{k-1}^m - 2n_k^m\right) \frac{\delta\tau}{\delta\xi^2} \tag{5.43}$$

$$n_0^{m+1} = n_0^m + \left(n_1^m - n_0^m\right) \frac{\delta\tau}{\delta\xi^2} - Q\, n_0^m (1-\theta^m) \frac{\delta\tau}{\delta\xi} \tag{5.44}$$

$$\theta^{m+1} = \theta^m + n_0^m (1-\theta^m)\, \delta\tau \tag{5.45}$$

Together with the initial conditions $n_k^0 = 1$ and $\theta^0 = 0$ and the boundary condition $n_N^m = 1$, we now are able to calculate the time dependence of both the surface density and the concentration profile.

Is this algorithm stable? Suppose only bin k at $\xi = \xi_k$ with width $\delta\xi$ is populated, i.e. $n_k^m > 0$ and $n_{k-1}^m = n_{k+1}^m = 0$. In that case one must demand $\delta\tau/\delta\xi^2 < 1/2$ otherwise $n_k^{m+1} < 0$. Moreover, considering bin 0, we should have $Q\,\delta\tau/\delta\xi < 1$. At last $\delta\tau < 1$ otherwise $\theta^{m+1} > 1$. Therefore the algorithm is stable if:

$$\delta\tau < \min\{\tfrac{1}{2}\delta\xi^2,\ \delta\xi/Q,\ 1\} \tag{5.46}$$

So, for large Q it is wise to start with $\delta\tau = 0.1\ \delta\xi/(Qn_0)$ until $0.1\ \delta\xi/(Qn_0) > 0.01\ \delta\xi^2$. From there on we'll use $\delta\tau = 0.01\ \delta\xi^2$.

We use Eqs. (5.43)-(5.45) to calculate the time evolution of the particle density at the surface.

6 Adsorption and interactions of soft microgel particles at oil-water interfaces

Abstract We address the influence of temperature on the adsorption and the interactions of PNIPAM microgel particles at a water-decane interface. Owing to their polymeric nature, the particles are found to readily adsorb onto a water-decane interface. Under compression, they do not desorb from the interface even when subjected to high loads. As the temperature is increased from 24°C to 36°C, the inter-particle interaction changes from predominantly steric to largely electrostatic repulsion. This is inferred from the observed increase in the zeta potential, and is explained using a simple theory that takes into account the change in charge distribution.

6.1 Introduction

Microgel particles are made of chemically cross-linked polymer that can be swollen by a solvent. The degree of swelling depends on solvent quality and cross-link density[1, 2]. Microgel particles made from the thermo-sensitive polymer poly N-isopropyl acrylamide (PNIPAM) undergo reversible swelling/shrinking transitions at temperatures around the body temperature, and therefore are considered as promising particles for thermo-stimulated control of drug delivery[3, 4]. In this context, the particle chemistry can also be varied, e.g., by incorporating charged co-monomers like (meth) acrylic acid to make them responsive to pH.

Another possibility which has only recently come under scrutiny is their possible use as so-called Pickering stabilizers of emulsions and foams[5–9]. This application hinges on their hybrid character somewhere between flexible polymer and colloidal particle. On one hand they share with the former the ability to easily adsorb to water/air or water/oil interfaces, while on the other hand they share with the latter the very strong anchoring at the interface, making their adsorption practically irreversible[10, 11]. Given this context, knowledge about aspects such as adsorption dynamics, interfacial interactions, microstructure and rheology of these particles are key to intelligent design of these systems. Although significant advances have recently been made in understanding these aspects[5–9], a comprehensive knowledge is still lacking.

The stability of conventional Pickering emulsions comes from the strong repulsion between the colloidal particles produced by (hard sphere) steric interactions and long-range electrostatic forces due to surface charges. In contrast, microgel particles deform strongly due to interfacial tension upon adsorption to solid - liquid[12] and liquid - liquid interfaces[6, 7, 13–16]. The nature of the mutual interactions and the interfacial assembly of such soft deformable colloidal particles at the interface is not yet clearly understood. Furthermore, the statics and kinetics of adsorption (in particular as a function of temperature), have not been very well studied, which is surprising. For example, it is currently not very clear which particle properties control the density and pressure at which spontaneous

adsorption saturates.

This lack of knowledge has prompted us to study layers of PNIPAM particles at a water-decane interface, focusing on the effect of temperature on the adsorption and interactions. We study the interfacial tension response of spontaneously adsorbed layers when they are subjected to compression, by reducing the interfacial area or by cycling the temperature. We also study the dilatational rheology of these adsorbed layers. To explain our observations, we corroborate a (previously proposed) mechanism in which the distribution of ions changes drastically upon crossing the phase transition temperature of the microgel. This explanation is supported by measurements of the zeta potential as a function of temperature.

6.2 Materials & Methods

6.2.1 Chemicals:

PNIPAM microgels are synthesized by batch suspension polymerization from NIPAM as monomer with 2 mol% N-N' methylene bisacrylamide as cross-linker, in the presence of sodium dodecyl sulfate (SDS) and using potassium persulfate as the initiator[17, 18]. No acidic monomers like methacrylic acid or acrylic acid are used, so that the particles only carry a slight negative charge due to persulfate groups. The particles are purified by repeated centrifugation at 18000g and replacing the supernatant with fresh Milli-Q water; the process is repeated 5-6 times which is enough to remove all the SDS. The particles are then freeze-dried and stored. Suspensions are prepared by adding a weighed amount of particles to Milli-Q water and stirring the suspension for at least 24 hours. The n-decane used as the oil phase (Merck) is purified by passing over an alumina column 5 times, to remove surface-active impurities. The purity is evaluated by checking that the interfacial tension of the decane-water interface to be equal to the value of the pristine interface (51 mN/m). The value of the bare water-oil interfacial tension drops by less than 3 mN/m over a period of 8 hours.

6.2.2 Particle characterization

The temperature dependent size of the microgel particles is measured by Dynamic Light Scattering (DLS) on a Malvern Zeta Sizer. We used the same instrument to measure the Electrophoretic Mobility (μ) and the Zeta Potential (ζ) of the particles at various temperatures. The zeta sizer uses the Stokes-Einstein relation ($D = k_BT/6\pi\eta R_H$, where k_B is the Boltzmann constant, T is the absolute temperature and η is the viscosity of the solvent) to calculate the hydrodynamic radius (R_H) from the measured diffusion coefficient (D) of the particles. The electrophoretic mobility of the particles is measured using Laser Doppler Micro-electrophoresis. Since the suspending medium is water, Smoluchowski approximation (Henry's function $f(Ka) = 1$) can be applied to the Henry's equation ($\mu = \varepsilon_r\varepsilon_0\zeta f(Ka)/\eta$, where ε_0 is the dielectric permittivity of vacuum, ε_r is the relative permittivity of the medium) to calculate the zeta potential from the electrophoretic mobility[19]. Microgel particles are also characterised by Static Light Scattering (SLS) by fitting the form factor, to find the molar mass and the light scattering radius (R_{SLS}) (for an equivalent homogeneous sphere) of these particles.

6.2.3 Pendant drop measurements

Water/decane interfacial tensions (IFT) are measured with an accuracy of ±0.1 mN/m from drop image analysis using a Data Physics OCA apparatus. A drop of water containing a known concentration of microgel particles is formed at the end of a needle, and the interfacial tension is determined as a function of time, while the particles adsorb onto the initially clean interface. The temperature is maintained by means of a heating stage and measured in the oil phase using a thermocouple. Measurements are started when the temperature is uniform ($\pm 0.1^oC$)throughout the system. For the interfacial tension measurements to be accurate, we make sure that the drop is big enough so that it is substantially deformed by the buoyancy forces. This criterion can be expressed in terms of the Bond number defined as $Bo = \Delta\rho g R^2/\gamma$ (where, $\Delta\rho$ is the density difference between the fluids, R is the radius of the drop and γ is the interfacial

tension). For accurate measurements, we make sure that Bo always lies between 0.1 and 1[20].

In compression experiments, a drop is formed at a given temperature and allowed to equilibrate for 30 minutes. The suspension is then slowly withdrawn through the needle at a rate of 0.5 μl/s. The IFT response is measured instantaneously as the liquid is withdrawn from the drop. In the so called step compression experiments, a similar protocol is followed except that the drop is withdrawn rapidly at a rate of 5.0 μl/s, and only the initial and final IFT, after 10 minutes of equilibration, are considered.

For dilatational rheology measurements we use the oscillating drop method on the OCA apparatus. The volume and surface area of the drop are modulated by periodically withdrawing and injecting small volumes of liquid using a small piston driven by a piezoelectric element. The corresponding sinusoidal IFT response is measured, after which the complex dilatational modulus E* is determined from the normalised amplitude and phase lag[21].

6.3 Results

For our microgel particles, the Volume Phase Transition Temperature (VPTT)[22] lies between 32°C and 36°C. The molar mass of the particles as measured from static light scattering is 1.82×10^6 kg/mol. As expected, the PNIPAM particles swell considerably upon decreasing the temperature. Particle size measured using static and dynamic light scattering are plotted as a function of temperature in figure 6.1, where it is seen that the hydrodynamic radius (R_H) as determined by DLS, drops from about 255±7 nm to 110±3 nm, which implies approximately a 12-14 fold reduction in volume. The radius (R_{SLS}) measured using SLS is smaller than the hydrodynamic radius (R_H) for temperatures below VPTT. At these temperatures, a small R_{SLS}/R_H ratio ($R_{SLS}/R_H < 1$) is due to the fact that in their swollen state, the particles have highly cross-linked cores with a number of loose polymer ends at the periphery. Thus the R_{SLS} that is calculated assuming a optically homogeneous particles may be less than the actual size of the particles. Above the VPTT, both the loose polymer

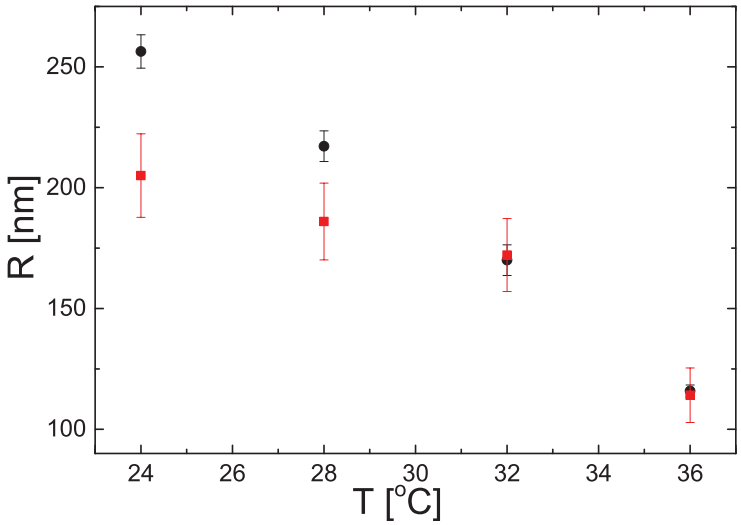

Figure 6.1: Size of PNIPAM microgel particles as a function of temperature. (■) Radius (R_{SLS}) measured using SLS and (●) Hydrodynamic radius (R_H) measured using DLS.

chains as well as the cross-linked particle core collapse and the particle behaves like a homogeneous particle leading to values of $R_{SLS}/R_H \cong 1$[23].

Anticipating changes in the charge distribution (ionized groups on the particle and counterions in the liquid phase), we also measure the electrophoretic mobility of our particles as a function of temperature. The results shown in figure 6.2 correspond to the particles in bulk. But we expect them to be important in understanding the interactions between adsorbed particles as well. Ohshima [24] has derived a simple approximate formula for predicting the electrophoretic mobility of core-shell type colloidal particles:

$$\mu = \frac{\varepsilon_r \varepsilon_0}{\eta}\left(\frac{\psi_0 \lambda + \psi_D \kappa_m}{\lambda + \kappa_m}\right) f\left(\frac{d}{a}\right) + \frac{\rho}{\eta \lambda^2} \tag{6.1}$$

Here, ε_0 is the dielectric permittivity of vacuum, ε_r is the relative permittivity of the medium, η is the viscosity of water, ψ_D is the Donnan potential in the particle, ψ_0 is the surface potential, κ_m is the Debye-Hückel

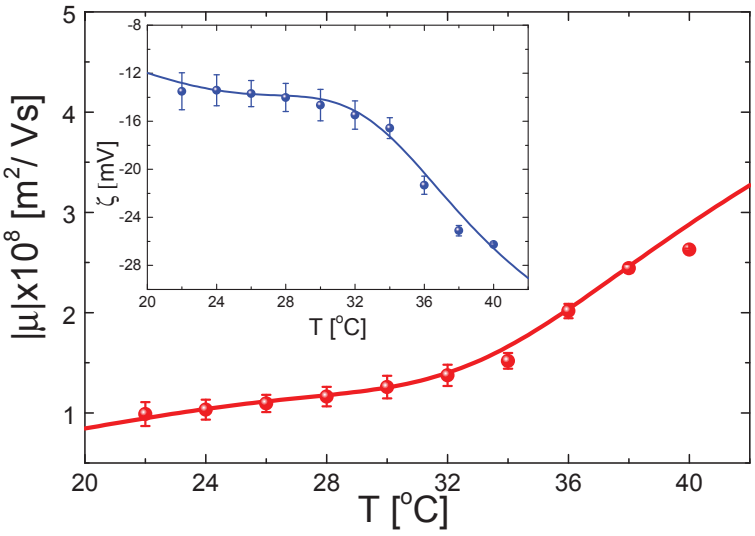

Figure 6.2: Electrophoretic mobility (μ) as a function of temperature. Solid line is theoretical calculation using Equation(1). Inset shows the variation of the Zeta Potential (ζ) as a function of temperature. Solid line is calculated from Henry's equation using the values of mobility computed by Equation(1).

parameter, ρ is the charge density in the particle (number of elementary charges per unit volume of the particle) and $1/\lambda$ is the softness parameter. The function $f(d/a)$ denotes the relative size if the radius of the particle core to the thickness of polyelectrolyte shell. In limiting cases when the particle is a spherical soft polyelectrolyte with no particle core ($d \gg a$) $f(d/a) = 2/3$[24, 25]. Garcia-Salinas *et al.* [26] point out that in case of PNIPAM microgel particles, even if the number of charges per particle remains constant, ρ varies with temperature since the volume of the particle varies significantly with temperature. Thus if the number of charges per particle is kept fixed, shrinking implies an increase in charge density. Using λ as a fit parameter to match their experimental results with the theoretical expression, they observe that changes in λ as a function of temperature are also closely related to changes in the size of the particle.

We use these findings also for analysing our data. Assuming 3000 ele-

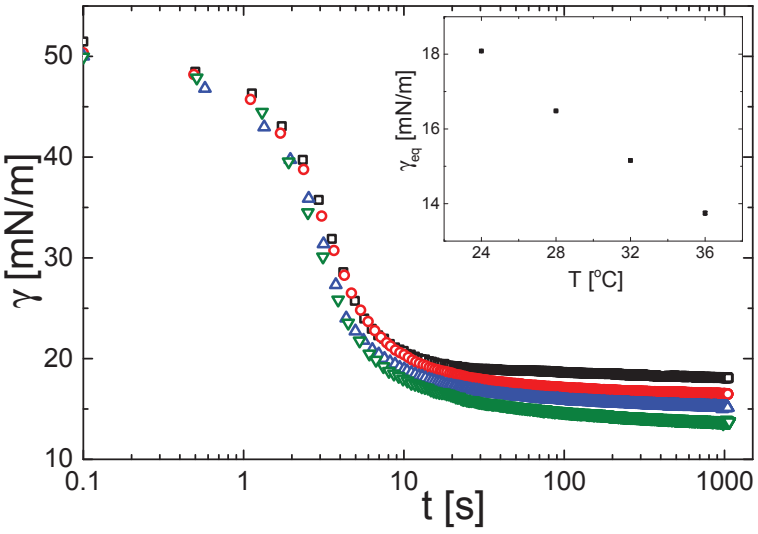

Figure 6.3: Decay in the IFT of an interface between n-decane and 0.5 g/l aqueous suspension of PNIPAM microgel particles at (□) 24°C, (◯) 28°C, (△) 32°C and (▽) 36°C.The inset shows the equilibrium surface tension versus the temperature.

mentary charges per particle, and using the typical values of temperature-dependent softness for PNIPAM[26] , we calculate the mobility as a function of temperature. The experimental data agree fairly well with the calculated predictions. The mobility decreases with decreasing temperature because in swollen particles, the charges are more dilute and hydrodynamically screened by the dangling polymer segments. Upon collapse the particles feature a higher charge density and a smoother surface which allow the surrounding medium and the counterions to move more easily resulting in a higher mobility. These findings are also in qualitative agreement with the outcome of model calculations by Moncho-Jordá[27], who found that upon shrinking of the microgel particles, the counterions are squeezed out from the interior of the particles to the surface. For sufficiently charged particles, this results in more repulsive effective interactions.

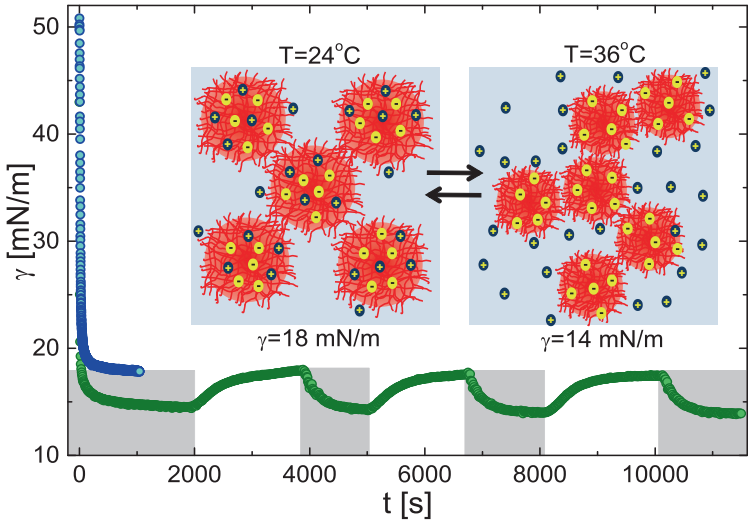

Figure 6.4: IFT response to changes in temperature. Green data points show response of a drop created at 36°C and subjected to temperature cycles between 36°C and 24°C. The blue data points show the response of a drop created at 24°C. The grey areas denote the part of temperature cycle at 36°C and the blank spaces at 24°C. Inset shows a schematic of the proposed particle conformations in aqueous phase at both temperatures.

The decrease of IFT as a function of time is presented in figure 6.3, for four temperatures (24°C, 28°C, 32°C and 36°C). In all cases, the initial interfacial tension γ_0 of the clean surface is ~ 51 mN/m. The temperature coefficient $d\gamma/dT$ for this system is about 0.069 mN/K so that γ_0 varies by less than 1 mN/m over the range studied[28]. For the 0.5 mg/l PNIPAM dispersion the tension drops in about 15 minutes to values around 18 mN/m, indicating that particles adsorb and a surface pressure builds up. The final tension depends weakly on concentration[29] but significantly on T, ranging from nearly 18 mN/m for 24°C, to slightly above 13 mN/m for 36°C. The surface pressure, given by $\Pi = \gamma_0 - \gamma$, thus increases by about 5 mN/m (from about 33 to 38 mN/m) by going from the lowest to the highest temperature.

The response of the surface tension when the temperature is cycled between 24°C and 36°C is shown in figure 6.4. A drop surface saturated with microgels at 36°C is cooled to 24°C and kept at this temperature for 30 minutes (1800 sec) after which it is heated back to 36°C and kept there for about 20 minutes (1200 sec). This cycle is repeated three times. As can be seen, the response is entirely reversible. The tension slowly adjusts to each imposed temperature reaching a steady value after about 1000 seconds, which is partly due to slow adjustment of the bath temperature to the new setpoint (~ 500 sec) and partly due to relaxation of the tension itself (~ 500 sec). In principle, this could mean that the particle surface density reversibly adjusts during the temperature cycles. However the compression experiments discussed below exclude any desorption. Therefore we must also rule out extra adsorption. This means that the surface density of the particles is the same at both temperatures and no adsorption or desorption of particles occurs upon changing the temperature.

Even though the spontaneous adsorption saturates, the surface pressure still responds to further compression, either carried out slowly and continuously, or carried out step-wise, allowing for a 10 minute waiting time between measurements. The results of such measurements (carried out on a surface which is first allowed to spontaneously fill with particles from solution) are shown in figures 6.5 and 6.6. For our analysis we define the excess surface pressure($\Delta\Pi$) due to compression of the drop, by subtracting the equilibrium surface pressure due to spontaneous adsorption of the particles(Π_{sp}) at the oil-water interface from the instantaneous surface pressure(Π). The excess pressure is thus a measure of the extra interactions between microgel particles upon compression. Compressing the surface by a factor of about 4 (from 40 to 10 mm^2) leads to an excess pressure increase of 3-5 mN/m depending on the temperature as shown in figure 6.5. At the lowest temperature, for which the pressure due to spontaneous adsorption is lowest, the increase is strongest, and vice versa.

If the particles were to desorb, it would cause the surface pressure to relax. At short times, this relaxation to equilibrium is expected to be dictated by the transport of the expelled particles away from the interface.

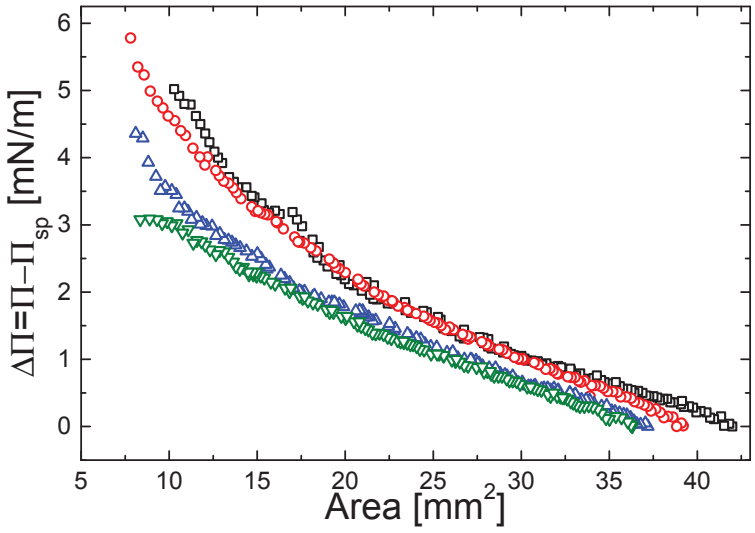

Figure 6.5: Evolution of excess surface pressure ($\Delta\Pi$) due to compression of the interfacial area for (□) 24°C, (◯) 28°C, (△) 32°C and (▽) 36°C. The compression was carried out by reducing the drop volume at a rate of 0.5 μl/s.

At long times local particle rearrangements that ensue after desorption of particles may lead to a slow relaxation in pressure. No such relaxation was observed even when the interface was rapidly compressed as seen in figure 6.6(b). This clearly means that no particles leave the (compressed) surface i.e. no desorption. Moreover, Figure 6.6(c) shows that the response upon compression is nearly instantaneous, so that the pressures found depend only on the extent of compression, and not on the rate of compression.

Finally, we present in figure 6.7 values of the dilatational modulus (E^*) as a function of frequency for the same four temperatures. The moduli turn out to be low, in the range 2-7 mN/m; the lowest modulus is found for the highest temperature. The frequency dependence is nearly absent for 36°C whereas there is a modest and increasing frequency dependence for the other three temperatures. It indicates existence of very soft layers at the interface that tend to get even softer as the temperature increases[30].

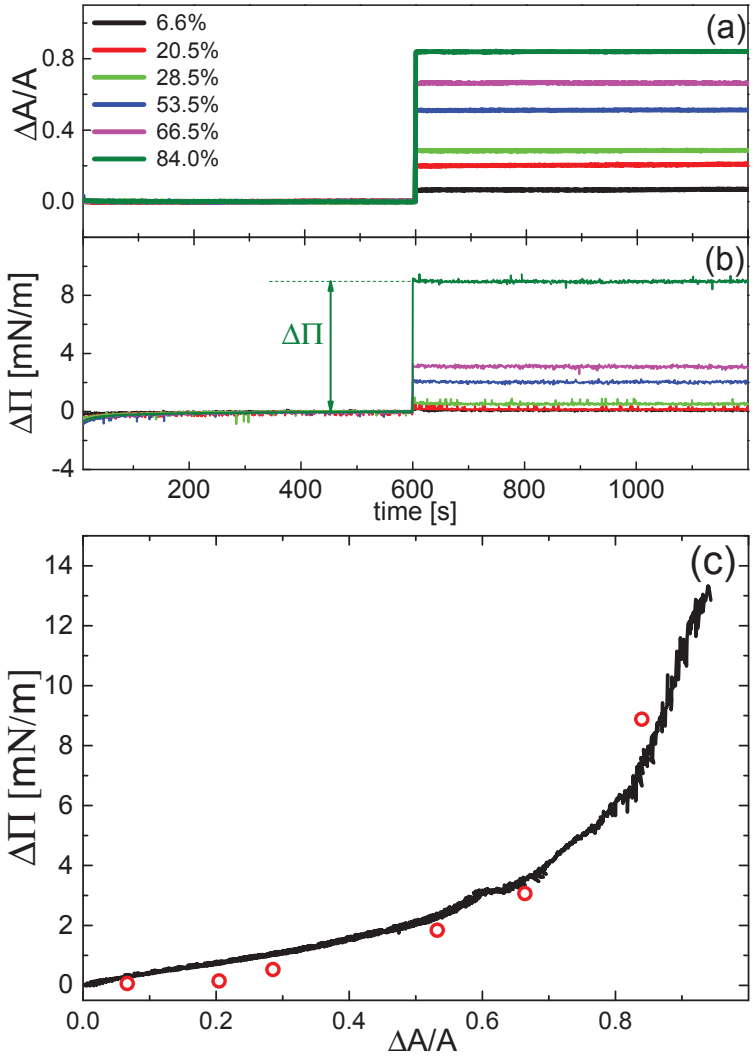

Figure 6.6: Surface pressure response to a step compression in the interfacial area. (a) The applied deformation (strain) at 24°C. (b) The corresponding response of surface pressure (stress) is the difference between the instantaneous pressure and the pressure due to spontaneous adsorption.(c)Comparison of the surface pressure response to a step change in the interfacial area(open circles) or to a continuous compression of the interface (solid line).

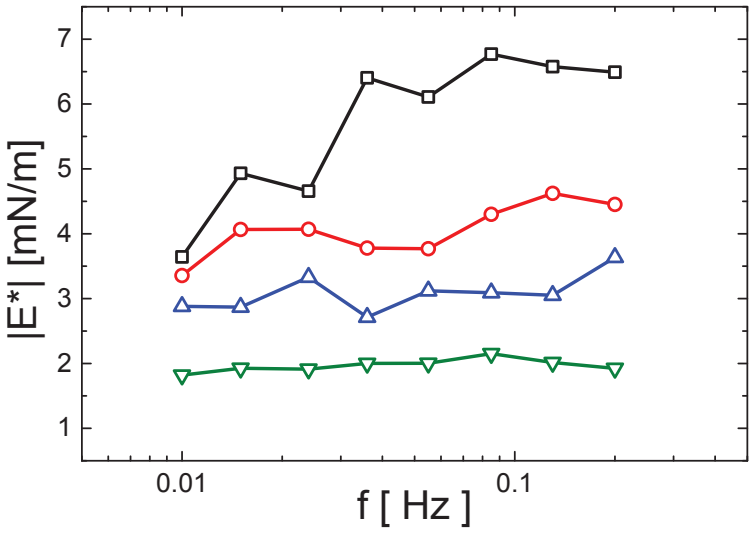

Figure 6.7: Complex dilatational viscoelastic modulus E^* as a function of frequency for (□) 24°C, (◯) 28°C, (△) 32°C and (▽) 36°C.

We can also roughly calculate the moduli from figure 6.5 by considering the IFT response at small area compressions. The moduli calculated thus are comparable to the values obtained from dilatational rheology.

6.4 Discussion

The interfacial tension data clearly indicate that the (negatively charged) PNIPAM microgel particles adsorb rapidly onto the water-decane interface. This is also found by other investigators[31]. The adsorption is as expected faster at higher temperatures due to a higher diffusion coefficient which, in turn, comes from a combined effect of the decrease in viscosity and the de-swelling of particles[29]. Moreover, once adsorbed, they stick firmly to the interface; compression/expansion cycles show no sign of particle desorption from the interface, in contrast to the typical behaviour of small molecules. It has been argued that this is simply related to the much larger contact area that colloidal particles can have with the inter-

face causing an anchoring free energy exceeding the thermal energy by orders of magnitude. Yet, colloidal particles do not always adsorb easily. In fact, it has been found that the adsorption of hard colloidal particles is strongly affected by the electrostatic interactions between the particles and the air-water interface[32]. Negatively charged particles tend to experience a strong adsorption barrier of electrostatic origin towards clean water-air and water-oil interfaces. It is therefore remarkable that the negatively charged microgel particles adsorb fairly easily implying a low barrier, if any. It seems likely that the polymer chains at the periphery of the particles allow for shape fluctuations by which they can establish a first contact with the interface without a large penalty of electrostatic energy.

As we have shown in a previous paper[29], at room temperature for an air-water interface (when the particles are in the swollen state in the bulk), the particles already start to exert measurable surface pressures at low surface loadings, where the area per particle is a multiple of its cross section in solution. This must be largely ascribed to the fact that these particles deform very strongly under the action of the bare interfacial tension. The extent of deformation (increase in cross section) scales as γ_0/ε, where ε is the elastic modulus of the particle. Using literature values of ε determined for PNIPAM particles[33, 34], we estimate a value of about 50 kPa, which leads to deformations on the order of 10^{-6} m, which is of the same order of magnitude as the particle diameter. It is therefore not surprising that adsorbed microgels assume cross sections 5-10 times larger than their unperturbed diameter. Upon filling the surface, the particles retract thereby reducing their elastic energy and presenting a larger polymer chain density at the interface. This shows up as a decrease in surface tension or, equivalently as an increase in pressure.

A key result of the present study is that an increase in temperature leads to an increase in pressure. From the data in figure 6.6 we can rule out that particles leave the interface and from figure 6.4 we know that the number of particles does not increase during temperature cycles. Hence, we have to conclude that the adsorbed amount remains constant during changes in temperature. At first sight it is truly puzzling that an increase

in temperature, which tends to lead to particle shrinking, can lead to an increase in pressure.

This apparent contradiction can be clarified by looking at the measurements of the zeta potential as a function of temperature, presented in the inset in figure 6.2. Here, we see that ζ increases 2.5 times from around -10 mV at 22°C to -26 mV at 40°C. Standard theories for the diffuse double layer predict hardly any effects of temperature so they cannot explain this finding, but the temperature-induced shrinking, together with the Ohshima theory[24, 25] for microgel particles offers a quantitative explanation. The negative charge most likely must be attributed to sulfate groups originating from the persulfate initiator. These are almost entirely deprotonated at neutral pH, so that any temperature effect on the protonation must also be ruled out. We therefore must suppose a constant number of charges per particle.

Due to the negative charge, the particles repel. The fact that these particles are at an oil-water interface adds to this electrostatic repulsion. Decane has a much smaller relative dielectric constant (~ 2)[35] as compared to water (~ 80)[36]. Thus the asymmetry in the charge dissociation at the interface causes the particles to become dipoles, which in turn leads to an enhancement in the range as well as the strength of electrostatic repulsion between the particles[37–40] which then contributes to a higher surface pressure. Having said that, increase in temperature also causes a coil to globule transition in the polymer. Hence the particle do experience attractive forces at short range owing to the interactions between hydrophobic polymer segments. We therefore propose that the increase in surface pressure is the net effect of a contribution from electrostatic repulsion and the formation of a network of particles due to short range attractive interactions. Hence, it is not surprising that the effect is small. The morphology of the particle layer thus changes from a ordered structure with particle interacting sterically via loose polymer brushes at low temperatures to an open network consisting of clusters of particle at higher temperatures.

This scenario of increased electrostatic interactions coupled with a network of particles at higher temperatures is consistent with the results of

the dilatational rheology as well as the drop compression experiments. At low T, where the interfacial layer is ordered and dense, the interaction is mostly steric in nature, the modulus increases with frequency, because the polymeric network needs time to adjust to changes in density. At high temperature, the moduli are low due to a gel like network formed at the interface.

6.5 Conclusion

PNIPAM microgel particles despite being negatively charged, adsorb readily to an oil water interface. This is possible because of the polymeric character of the particles that allow for deformation and shape fluctuations at the interface enabling adsorption to the interface without any electrostatic energy barrier. Once equilibrated, the surface density of particles remains constant even if the drop is subjected to temperature cycles. The particles are irreversibly adsorbed on to the interface and do not leave the interface even when the interfacial area is reduced by a large extent. The increase in temperature causes an increase in surface pressure. This can be explained by a cross-over in the inter-particle interactions that change from predominantly steric at lower temperatures to predominantly electrostatic at higher temperatures. The increase in electrostatic interactions are verified by the Zeta potential measurements which show a 2.5 fold increase as the temperature increases from 24^{o}C to 40^{o}C.

Acknowledgement

The authors thank Remco Fokkink (Wageningen University) for help with the SLS characterisation. This work has been supported by the Foundation for Fundamental research on Matter (FOM), which is financially supported by the Netherlands Organization for Scientific Research (NWO).

Bibliography

[1] Brian R. Saunders and Brian Vincent. Microgel particles as model colloids: theory, properties and applications. *Advances in Colloid and Interface Science*, 80(1):1 – 25, 1999.

[2] H. Senff and W. Richtering. Influence of cross-link density on rheological properties of temperature-sensitive microgel suspensions. *Colloid and Polymer Science*, 278(9):830–840, 2000.

[3] Ying Guan and Yongjun Zhang. Pnipam microgels for biomedical applications: from dispersed particles to 3d assemblies. *Soft Matter*, 7:6375–6384, 2011.

[4] Christine T. Schwall and Ipsita A. Banerjee. Micro- and nanoscale hydrogel systems for drug delivery and tissue engineering. *Materials*, 2(2):577–612, 2009.

[5] Bastian Brugger and Walter Richtering. Emulsions stabilized by stimuli-sensitive poly(n-isopropylacrylamide)-co-methacrylic acid polymers: Microgels versus low molecular weight polymers. *Langmuir*, 24(15):7769–7777, 2008.

[6] Bastian Brugger, Brian A. Rosen, and Walter Richtering. Microgels as stimuli-responsive stabilizers for emulsions. *Langmuir*, 24(21):12202–12208, 2008.

[7] Mathieu Destribats, Veronique Lapeyre, Melanie Wolfs, Elisabeth Sellier, Fernando Leal-Calderon, Valerie Ravaine, and Veronique Schmitt. Soft microgels as pickering emulsion stabilisers: role of particle deformability. *Soft Matter*, 7(17):7689–7698, 2011.

[8] To Ngai, Sven Holger Behrens, and Helmut Auweter. Novel emulsions stabilized by ph and temperature sensitive microgels. *Chemical Communications*, (3):331–333, 2005.

[9] To Ngai, Helmut Auweter, and Sven Holger Behrens. Environmental responsiveness of microgel particles and particle-stabilized emulsions. *Macromolecules*, 39(23):8171–8177, 2006.

[10] Bernard P. Binks. Particles as surfactants—similarities and differences. *Current Opinion in Colloid & Interface Science*, 7(1–2):21–41, 2002.

[11] L. Andrew Lyon and Alberto Fernandez-Nieves. The polymer/colloid duality of microgel suspensions. *Annual Review of Physical Chemistry*, 63(1):25–43, 2012.

[12] Sarah Höfl, Lothar Zitzler, Thomas Hellweg, Stephan Herminghaus, and Frieder Mugele. Volume phase transition of "smart" microgels in bulk solution and adsorbed at an interface: A combined afm, dynamic light, and small angle neutron scattering study. *Polymer*, 48(1):245 – 254, 2007.

[13] Mathieu Destribats, Véronique Lapeyre, Elisabeth Sellier, Fernando Leal-Calderon, Valérie Ravaine, and Véronique Schmitt. Origin and control of adhesion between emulsion drops stabilized by thermally sensitive soft colloidal particles. *Langmuir*, 28(8):3744–3755, 2012.

[14] Karen Geisel, Lucio Isa, and Walter Richtering. Unraveling the 3d localization and deformation of responsive microgels at oil/water interfaces: A step forward in understanding soft emulsion stabilizers. *Langmuir*, 28(45):15770–15776, 2012.

[15] Mathieu Destribats, Mayalen Eyharts, Véronique Lapeyre, Elisabeth Sellier, Imre Varga, Valérie Ravaine, and Véronique Schmitt. Impact of pnipam microgel size on its ability to stabilize pickering emulsions. *Langmuir*, 2014.

[16] Walter Richtering. Responsive emulsions stabilized by stimuli-sensitive microgels: Emulsions with special non-pickering properties. *Langmuir*, 28(50):17218–17229, 2012.

[17] Roberta Acciaro, Tibor Gilanyi, and Imre Varga. Preparation of monodisperse poly(n-isopropylacrylamide) microgel particles with homogenous cross-link density distribution. *Langmuir*, 27(12):7917–7925, 2011.

[18] X. Wu, R. H. Pelton, A. E. Hamielec, D. R. Woods, and W. McPhee. The kinetics of poly(n-isopropylacrylamide) microgel latex formation. *Colloid and Polymer Science*, 272(4):467–477, 1994.

[19] R.J. Hunter. *Zeta Potential in Colloid Science: Principles and Applications*. Colloid science. Academic Press, 1981.

[20] Riëlle de Ruiter, R. Willem Tjerkstra, Michèl H. G. Duits, and Frieder Mugele. Influence of cationic composition and ph on the formation of metal stearates at oil–water interfaces. *Langmuir*, 27(14):8738–8747, 2011.

[21] R. Miller and L. Liggieri. *Interfacial Rheology*. Progress in Colloid and Interface Science. Taylor & Francis, 2009.

[22] A. Fernandez-Nieves, H. Wyss, J. Mattsson, and D.A. Weitz. *Microgel Suspensions: Fundamentals and Applications*. Wiley, 2011.

[23] Imre Varga, Tibor Gilányi, Róbert Mészáros, Genoveva Filipcsei, and Miklós Zrínyi. Effect of cross-link density on the internal structure of poly(n-isopropylacrylamide) microgels. *The Journal of Physical Chemistry B*, 105(38):9071–9076, 2001.

[24] Hiroyuki Ohshima. Electrophoretic mobility of soft particles. *Journal of Colloid and Interface Science*, 163(2):474 – 483, 1994.

[25] Hiroyuki Ohshima. Electrophoresis of soft particles: Analytic approximations. *ELECTROPHORESIS*, 27(3):526–533, 2006.

[26] M.J. Garcia-Salinas, M.S. Romero-Cano, and F.J. de las Nieves. Electrokinetic characterization of poly(n-isopropylacrylamide) microgel particles: Effect of electrolyte concentration and temperature. *Journal of Colloid and Interface Science*, 241(1):280 – 285, 2001.

[27] A. Moncho-Jordá. Effective charge of ionic microgel particles in the swollen and collapsed states: The role of the steric microgel-ion repulsion. *The Journal of Chemical Physics*, 139(6):–, 2013.

[28] Susana Zeppieri, Jhosgre Rodríguez, and A. L. López de Ramos. Interfacial tension of alkane + water systems†. *Journal of Chemical & Engineering Data*, 46(5):1086–1088, 2001.

[29] Omkar Suresh Deshmukh, Armando Maestro, Michel H. G. Duits, Dirk van den Ende, Martien A. Cohen-Stuart, and Frieder Mugele. Equation of state and adsorption dynamics of soft microgel particles at air-water interface. *Soft Matter*, 2014.

[30] Bastian Brugger, Jan Vermant, and Walter Richtering. Interfacial layers of stimuli-responsive poly-(n-isopropylacrylamide-co-methacrylicacid) (pnipam-co-maa) microgels characterized by interfacial rheology and compression isotherms. *Physical Chemistry Chemical Physics*, 12(43):14573–14578, 2010.

[31] Zifu Li, Karen Geisel, Walter Richtering, and To Ngai. Poly(n-isopropylacrylamide) microgels at the oil-water interface: adsorption kinetics. *Soft Matter*, 9(41):9939–9946, 2013.

[32] Sarah L. Kettlewell, Andreas Schmid, Syuji Fujii, Damien Dupin, and Steven P. Armes. Is latex surface charge an important parameter for foam stabilization? *Langmuir*, 23(23):11381–11386, 2007.

[33] Anna Burmistrova, Marcel Richter, Michael Eisele, Cagri Üzüm, and Regine von Klitzing. The effect of co-monomer content on the swelling/shrinking and mechanical behaviour of individually adsorbed pnipam microgel particles. *Polymers*, 3(4):1575–1590, 2011.

[34] Eko H. Purnomo, Dirk van den Ende, Siva A. Vanapalli, and Frieder Mugele. Glass transition and aging in dense suspensions of thermosensitive microgel particles. *Phys. Rev. Lett.*, 101:238301, Dec 2008.

[35] C. Wohlfarth. Dielectric constant of decane. *Landolt Börnstein*, 17:469, 2008.

[36] D. P. Fernández, Y. Mulev, A. R. H. Goodwin, and J. M. H. Levelt Sengers. A database for the static dielectric constant of water and steam. *Journal of Physical and Chemical Reference Data*, 24(1):33–70, 1995.

[37] Pawel Pieranski. Two-dimensional interfacial colloidal crystals. *Phys. Rev. Lett.*, 45:569–572, Aug 1980.

[38] A J Hurd. The electrostatic interaction between interfacial colloidal particles. *Journal of Physics A: Mathematical and General*, 18(16):L1055, 1985.

[39] Bum Jun Park, John P. Pantina, Eric M. Furst, Martin Oettel, Sven Reynaert, and Jan Vermant. Direct measurements of the effects of salt and surfactant on interaction forces between colloidal particles at wateroil interfaces. *Langmuir*, 24(5):1686–1694, 2008.

[40] Eric M. Furst. Directing colloidal assembly at fluid interfaces. *Proceedings of the National Academy of Sciences*, 108(52):20853–20854, 2011.

Summary

In this thesis we study the properties of oil-water and air-water interfaces. They determine the behavior and stability of for instance foams and emulsions. These properties can be changed by adding particles to the interface. Often hard colloidal particles are used for that purpose. This is called Pickering stabilization. We investigate the use of soft microgel particles based on poly-N-isopropylacrylamide (PNIPAM) and try to understand the interactions between these particles at an air-water or oil-water interface. These interactions also affect the adsorption process of such soft particles. PNIPAM microgel particles are sensitive to external stimuli as temperature. Hence, also the effect of temperature on the adsorption kinetics and the interfacial behaviour of these particles will be studied. A deeper understanding of the adsorption kinetics as well as the particle interactions and the resulting microstructure at the interface is crucial in the intelligent design of these microgel particles for applications like Pickering stabilisation of foams and emulsions.

We start our research in *Chapter 2* with a detailed review of the existing literature regarding particles at fluid interfaces. The existing understanding of the adsorption kinetics, particle interactions, interfacial microstructure and interfacial rheology is based on stiff colloidal particles. The soft and deformable nature of microgel particles adds another level of complexity. The deformation enables them to adsorb readily on to an interface allowing for shape fluctuations which help them overcome the electrostatic adsorption barrier faced by charged colloidal particles. In the study of adsorption kinetics of both stiff as well as soft microgel particles, an ideal gas equation of state is often used to relate the surface pressure and the surface concentration. However, a linear relation between pressure and loading is not valid and results in erroneous values of

diffusion coefficients that differ by a factor of 10^{12} - 10^{13}. In case of hard colloidal particles at interfaces, the particles posses a well defined shape, contact line at the interface and charge distribution at the surface of the particle. This makes the estimation of electrostatic, Van der Waals and capillary forces between hard particles at interface relatively easy. The literature is thus replete with numerous articles covering the experimental and theoretical estimation of interaction between hard particles at fluid interfaces. The soft, deformable and permeable nature of the PNIPAM microgel particles make it difficult to define a shape, a contact line or even the surface of the particle. We highlight the lack of a concrete theoretical or experimental investigation into the nature of interactions between microgel particles at the interface. The stimuli responsive nature of the microgel particles also results in changes in the interfacial microstructure of these particles with changes in the environmental conditions such as temperature and pH. These microstructural changes reflect in the interfacial rheological measurements.

In *Chapter 3*, we provide an overview of the materials and the various experimental methods used in the research. The PNIPAM microgel particles used during all the experiments have been synthesized in-house. We provide a detailed description of the synthesis and the characterisation of these microgel particles. We further discuss the theoretical background of the most important experimental techniques used for our research, namely compression isotherms of spread monolayers using the Langmuir balance and interfacial tension measurement using the axisymmetric drop shape analysis method. Minute details of the protocol followed during each of the experiments have been discussed separately in respective chapters.

In *Chapter 4*, we aim to study the adsorption dynamics of microgel particles at an air-water interface. As pointed out in the literature review, an ideal gas like EOS is insufficient to describe the relation between the surface pressure and surface concentration. Hence we experimentally determine such a relation (an EOS) using compression isotherms of spread monolayers of microgel particles. The pressure-area isotherms reveal some interesting observations. The isotherms detect measurable surface pressures at inter-particle distances that are much greater than the particle

diameter. This suggests that the particles are strongly deformed. Using a simple scaling argument we show that the surface pressure detected at very low loading is a measure of the internal elasticity of the particles. We compare our experimental findings to the scaling relation proposed by Groot and Stoyanov. The length scale d_{eff} = 1.25 nm that arises out of this scaling relation is the effective distance between the crosslinks in the microgel particle. We use this experimentally determined EOS to study the adsorption dynamics of these microgel particles. The adsorption process is clearly comprised of two regimes. An initial diffusion limited regime which is later taken over by a barrier limited adsorption regime where the crowding of the particles at the interface causes a barrier for the subsequent particles to adsorb on to the interface.

In *Chapter 5* we have extended the experimental observations of Chapter 4 to different temperatures in order to study the effect of temperature on the adsorption dynamics. We establish separate EOS for various temperatures. The compression isotherms show a softer response with increasing temperature. This softness is speculated to be a result of increasing electrostatic repulsion between the particles combined with short range attractive interactions between loose polymer segments along the periphery of the particle. This leads to a change in the interfacial microstructure from a dense ordered monolayer at lower temperatures to a network of particles consisting of clusters of particles at higher temperatures. The experimental EOS has been used to study the adsorption kinetics of microgel particles. Based on the observations in the previous chapter, a simple model that takes into account diffusion limited adsorption at short times and a barrier limited adsorption at long times has been developed. Such a model described the entire process very well. The solution to such a model is fitted to the experimental data using diffusion coefficient and adsorption rate constant as fit parameters. The diffusion coefficient thus extracted agreed well with ones measured using DLS.

Chapter 6 deals with microgel particles adsorbed on an oil-water interface. We equilibrate the surface of drops so that the drop surface is covered with particles. We then subject the drops to changes in temperature as well as in the surface area. Cyclic changes in the temperature

invoke a perfectly reversible response in the interfacial tension. When the drop is subjected to a change in the interfacial area the result is a change in the surface pressure. Any desorption of particles caused by the decrease in the interfacial area should reflect as a relaxation in the surface pressure. However, no such relaxation is observed even if the drop was deformed by a large extent. Moreover, the change in surface pressure is independent of the rate of compression. These confirm the fact that the particles are irreversibly adsorbed on the oil-water interface. The electrophoretic measurements suggest a 2.5 fold increase in the effective surface potential over the range of temperatures studied. The asymmetric charge distribution at the oil-water interface causes the particles to interact via long range dipole-dipole interactions. In addition to this the particles also experience a short range attraction owing to the hydrophobic interactions between the loose polymer segments along the periphery of the particles. The net effect is that the interfacial microstructure goes from a dense, ordered structures at lower temperatures to a more open network of particles at higher temperatures. This change can be observed indirectly through the interfacial dilatational rheology measurements. At low temperatures the dense network results in a higher modulus whereas at higher temperatures the dilatational elasticity is reduced. These insights will prove crucial if PNIPAM based microgel particles are to be used as Pickering stabilisers for foams and emulsions. Their stimuli responsive nature provides us with a handle to control the particle interactions, their interfacial microstructure and interfacial rheology and consequently on the stability of foams and emulsions prepared using such particles as stabilisers. Suitable modifications in the chemistry of these particles can enable us to manufacture particles that are tailor made for very specific applications.

Samenvatting

In dit proefschrift bestuderen we de eigenschappen van olie-water en lucht-water grensvlakken. Deze eigenschappen bepalen het gedrag en de stabileit van schuimen en emulsies. Men kan ze beinvloeden door deeltjes aan het grensvlak toe te voegen. Vaak worden hiervoor harde colloïdale deeltjes gebruikt; men spreekt dan van Pickering stabilisatie. In deze studie beschouwen we zachte microgel deeltjes op basis van poly-N-isopropylacrylamide (PNIPAM). Belangrijke vragen hierbij zijn: hoe adsorberen deze deeltjes aan het grensvlak en wat is de wisselwerking tussen deze deeltjes in het grensvlak. Omdat de deeltjes bij omgevingstemperaturen beneden de karakteristieke overgangs temperatuur (TT) sterk gezwollen zijn en boven deze temperatuur juist sterk gekrompen, is het van belang de temperatuurafhankelijkheid van deze processen te bestuderen. Met deze kennis kan men vervolgens de eigenschappen van stabilisatoren verder verbeteren en toespitsen op de specifieke eisen die men aan het product stelt, waarin ze toegepast worden.

We beginnen onze studie in *Hoofdstuk 2* met een uitgebreid overzicht van de reeds beschikbare literatuur op dit gebied. De beschrijving van de deeltjes wisselwerking, de adsorptie kinetiek en de daaruit voortvloeiende grensvlak structuur en reologie is meestal gebaseerd op het gedrag van harde deeltjes. Voor zachte, vervormbare deeltjes verandert deze beschrijving enigszins: door hun vervormbaarheid kunnen ze makkelijker de barrière opgeworpen door de elektrisch lading op de deeltjes, overwinnen. Daardoor adsorberen ze makkelijker aan het grensvlak dan harde colloïdale deeltjes. De adsorptie kinetiek hangt mede af van de toestandsvergelijking (de relatie tussen grensvlakspanning en grensvlakbezetting) van de deeltjes in het grensvlak. Meestal wordt zowel voor harde als voor vervormbare deeltjes de ideale gaswet verondersteld. Deze

lineaire relatie is echter onjuist en leidt bij voorbeeld tot waarden van de diffusie constante die twaalf tot dertien ordes van grootte mis zijn. In geval van harde colloïdale deeltjes met een goedgedefinieerde vorm is de contactlijn van het grensvlak met het deeltje en de elektrische lading van het deeltje goed gedefinieerd. Daardoor zijn de elektrostatische, de van der Waals en de capillaire krachten goed te schatten. Hierover is dan ook een schat aan informatie te vinden in de literatuur. Het zachte, vervormbare en doordringbare karakter van de PNIPAM microgel deeltjes maakt het moeilijk om de vorm, het oppervlak en de contactlijn te precies vast te stellen. Er zijn dan ook weinig theoretische of experimentele artikelen te vinden die de wisselwerking tussen de microgel deeltjes in het grensvlak adequaat beschrijven. De temperatuur (en pH) afhankelijkheid van deze deeltjes heeft ook zijn invloed op de microstructuur in het grensvlak, zoals zichtbaar wordt in de oppervlakte reologie van het grensvlak.

In *Hoofdstuk 3* wordt een overzicht gegeven van de in dit proefschrift gebruikte technieken en materialen. In dit hoofdstuk beschrijven we ook de synthese van de gebruikte microgel deeltjes en hoe we deze deeltjes gekarakteriseerd hebben in termen van afmeting en oppervlaktepotentiaal. Verder wordt de Langmuir balans en de "pendant drop" methode in detail besproken. De gevolgde protocollen worden in de desbetreffende hoofdstukken nader uitgewerkt.

In *Hoofdstuk 4* bestuderen we het adsorptie proces van microgel deeltjes aan een lucht-water grensvlak. Zoals al eerder aangegeven beschrijft de ideale gas toestands-vergelijking de grensvlakspanning versus grensvlakbezetting relatie onjuist. Daarom bepalen we deze relatie experimenteel door met een Langmuir balans de compressie isothermen op te nemen van monolagen van deze microgel deeltjes. Deze compressie isothermen vertonen een interessant gedrag. De grensvlakspanning is al voelbaar als de afstand tussen de deeltjes nog veel groter is dan de deeltjes diameter. Dit geeft aan dat de deeltjes de neiging hebben om zich in het grensvlak te spreiden waarbij ze sterk moeten vervormen om dat mogelijk te maken. Met simpele schalings relaties kunnen we laten zien dat de grensvlakspanning bij lage oppervlakteconcentratie wordt bepaald door de elasticiteit van de microgel deeltjes. Door onze resultaten te vergelijken met theo-

retisch werk van de Groot en Stoyanov krijgen we een indruk van de effectieve afstand tussen de "cross-link" posities binnen een microgel deeltje: d_{eff} = 1.25 nm. Vervolgens gebruiken we de experimenteel gevonden toestandsvergelijking om de grensvlakspanning, gemeten als functie van de tijd, te vertalen naar een oppervlaktebezetting versus tijd relatie. Het onderliggende adsorptieproces laat duidelijk twee regimes zien. Aanvankelijk is het proces diffusiegelimiteerd maar als de bezettingsgraad in het grensvlak toeneemt, levert dit een barrière op voor verdere adsorptie en bepaalt deze de adsorptie snelheid.

In *Hoofdstuk 5* trekken we de lijn van Hoofdstuk 4 verder door en bestuderen we in detail de temperatuurafhankelijkheid van het adsorptie proces. Daartoe bepalen we eerst de temperatuurafhankelijkheid van de toestandsvergelijking. De compressie isothermen vertonen met toenemende temperatuur een "zachtere" respons, dat wil zeggen de drukvariatie met varierende oppervlaktebezetting neemt af als de temperatuur toeneemt. Aangezien de deeltjes met toenemende temperatuur steeds meer krimpen, vermoeden we dat dit gedrag veroorzaakt wordt door een toenemende elektrische ladingsdichtheid op de deeltjes waardoor deze elkaar over relatief lange afstand afstoten. Ook kan er een korte dracht aantrekkingskracht tussen de polymeeruiteinden van de microgel deeltjes aanwezig zijn omdat water bij deze temperaturen een slecht oplosmiddel is. Hierdoor lijkt de microstructuur in het grensvlak te verschuiven van een geordende monolaag bij lage temperaturen beneden de TT naar een tweedimensionaal netwerk van aggregerende deeltjes bij temperaturen boven de TT. Ook de temperatuurafhankelijkheid van de adsorptie kinetiek is nader bestudeerd. Uitgaande van de waarnemingen in vorig hoofdstuk hebben we een eenvoudig model geformuleerd waarmee zowel de invloed van de diffussie in de sublaag als van de adsorptie barriëre theoretisch kan worden bestudeerd. De model berekingen zijn gefit aan de gemeten adsorptie karakteristieken. Hierbij zijn de diffusieconstante en de adsorptiesnelheids constante gebruikt als fitparameter. De gevonden waarden voor de diffusieconstante blijken goed overeen te komen met de waarden gemeten met dynamische lichtverstrooing.

Hoofdstuk 6 gaat over het gedrag van microgel deeltjes die aan het

grensvlak van een oliedruppel in een waterbad adsorberen. Hierbij laten we het grensvlak eerst tot evenwicht komen met de waterfase die een hoge concentratie microgel deeltjes bevat. Daarbij wordt het grensvlak volledig bezet met deeltjes. Zodra dit evenwicht zich heeft ingesteld onderwerpen we de druppel aan temperatuur en oppervlakte veranderingen. Het cyclisch variëren van de temperatuur leidt tot een volledig reversibele respons van de grensvlakspanning. Ook het variëren van de grootte van het oppervlak leidt tot een nagenoeg instantane verandering van de oppervlaktedruk. Als ten gevolge van deze oppervlakte variatie deeltjes zouden ad- dan wel desorberen, zou de oppervlakte druk relaxeren naar zijn oorspronkelijke waarde. Deze relaxatie wordt niet waargenomen ook niet als het druppeloppervlak aanzienlijk vergroot wordt. Bovendien is de drukvariatie onafhankelijk van de compressiesnelheid. Daaruit concluderen we dat de deeltjes inderdaad irreversibel in het olie-water grensvlak zijn geadsorbeerd. Elektroforese metingen suggereren dat de ladingsdichtheid en de corresponderende elektrische potentiaal sterk temperatuurafhankelijk zijn: de potentiaal varieert met een factor 2.5 over het beschouwde temperatuur bereik. Omdat in het grensvlak de ladingsverdeling niet symmetrisch is, ontstaat er een dipool-dipool wisselwerking in het grensvlak welke ook sterk temperatuur afhankelijk is. Dit is in overeenstemming met de in Hoofdstuk 5 geschetste verschuiving van de microstructuur van een compacte ordening bij temperaturen beneden de TT naar een meer open netwerkstructuur bij temperaturen boven de TT. Deze veranderingen zien we indirect terug in de opervlakte reologie van de druppel. De compacte ordening bij lage temperaturen heeft een hoge elasticiteitsmodulus tot gevolg. Bij hoge temperatuur blijkt deze dilatatie elasticiteit veel kleiner te zijn ten gevolge van de meer open netwerkstructuur. Op basis van deze bevindingen kunnen in de toekomst hopelijk PNIPAM microgel deeltjes gebruikt worden als Pickering stabilizatoren waarbij de temperatuur (en pH) afhankeijkheid van deze deeltjes het mogelijk zullen maken de structuur van het olie-water of lucht-water grensvlak te beheersen en daarmee ook de stabilteit van bij voorbeeld emulsies of schuimen. Door de chemie van de microgel deeltjes aan te passen kan men de producten waarin ze gebruikt worden, verder optimaliseren voor hun specifieke toepassing.

Acknowledgements

Finally it comes to the moment as I write the final few lines in my thesis. There was a time in my PhD when it felt as if this moment would never occur. But it was the wonderful people around me and those whom I have met over the past 5 years who have, in one way or the other played an important role in me completing my work.

I would begin with extending my thanks to my advisor Prof. Frieder Mugele for allowing me to be a part of the PCF group and letting me work on a topic which was originally not supposed to be my thesis. He kept his faith in me at times when probably anyone else would have lost all hope. My daily supervisor Dr. Dirk van den Ende has always been a source of inspiration for me. I would fall short of words if I begin to thank you. I always have learnt something from each of our discussions regardless of whether it was about scientific or personal issues. I am truly in awe of the breadth as well as the depth of knowledge that you posses. As of now, I don't know where my life will take me next. But if I ever land up in a career in academia, I would strive to be like you. Without Prof. Martien Cohen Stuart, this thesis was truly impossible. He was truly the lighthouse to my ship which was lost in rough seas. I simply loved his ability to distil out simple tangible numbers out of seemingly intricate physical phenomena to get a judgement of whether we are moving in the right direction. It was his number crunching that led us to realise the inaccuracy of the ideal gas EOS for particle adsorption and which finally lead to our first article. Dr. Michel Duits even in his busiest of times always managed to spare a few minutes to listen to my ideas. I would especially want to appreciate his help in writing and the subsequent iterations of the review article about particles at interfaces. His profound knowledge about the state of the art in the field of colloids was the only

reason we could submit the article before the stipulated deadline.

My stay at the PCF group was a memorable one, thanks to the wonderful colleagues I have had the privilege to work with over the past 5 years. I would like to thank the current members of PCF Bijoy, Jolet, Davood, Fei, Reille, Arjen, Andrea, Aram, Igor, Carla, Olena, Lei and Yan for all the fun and many interesting discussions that covered a wide range of topics. I will surely miss the interesting discussions at the coffee corner. Mariska, I thank you for your help with the experiments towards the end of my thesis. It took quite a burden off my shoulders. Daniel, Cunlu, Zhantao, Hao, Pablo, Alberto and Arun. You guys were amazing officemates. Daniel, your jokes and witty comments always kept me cheerful. I would also like to thank all the past members of the PCF group. Hao, Pablo, Gor, Burak, Sissi, Agata, Tarun, Dhirendra, Dileep, Jung, Dieter, Ivo, Huub, Arun Gnanappa, Arun Banpurkar, Daniel Ebeling, Daniel Hagedoorn, Mathijs, I learnt a lot from you guys. Arjen and Daniel H., I thank you for not hurting my feelings and sentiments and not passing any offensive remarks on or around me. I wonder if I will find such caring and sensitive colleagues ever again. I would like to especially thank Armando. Your new ideas and insights kept me motivated. Naveen, Kartikeya, Somnath, Chandra, Aditya. You guys and your chai/bakchodi sessions were truly memorable. I would also like to thank Martijn who was my first student. Annelis, Lisette, Edith and Isabelle, thanks to you, I never had to worry about any paperwork.

Prof. Vinod Subramaniam allowed me to work on the Kibron LB trough at AMOLF. Those experiments form the heart of my thesis. I can't thank you enough for that. Aditya Iyer was a perfect host whenever I visited AMOLF. Martin Bennink not only allowed me to work on the OT setup in his lab but at times even came into the lab and helped me with troubleshooting. It is a pity that after all the hard work that we put in neither the OT nor the microrheology project with Ramesh could bear fruit. But I have admired your enthusiasm and passion for science and I thank you for all those wonderful discussions. I also thank Hans and Burcu for letting me use their microscope for my interfacial microrheology experiments. I sincerely thank Remko Fokkink for the SLS experiments.

Just when I started writing my thesis, I came to know about the sad demise of my Bachelors thesis supervisor, Prof. S. R. Patwardhan. He was one of my role models. It was he who motivated me to join PhD. His excitement for science and his discipline has left an everlasting imprint on me.

Dina, Tiyo, Niro and Ernest proved to be the best house mates I could get. Unai and Ramazan were not just house mates but brothers. I thank you for some of the best moments in my life. I really appreciate Unai and Naiara coming all the way to India to attend my wedding.

The Indian community in Enschede was a big part of my life in Enschede. Chandu-Meenakshi and Pramod-Vishakha were our family here in Enschede. I can never forget their help especially at the time when Amogh was born. When it came to scientific as well as personal discussions, Abhi was always available. Our friendship started with a wonderful trip to Corsica and has kept on growing ever since. I was blessed to have friends like Rohit, Shushil, Nishant, Sourabh, Gargi, Harini, Siddharth, Nupur, Arpita, Raja, Vivek, Ragha, Tushar, Rajesh, Maulik and Gaurav. I (on behalf of Sampada and Amogh as well) would also like to thank Abhi-Shruti, Pandu-Pallavi, Shodhan-Chaitanya, Jigar-Falguni, Dhaval-Hinal, Mayur-Tina, Saurabh-Neha, Hanumant-Neeru, Jitendra-Neelam, Giri-Varsha, Kishore-Hema, Shrikrishna-Gayatri, Chintan-Usha, Raman-Priyanki, Supriyo-Anandita, Vishwas-Sarika, Himanshu-Shablika, Harsh-Lakshmi, Jay-Bhavana, Ravi-Anne, Prince-Aditi, Arun-Aarti, Kartikeya-Harshita for all the wonderful memories. Amit-Kiranmayee, our friendship from IIT days continued even here in NL. I just hope it keeps going on in the future as well. I also thank AADHAAR and all its members for giving me an opportunity to work for a good cause. Ajit-Vrunda, you were our only relatives so far away from home. Thank you for all the wonderful time and memories. The Bhasad gang: Aditya I., Naveen, Prince, Kartikeya, Himanshu, Naveen, Praneeth, Deepak, Mitava, Yashashwini, Aditya N. and Ravi. Thank you guys for the jokes, the *'relaxing'*, the *'Lunch? at 3AM'* and all the bakaiti. To you guys I can just say, *"Direct wahi milo!!"*. My friends over the years: Vineet, Rohan, Vinit, Mandar, Harsh, Devesh, Dwaipayan, Meenesh, Amit, Arijit and , Meenakshi. Your

friendship has always been and will continue to be my strength.

My family has truly made me what I am today. Aditya you have been my best friend rather than my younger brother. I have been proud of your achievements and I am sure you'll manage to achieve greater heights in the future. Sampada's parents have treated me as their son rather than a son-in-law. I thank them as well as Piyu-Tushar for accepting me whole heartedly in their family. My late grandparents Anna and Aaji were the ones who inculcated in me the importance of hard-work and dedication. Madhu kaka, I have always admired the way you have tied the entire Deshmukh family together. I also owe my love for mathematics to you. My parents have supported me in each and every decision that I have made. They allowed me to develop my thoughts independently and have always provided me with their support and guidance when I faced even slight difficulty. Aai-Baba I will forever be indebted for your love and blessings that you have showered on me. I can only hope I can continue to work hard and make you proud in the future as well. Sampada, you have truly been my better half for the past 4 years. I have spent time on research, working on weekends and nights; time that I should have ideally spent with you and Amogh. But you understood me and tried to keep me cheerful in whatever little time I could spend with you. Amogh, your smile and a hug at the end of the day made me forget all the worries in the world. You have been the best thing that has ever happened to me.I love you both! Last but not the least I would also like to thank the Almigthy for giving me an amazing life full of opportunities and the courage and strength to face all the challenges in life.

Output

Publications

1. Omkar. S. Deshmukh, Armando Maestro, Michel H. G. Duits, Dirk van den Ende, Martien Cohen Stuart and Frieder Mugele. **An equation of state and adsorption dynamics of soft microgel particles at air-water interface**, Soft Matter, 2014, 10, 7045-7050. DOI: 10.1039/C4SM00566J.
2. Omkar S. Deshmukh, Dirk van den Ende, Martien Cohen Stuart, Frieder Mugele and Michel H. G. Duits. **Hard and soft colloids at fluid interfaces: Adsorption, interactions, assembly and rheology.**, Advances in Colloid and Interface Science, 2014. DOI: 10.1016/j.cis.2014.09.003.
3. Omkar S. Deshmukh, Armando Maestro, Dirk van den Ende, Martien Cohen Stuart, Frieder Mugele and Michel H. G. Duits. **Adsorption and interactions of soft microgel particles at oil-water interfaces**, Manuscript in preparation.
4. Armando Maestro, Omkar S. Deshmukh, Frieder Mugele and Dominic Langevin. **Shear Rheology of surfactant-decorated nanoparticles adsorbed at fluid interfaces: Evidences of a 2D - glassy state**, Manuscript in preparation
5. Omkar S. Deshmukh, Mariska H. P. van der Weide, Michel H. G. Duits, Dirk van den Ende, Martien Cohen Stuart and Frieder Mugele. **Temperature effect on adsorption dynamics of soft microgel particles at air-water interface.**, Manuscript in preparation.

Presentations

- "Soft microgel particles: New insights into their adsorption at fluid interfaces", Annual European Rheology Conference,2013, Leuven, Belgium.
- "Particle tracking microrheology in dense microgel suspensions", Jamming and Rheophyiscs Meeting, 2010, Corsica, France
- "On the theory of Brownian motion", Guest lecture at the Sinhgad College of Engineering, 2010, Pune, India.

Poster presentations

- "Temperature dependent adsorption dynamics of soft microgel particles on air-water interfaces", CompFlu2014 - Symposium on Rheology of Complex Fluids, 2014, Bengaluru, India.
- "PNIPAM microgels: A novel insight into their adsorption and interactions at fluid interfaces", 9th Liquid Matter Conference, 2014, Lisbon, Portugal.
- "Adsorption of PNIPAM microgel particles at interfaces", Soft Matter Conference, 2013, Rome, Italy.
- "Interfacial rheology of microgel suspensions", International Congress on Rheology, 2012, Lisbon, Portugal.
- "Microrheology on a thermosensitive microgel particle suspension near the jamming transition", FOM Physics, 2012, Veldhoven, Netherlands.

Biography

Omkar Suresh Deshmukh was born at his maternal place in the city of Solapur in India on 20th March 1985. His father's job transfers meant he travelled across various cities such as Ahmedabad, Jalna and Aurangabad before finally settling down in Pune, India where he completed his school education. He later joined the Sinhgad College of Engineering, Pune for Bachelor of Engineering degree in Chemical Engineering. He worked on his Bachelors thesis titled "Design of Lo-Cat process for Gas sweetening" under the guidance of Prof. S. R. Patwardhan and Dr. C. V. Rode (NCL, Pune). He went on to study M.Tech in Chemical Engineering at the Indian Institute of Technology, Bombay. There he worked with Prof. P. Sunthar on his thesis titled " Drop detachment dynamics of dilute polymer solutions". After his masters he worked as a Research Assistant under Dr. Ashish Lele at the Complex Fluids and Polymer Engineering (CFPE) group at the National Chemical Laboratory, Pune. He joined the Physics of Complex Fluids (PCF) group at the University of Twente in The Netherlands as PhD student in November 2009. At the PCF group he worked on interfacial dynamics of soft microgel particles at fluid interfaces. His work has been presented in several international conferences and has resulted in journal publications in reputed peer-reviewed journals.